Title
Arsenic Mobilization and Sorption in Subsurface Environments: Experimental Studies, Geochemical Modeling, and Remediation Strategies

Author
Hafeznezami, Saeedreza

Publication Date
2015

Peer reviewed|Thesis/dissertation

UNIVERSITY OF CALIFORNIA

Los Angeles

Arsenic Mobilization and Sorption in Subsurface Environments: Experimental Studies, Geochemical Modeling, and Remediation Strategies

A dissertation submitted in partial satisfaction of the requirements for the degree Doctor of Philosophy in Civil Engineering

By

Saeedreza Hafeznezami

2015

ABSTRACT OF THE DISSERTATION

Arsenic Mobilization and Sorption in Subsurface Environments:
Experimental Studies, Geochemical Modeling, and Remediation Strategies

by

Saeedreza Hafeznezami
Doctor of Philosophy in Civil Engineering
University of California, Los Angeles, 2015
Professor Jennifer Ayla Jay, Chair

Contamination of groundwater resources with naturally occurring arsenic (As) is a major health concern globally that affects millions of people. Experimental studies and geochemical modeling can be useful tools for understanding the mechanisms controlling speciation and partitioning of As, predicting the mobility and transfer of As, assessing the risks, and developing effective in-situ remediation schemes for affected areas.

The wide variety of experimental details used in the published adsorption studies, and limited number of studies conducted for adsorption of As on natural samples underscores the need for further research in this area. Application of currently available empirical models, and mechanistic surface complexation modeling (SCM) approaches for describing the adsorption of

As on natural sediments is also challenging due to the complexity of the heterogeneous solid phases of porous media.

In Chapter 2, we compare different kinetic and equilibrium adsorption models for describing the adsorption data from batch experiments conducted on natural sediment samples collected from a contaminated site in New England, USA. We evaluate the capability and sensitivity of commonly used empirical models for modeling the concentrations of dissolved As as well as the relations between the derived model parameters and chemical/physical characteristics of sediments.

In Chapter 3, four different SCMs are developed to model the data from batch experiments conducted on natural sediment and groundwater samples. The SCMs used in this study vary in terms of 1) method for estimating the total number of sorption sites, 2) method for describing the surface site heterogeneity, and 3) method for applying electrostatic and pH-dependent correction factors to surface reaction constants. we utilize the easily-accessible modeling tools PHREEQC and FITEQL to predict and simulate the experimental results.

Chapter 4 focuses on batch and column experiments conducted to study the effectiveness of applying chemical amendments with the purpose of facilitating and enhancing natural attenuation of As in contaminated subsurface environments. The results will provide a qualitative basis for evaluating the suitability and efficiency of applying these methods in actual contaminated sites.

The dissertation of Saeedreza Hafeznezami is approved.

Michael K. Stenstrom

Keith Stolzenbach

Irwin Suffet

Jennifer Ayla Jay, Committee Chair

Dedication Page

I want to dedicate this work to Seyed Mahmoud Aghazadeh and his lovely family for giving me the biggest opportunity in life. I am forever in your debt.

Thank you Farah and Ali, my kind and caring mom and dad for all your sacrifices and bearing with me.

Thanks to Mohammadreza, Alireza, and Hamidreza my three brothers for all their helps.

Table of Contents

Chapter 1 – Introduction 1

Chapter 2 – Adsorption and Desorption of Arsenate on Sandy Sediments from Contaminated and Uncontaminated Saturated Zones: Kinetic and Equilibrium Modeling 8

ABSTRACT 8

INTRODUCTION 9

MATERIALS AND METHODS 10

RESULTS 15

DISCUSSION 22

CONCLUSIONS 26

REFERENCES 49

Chapter 3 - Arsenic Mobilization in an Oxidizing Alkaline Groundwater: Experimental Studies, Comparison and Optimization of Geochemical Modeling Parameters 52

ABSTRACT 52

INTRODUCTION 53

MATERIALS AND METHODS 58

RESULTS 67

DISCUSSION 74

CONCLUSIONS 81

REFERENCES 100

Chapter 4 – Remediation of As(V) Contaminated Groundwater Through Enhanced Natural Attenuation: Batch and Column Studies 107

INTRODUCTION 107

MATERIALS AND METHODS 109

RESULTS 114

DISCUSSION 117

CONCLUSIONS 120

CHAPTER 5-SUMMARY 134

REFERENCES 137

LIST OF FIGURES

Figure 1.1. Arsenic mobilization and sorption mechanisms 5

Figure 2.1. As(V) concentration remaining in solution versus time 28

Figure 2.2. Plots of Ln(C/C0) versus time 29

Figure 2.3. Plots of t/q versus time 31

Figure 2.4. Freundlich isotherm model fits to adsorption data 33

Figure 2.5. Langmuir isotherm fits to adsorption data 36

Figure 2.6. Desorption of As over time 39

Figure 2.7. Solid phase distribution (%) of As, Fe, P, Ca, and Al 40

Figure 2.8. Molar ratios of As/Fe and P/Fe extracted from the different solid phases 43

Figure 2.9. Comparison between the Langmuir St and characteristics of sediments 44

Figure 3.1. Map of the site 84

Figure 3.2. Schematic framework of geochemical modeling 84

Figure 3.3. As concentrations and pH values at monitoring wells 85

Figure 3.4. Distribution of solid phase As concentrations 86

Figure 3.5. Experimental As(V) adsorption as a function of equilibrium concentration 86

Figure 3.6. Experimental and modeling results for acid titrations 87

Figure 3.7. Dissolved As(V) in acidification experiments compared with the modeling simulations 88

Figure 3.8. Simulated distribution (%) of surface species at pH 7 90

Figure 3.9. Surface site concentration calculated from four different methods 92

Figure 3.10. Hybrid-Isotherm Model predictions for different potential remediation schemes 92

Figure 4.1. Acid titration of sediment suspensions 122

Figure 4.2. Average effect of remediation treatments on increased As(V) removal 120

Figure 4.3. Adsorption isotherm results for three levels of Ca 123

Figure 4.4. Concentrations of As and PO_4 from acidification experiments 124

Figure 4.5. Concentrations of As and PO_4-P in the effluents of columns 125

Figure 4.6. Summary of maximum removal rates (%) for As and PO_4 128

Figure 4.7. Solid phase concentrations of Fe and As (mg/kg) along the column profile 129

LIST OF Tables

Table 2.1. Chemical and physical properties of sediments 46

Table 2.2. Pseudo-first order kinetic model parameters 45

Table 2.3. Pseudo-second order kinetic model parameters 47

Table 2.4. Freundlich adsorption isotherm model parameters 47

Table 2.5. Langmuir adsorption isotherm parameters 48

Table 2.6. Arsenic desorption rates from original and As-loaded sediments 48

Table 3.1. Sediment samples properties and descriptions 94

Table 3.2. Sequential extraction method modified from Keon et al (2001) 94

Table 3.3. Surface Complexation Model parameters and assumptions 95

Table 3.4. Surface complexation stoichiometry and reaction constants used in the diffuse double layer model for HFO 95

Table 3.5. Distribution of solid phase As concentrations from sequential extractions 96

Table 3.6. Langmuir Isotherm parameters derived from adsorption experiments 97

Table 3.7. Acidification Experiment Results 97

Table 3.8. Comparison of the goodness of fit values (NRMSE, %) 98

Table 3.9. Surface complexation reaction constants modified for Hybrid-Isotherm model 98

Table 3.10. Surface complexation constants optimized by FITEQL for GC-BET model 98

Table 4.1. Column physical properties 131

Table 4.2. Groundwater quality data 131

Table 4.3. Results of factorial remediation experiments 132

Table 4.4. Acidification experiment data 133

Acknowledgements

First and foremost I like to thank my amazing advisor and mentor, Professor Jay who always believed in me and motivated me to work harder and learn more.

I like to thank my committee members Professor Stenstrom, Professor Stolzenbach, and Professor Suffet for their guidance and feedback.

I want to thank Matthew Reynolds for supporting the project, sample collection, and providing data. I thank Dr. James A. Davis for sharing his vast knowledge in the geochemical modeling field with me. I like to express my deepest gratitude and respect to Dr. Hillary Godwin and Chong Hyun Chang for their vital assistance to this work without any expectations.

I acknowledge all the wonderfully kind and talented graduate, undergraduate, and volunteer researchers who worked in the Jay lab team over the years. I am forever grateful to Amity Zimmer-Faust for her unconditional help. I want to thank my good friend Dukwoo Jun for always being there when I needed him. All the undergraduate assistants who helped me throughout the years, the mighty "Metals Team", I thank and salute you.

I like to thank all the staff at the UCLA CEE department for the administrative and logistical support that made this work possible.

Finally, thank you my selfless, loving and patient family for supporting me throughout this journey. I love you.

VITA

Education

2010	M.S. Civil & Environmental Engineering, California State University, Long Beach. Research project title: Evaluating removal efficiency of heavy metals in constructed wetlands
2008	B.S. Civil & Environmental Engineering, Polytechnic University of Tehran

Employment

2011 – 2015	UCLA Civil and Environmental Engineering Department, research and teaching assistant

Teaching Experience

Spring 2012	Teaching assistant, CEE 110: Introduction to Probability and Statistics for Engineers
Summer 2012	Teaching assistant, ENV 12: Sustainability and Environment
Fall 2012	Teaching assistant, CEE 153: Introduction to Environmental Engineering
Spring 2013	Teaching assistant, CEE 110: Introduction to Probability and Statistics for Engineers
Summer 2013	Teaching assistant, ENV 12: Sustainability and Environment
Fall 2013	Teaching assistant coordinator, CEE 495: Teaching Assistant Training Seminar
Spring 2014	Teaching assistant, CEE 110: Introduction to Probability and Statistics for Engineers

Spring 2015 Teaching assistant, CEE 110: Introduction to Probability and Statistics for Engineers

Publications and Conference Presentations

- Hafeznezami, S., Reynolds, M., Davis, J. A. and Jay, J. A. Arsenic Mobilization in an Oxidizing Alkaline Groundwater: Experimental Studies, Comparison and Optimization of Geochemical Modeling Parameters. (Submitted to Applied Geochemistry, August 2015)

- Hafeznezami, S., Lin, T.Y. and Jay, J.A. Redistribution of Solid Phase Arsenic and Effect of NOM in Microcosms of Aquaculture Pond Sediments. Poster presentation delivered at the American Chemical Society national meeting, Denver, CO, March 2015.

- Hafeznezami, S., Kim, J., and Redman, J. (2012). Evaluating Removal Efficiency of Heavy Metals in Constructed Wetlands. Journal of Environmental Engineering. 138(4), 475–482.

Awards

- Received UCLA's 2014-2015 Dissertation Year Fellowship
- Selected to the 2010 Graduate Dean's List of University Scholars (Top one percent of the graduate students)
- Selected as a member of Chi Epsilon, the National Civil Engineering Honor Society

Professional Affiliations

- American Society of Civil Engineers
- American Chemical Society
- Association of Environmental Engineering and Science Professors

Chapter 1. Introduction: Geochemistry of Arsenic Mobilization in the Subsurface Environments

Arsenic (As) is a toxic element classified as a metalloid with atomic weight of 74.92. It is ubiquitous and found in the atmosphere, soil and natural waters. Chronic exposure to arsenic in drinking water can cause numerous negative health impacts and is a proven carcinogen linked to many cancers including skin, bladder and kidney among others (Mandal and Suzuki, 2002). The World Health Organization (WHO) and United States Environmental Protection Agency (USEPA) has set the maximum contaminant level of As for drinking water standards at 10 μg/L.

Some of the common As containing minerals in the environment include arsenopyrite (FeAsS), orpiment (As_2S_3), realgar (AsS), and arsenolite (As_2O_3). Arsenic concentrations in soils vary based on their geological characteristics, but the global average is reported as 5 to 10 mg/kg (Smedley and Kinniburgh, 2002; Matschullat, 2000).

Arsenic can be mobilized into the natural waters either through naturally occurring processes or as a result of human activities. Even though the use of As containing compounds in the various industries has decreased in the recent decades, the risks of large scale contaminations due to human activities is as high as ever. The anthropogenic influence can be direct in the form of point source pollution discharges or indirect by facilitating the natural processes leading to release of As. Activities such agricultural, industrial, mining, and landfilling could affect the geochemistry of the subsurface environments through land disturbance or introduction of other chemicals.

Arsenic speciation and mobility in the subsurface environments is controlled by a complex array of geochemical parameters such as pH, redox condition, presence of competing

ions, kinetics and levels of concentration, presence and type of organic matter, mineralogy of solid phase, microbial activities. These parameters drive processes such as oxidation, reduction, precipitation, dissolution, adsorption, desorption and bioaccumulation in various directions and to different extents, all of which influence the concentrations of As present as dissolved species in the aqueous phase.

Figure 1 (based on work of Polizzotto et al., 2006) shows a simplified illustration of naturally occurring processes that could cause to mobilization and release of As from solid into solution phase. Occurrence of any or combination of these processes has lead to As contamination of groundwaters in many countries around the world including Bangladesh, India, Cambodia, Vietnam, Argentina, USA, Hungry, Chile, Mexico and China. Arsenic mobilization from solid to solution phase can occur in reducing environments where reduction and dissolution of host minerals causes the release of bound arsenic or in oxidizing environments by desorption from solid surfaces due to presence of high pH and/or competing ions.

It is widely recognized that iron (Fe) oxides play an important role in controlling levels of As in the porous media by the strong adsorption affinity. Poorly crystalline (amorphous) Fe oxides such as ferrihydrite (also referred to as hydrous ferric oxide, HFO) are known to adsorb As and other contaminants at a much higher rate than crystalline phases due to the higher surface area and adsorption site density (Harrison and Berkheiser, 1982; Sadiq 1997; Lumsdon 2001; Dixit and Hering, 2003). These phases are commonly found in soils and sediments either as discrete minerals or as coatings on other solid particles (Pierce and Moore, 1982). Over time amorphous Fe oxides transform to more crystalline phase such as goethite or hematite with smaller surface area and therefore lose some of their adsorptive capacities.

Inorganic As in natural systems including ground water is mostly present as oxyanions with oxidation state of +III (arsenite) or +V (arsenate). Arsenic speciation is controlled by pH and redox potential (Eh) of water. Arsenate ($H_nASO_4^{n-3}$) is the dominant inorganic form in oxidizing and arsenite ($H_nASO_3^{n-3}$) in reducing conditions. Most toxic cation trace metals become increasingly insoluble with increasing pH and their concentrations are controlled by precipitation or adsorption to hydrous metal oxides, however oxyanions such as arsenate tend to become less strongly adsorbed as the pH increases. (Dzombak and Morel, 1990; Smedley et al., 2002)

Raven et. al (1998) studied the adsorption of arsenate and arsenite on ferrihydrite at varying pH levels, showing that arsenate adsorption was higher at lower pH due to net positive charge of the surface attracting $H_2AsO_4^-$ ions. At higher pH levels arsenate adsorption was limited due to increased repulsion between the more negatively charged arsenate species and the negatively charged surface sites while arsenite can be retained in much larger amounts at pH>7.5. The mechanism for adsorption of As(V) on surface of metal oxides has been characterized as formation of inner-sphere surface complexes through a ligand exchange reaction with the surface functional groups, hydroxyl groups (Goldberg, 2002; Sherman and Randall, 2003; Moldovan and Hendry, 2005).

Due to great severity of As contamination problem in Bangladesh and other regions in south and south-east Asia where reductive dissolution is the major mobilization mechanism (Brammer and Ravenscroft et al., 2009); majority of published studies have addressed reducing conditions with As(III) being the dominant species. Fewer studies have addressed oxidizing conditions, in which As(V) may be mobilized by desorption at high pH (Currel et al. 2011; Scanlon et al., 2009; Bhattacharya et al., 2006; Smedley et al., 2005).

In this work, sediment and groundwater samples collected from an oxidizing sandy aquifer in Maine, USA are used to study the factors controlling the rates of adsorption/desorption processes with the ultimate goal to guide designing the in-situ remediation schemes. Portions of this study site are located within a known contamination plume with pH values above background levels and varying levels of As(V) and phosphate.

In Chapter 1 samples from upgradient and downgradient portions of the impacted zone as well as un-impacted areas downgradient of the plume are studied for their adsorption capacity with respect to As(V). Kinetic and equilibrium adsorption models are utilized and compared for describing the experimental data, and the fitted parameters are related to the chemical and physical characteristics of the sediments.

In Chapter 2 , the mechanistic approach to modeling adsorption data, surface complexation modeling (SCM) is studied for application to heterogeneous environments such as this study site. Three models based on the currently used approaches in the literature as well as a new hybrid model are developed using laboratory and field data to predict and simulate the results of batch experiments. Models developed and calibrated to the batch experimental data are used for predicting dissolved concentrations of As(V) under different remediation schemes.

In Chapter 3, both batch and column experiments are conducted with the intent of evaluating the effectiveness of applying chemical amendments to enhance the natural attenuation capacity of sediments with respect to As(V) and phosphate present in groundwater.

Figures

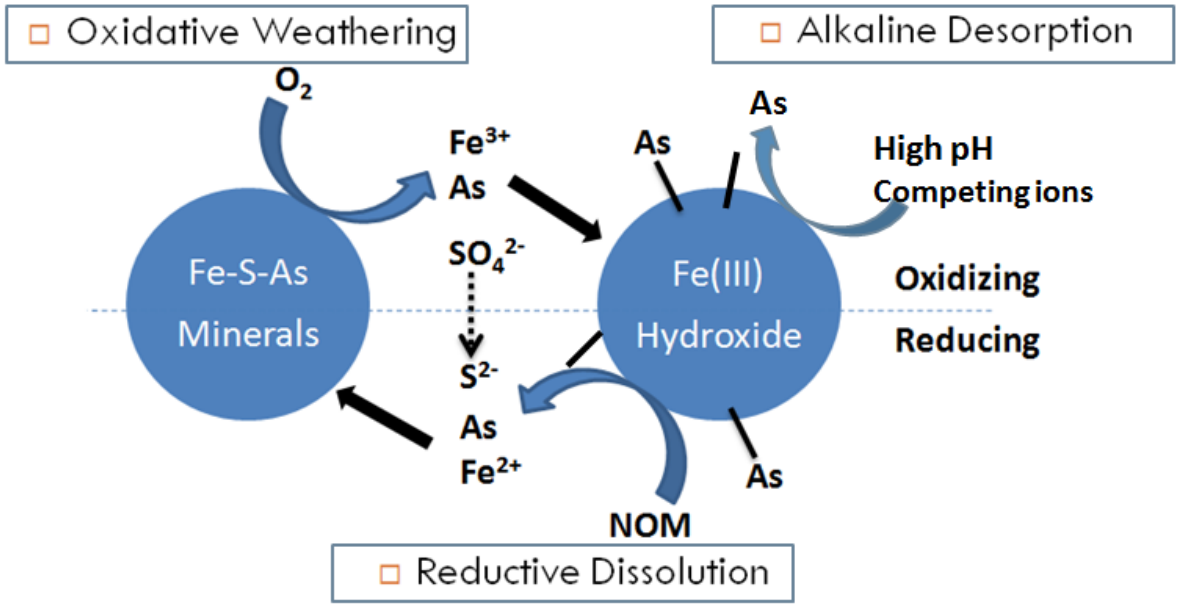

Figure 1. Schematic representation of As mobilization and sorption mechanisms in subsurface environments.

References

Arai, Y., Elzinga, E. J., & Sparks, D. L. (2001). X-ray absorption spectroscopic investigation of arsenite and arsenate adsorption at the aluminum oxide–water interface. *Journal of Colloid and Interface Science*, *235*(1), 80-88.

Bhattacharya, P., Claesson, M., Bundschuh, J., Sracek, O., Fagerberg, J., Jacks, G., … Thir, J. M. (2006). Distribution and mobility of arsenic in the Rio Dulce alluvial aquifers in Santiago del Estero Province, Argentina. *Science of the Total Environment*, *358*(1-3), 97–120.

Brammer, H., & Ravenscroft, P. (2009). Arsenic in groundwater: a threat to sustainable agriculture in South and South-east Asia. *Environment International*, *35*(3), 647-654.

Cances, B., Juillot, F., Morin, G., Laperche, V., Alvarez, L., Proux, O., ... & Calas, G. (2005). XAS evidence of As (V) association with iron oxyhydroxides in a contaminated soil at a former arsenical pesticide processing plant. *environmental science & technology*, *39*(24), 9398-9405.

Cornell, R. M., & Schwertmann, U. (2006). *The iron oxides: structure, properties, reactions, occurrences and uses*. John Wiley & Sons.

Currell, M., Cartwright, I., Raveggi, M., & Han, D. (2011). Controls on elevated fluoride and arsenic concentrations in groundwater from the Yuncheng Basin, China. *Applied Geochemistry*, *26*(4), 540–552.

Dixit, S., & Hering, J. G. (2003). Comparison of arsenic(V) and arsenic(III) sorption onto iron oxide minerals: implications for arsenic mobility. *Environmental Science & Technology*, *37*(18), 4182–9.

Dzombak, D. A., & Morel, F. M. (1990). *Surface complexation modeling: hydrous ferric oxide*. John Wiley & Sons.

Goldberg, S. (2002). Competitive adsorption of arsenate and arsenite on oxides and clay minerals. *Soil Science Society of America Journal*, *66*(2), 413-421.

Harrison, J. B., & Berkheiser, V. E. (1982). Anion interactions with freshly prepared hydrous iron oxides. *Clays Clay Miner*, *30*(2), 97-102.

Lumsdon, D. G., Meeussen, J. C. L., Paterson, E., Garden, L. M., & Anderson, P. (2001). Use of solid phase characterisation and chemical modelling for assessing the behaviour of arsenic in contaminated soils. *Applied Geochemistry*, *16*(6), 571-581.

Mandal, B. K., & Suzuki, K. T. (2002). Arsenic round the world: a review. *Talanta*, *58*(1), 201-235.

Matschullat, J. (2000). Arsenic in the geosphere—a review. *Science of the Total Environment*, *249*(1), 297-312.

Moldovan, B. J., & Hendry, M. J. (2005). Characterizing and quantifying controls on arsenic solubility over a pH range of 1-11 in a uranium mill-scale experiment. *Environmental science & technology*, *39*(13), 4913-4920.

Pierce, M. L., & Moore, C. B. (1982). Adsorption of arsenite and arsenate on amorphous iron hydroxide. *Water Research*, *16*(7), 1247–1253.

Polizzotto, M. L., Harvey, C. F., Li, G., Badruzzman, B., Ali, A., Newville, M., … Fendorf, S. (2006). Solid-phases and desorption processes of arsenic within Bangladesh sediments. *Chemical Geology*, *228*, 97–111.

Raven, K. P., Jain, A., & Loeppert, R. H. (1998). Arsenite and arsenate adsorption on ferrihydrite: Kinetics, equilibrium, and adsorption envelopes. *Environmental Science and Technology*, *32*(3), 344–349.

Ravenscroft, P., Brammer, H., & Richards, K. (2009). *Arsenic pollution: a global synthesis* (Vol. 28). John Wiley & Sons.

Sherman, D. M., & Randall, S. R. (2003). Surface complexation of arsenic (V) to iron (III)(hydr) oxides: structural mechanism from ab initio molecular geometries and EXAFS spectroscopy. *Geochimica et Cosmochimica Acta*, *67*(22), 4223-4230.

Sadiq, M. (1997). Arsenic chemistry in soils: an overview of thermodynamic predictions and field observations. *Water, air, and soil pollution*, *93*(1-4), 117-136.

Sherman, D. M., & Randall, S. R. (2003). Surface complexation of arsenic (V) to iron (III)(hydr) oxides: structural mechanism from ab initio molecular geometries and EXAFS spectroscopy. *Geochimica et Cosmochimica Acta*, *67*(22), 4223-4230.

Smedley, P. L., & Kinniburgh, D. G. (2002). A review of the source, behaviour and distribution of arsenic in natural waters. *Applied Geochemistry*, *17*(5), 517–568.

Smedley, P. L., Kinniburgh, D. G., Macdonald, D. M. J., Nicolli, H. B., Barros, a. J., Tullio, J. O., … Alonso, M. S. (2005). Arsenic associations in sediments from the loess aquifer of La Pampa, Argentina. *Applied Geochemistry*, *20*, 989–1016.

Scanlon, B. R., Nicot, J. P., Reedy, R. C., Kurtzman, D., Mukherjee, a., & Nordstrom, D. K. (2009). Elevated naturally occurring arsenic in a semiarid oxidizing system, Southern High Plains aquifer, Texas, USA. *Applied Geochemistry*, *24*(11), 2061–2071.

Chapter 2. Adsorption and Desorption of Arsenate on Sandy Sediments from Contaminated and Uncontaminated Saturated Zones: Kinetic and Equilibrium Modeling

Abstract

Understanding the rates and controlling factors for adsorption of contaminants such as arsenic (As) on natural sediments serves the objective of designing and implementing effective remediation schemes in contaminated soils and groundwaters. Sediment samples from contaminated and uncontaminated portions of a study site in Maine, USA were collected and investigated for adsorption of arsenate [As(V)]. Both the pseudo-first order and the pseudo-second order kinetic models were used to describe the results of the single solute batch adsorption experiments. Piecewise linear regression of data resulted in estimating a cutoff time point (14-19 h) describing the biphasic behavior of solute adsorption. During the rapid adsorption phase an average of 60-80% of total adsorption took place. Both Langmuir and Freundlich isotherms were able to fit the adsorption isotherm data. Langmuir derived maximum adsorption capacity (S_t) of the studied sediments ranged between 28.5 and 97.2 mg/kg. Solid phase content of As in the sediments was found to range from 3.8 to 10 mg/kg. Sequential extractions showed that while the As/Fe ratios are highest in the amorphous phase, majority of the solid phase phosphate exists in this fraction, outcompeting As. High-pH desorption experiments conducted on sediments before and after adsorption experiments showed that greater percentage of adsorbed As is released back into solution from experimentally-loaded sediments than from original samples suggesting that As(V) adsorption takes place on different reversible and irreversible surface sites.

1. Introduction

Consumption of groundwater contaminated with inorganic arsenic (As) is one of the principal pathways for chronic exposure of populations, increasing the risk of cancers as well as other negative health effects (Kapaj et al., 2006).

Mobility of arsenic As in the environment is primarily controlled by adsorption onto solid surfaces including oxides and hydroxides of metals such as iron (Fe) and aluminum (Al), layer silicates and clays, metal carbonates, natural organic matter (NOM). These natural adsorbents have different levels of affinity for As adsorption depending on various factors such as surface properties, aqueous speciation of As, redox condition, pH, and competing ions (Stollenwerk, 2003; Smedley et al., 2002). The mechanism of As adsorption on metal oxides is believed to be through formation of inner-sphere monodentate and bidentate complexes (chemisorption) based on evidence from zeta-potential measurements and spectroscopic data (Manning and Goldberg, 1996; Hiemstra and Riemsdijk, 1999; Goldberg and Johnston, 2001; Sherman and Randall, 2003; Lakshmipathiraj et al., 2006)

Adsorption of trace level contaminants such as As on solid phases have been described by both empirical isotherms and mechanistic surface complexation models (SCM). SCMs predict the adsorption phenomenon by defining complexation reactions between solutes and surface functional groups, and incorporating a description of electrical double layer theory. This covers both the chemical ligand exchange reactions as well as accounting for the attractive/repulsive electrostatic forces dependent on the sorbent surface charges (Antelo et al., 2005).

Commonly used SCM's include the Diffuse Double Layer model (DDLM), the Constant Capacitance model (CCM), the Triple Layer Model (TLM) and Charge Distribution-Multisite Complexation model (CD-MUSIC).

Empirical adsorption isotherms are mathematical equations that relate the concentration of adsorbed species on the solid phase at equilibrium to the concentration of adsorbate in the bulk solution without describing the chemical and electrostatic mechanisms of retention. There have been efforts at applying modified isotherm equations in lieu of using the more complex SCMs (Jeppu et al., 2012) or application of empirical models in transport models (Radu et al., 2008). However, application of empirical models can be challenging due to the uncertainty associated with fitting the experimental data and determination of adjustable parameters. Interpreting the experimental adsorption results on heterogeneous sorbents using these empirical models can particularly be difficult. A great number of studies have focused on use of isotherm equation for describing the adsorption of phosphate on soils and sediments and to a lesser extent on As adsorption.

In this research, adsorption of arsenate, As(V), on nine sediments collected from various locations and depths at a study site in Maine, USA is investigated.

The objectives of this study are: (1) investigate the kinetics of As(V) adsorption on sediments; (2) to use and compare empirical adsorption models for describing the adsorption of As(V) on natural sediments as a function of aqueous concentration; (3) to study the relation between the adsorption capacity of sediments and the solid phase distribution of major elements determined from chemical sequential extractions; and (4) to determine the rates of As(V) desorption from contaminated and un-contaminated sediment.

2. Materials and Methods

2.1. Sediment Samples

Sediments investigated in this study are from a site in Maine, USA with history of contamination with a high pH, PO4 and As plume. The sample locations are categorized by dividing the study

site into three areas: 1) upgradient portion within the plume (impacted upgradient), 2) downgradient portion within the plume (impacted downgradient), and 3) further downgradient beyond the current extent of the plume (Un-impacted). Three sediment samples from different depths at saturated zone of each area were collected in 2014, making a total of nine distinct samples in this study (Table 1). Sediments from locations within the plume have been in contact with groundwater enriched in As (61-604 μg/L). Arsenic levels in groundwater from un-impacted sites are all below 10 μg/L. Previous samplings have shown that arsenate [As(V)] is the predominant species in the oxidizing groundwater at this study site.

The natural pH of sediments were determined by suspending 5g of sediment in 12.5mL of de-ionized water and measuring the suspension pH after 1h of shaking and 0.5h of stabilization. The water and organic content of the sediments were estimated by measuring sequential loss on ignition (105°C for 24h, 440°C for 12h). Surface areas of samples were measured by N_2 and Kr adsorption isotherm using Micromeritics ASAP 2020 instrument by Brunauer–Emmett–Teller (BET) method. Particle size distribution was determined using the USDA (1972) method by drying 50 g of sediment and soaking in a sodium metaphosphate solution overnight followed by hydrometer measurements at standardized time increments.

2.2. Analytical Methods

Sediment samples were stored in sealed zip lock-bags upon collection and shipped in coolers on ice. All sediment and groundwater samples were stored refrigerated (4°C) in dark until use. Sediments were air-dried and <2mm fractions were used in all experiments. All lab-ware and containers were soaked in 1.2N HCl for 24h and rinsed with Milli-Q water five times prior to use. All solutions were prepared using Milli-Q water (18MΩ) purified by NANOpure deionization system. All chemicals used were of laboratory reagent grade (99.99% pure). pH of

solutions were measured using an Acumet Basic AB 15 pH meter, calibrated regularly with standard pH buffer solutions (4, 7, and 10).

Total As concentration in filtered solutions was measured by Graphite Furnace Atomic Absorption Spectrometry (GFAAS) (Perkin Elmer AAnalyst 700) with an electrodeless discharge lamp (EDL). All samples were preserved with 2%v/v HNO_3, refrigerated if not measured immediately, and analyzed in triplicates. 20uL of sample plus 5uL of matrix modifier ($Pd(NO_3)_2$ + $Mg(NO_3)_2$) was used for each measurement. The instrument was calibrated on a daily basis with minimum of five standard solutions (5-100 μg/L) prepared from stock solution obtained from Perkin Elmer. The analyses were conducted in triplicates and the relative standard deviations of measurements were below 5%. All experiments were conducted at least in duplicates with the average value reported and the relative percent difference between the duplicates was less than 15%.

2.3. Batch Kinetic Adsorption Experiments

Commonly used empirical isotherm models such as Langmuir and Freundlich are based on equilibrium assumption, however in natural environments often equilibrium conditions are not achieved. Therefore, understanding the kinetic behavior of As adsorption on natural sediments is important.

Five sediments S-6, S-7B, S-10, S-11, and S-12 were used to study the kinetics of As(V) adsorption at pH 7. In the first round of kinetic experiments, initial As(V) concentrations (C_0) of 0.5, 5, and 10 mg/L were used for S-10, S-6, and S-7B sediments. The electrolyte solution, solid/solution ratio, shaking and sampling methodology were same as those used for isotherm experiments, mentioned above. Samples were collected between 4 and 144 h reaction time.

In the second round, 25 g of un-impacted sediments S-10 and S-11 were added to 250 mL of background solution with three levels of As(V) (0.5, 1, 2.5 mg/L). These initial concentrations are selected to be relevant to contamination situations encountered in the field. Suspensions were sealed and placed on an orbital shaker and 1 mL samples were withdrawn at different time intervals (0.1-216 h) and syringe filtered (0.45 μm) into pre-acidified (2% HNO_3) vials. The volume of the suspensions were kept constant throughout the course of the experiment.

2.4. Batch Adsorption Isotherm Experiments

Single solute adsorption experiments were conducted in duplicates by equilibrating 3g of sediment samples with background electrolyte solutions (0.1M NaCl, 5mM HEPES) in polypropylene centrifuge tubes using a 1g:10mL solid/solution ratio. Sodium arsenate dibasic heptahydrate ($Na_2HAsO_4.7H_2O$, Sigma-Aldrich, ACS reagent grade) was used to prepare stock solutions (1000 ppm) and the serial dilutions needed to achieve the total concentration desired in the experiments. Initial concentrations (C_0) used in the experiments were 0.05, 0.1, 0.5, 1, 2.5, 5, 10, 15, and 30 mg/L.

pH of the suspensions were adjusted prior to addition of As(V) and maintained at 7 throughout the experiment by addition of 0.1N HCl or 0.1N NaOH. Preliminary kinetic tests showed that a mixing time of 7 days is needed to reach equilibrium. The suspensions were placed on rotary shakers in room temperature (25°C) for the course of the experiment. At the end of the 7-day experiment, The sediments were separated from solutions by centrifuging the suspensions at 7800 rpm for 15 minutes and supernatants were syringe filtered through 0.45 μm disposable MCE filters (EMD Millipore). The samples were acidified with HNO3 (2%) for preservation and refrigerated until analysis.

It is worth noting that the methodology and details used for conducting adsorption experiments are critical for interpreting and comparing the data. A search in the published literature shows that there is a wide variety of experimental details among adsorption studies. These experimental details include: reaction time, gas composition, method of pH control, background electrolyte composition and concentration, solid/solution ratio, and method of mixing.

Maintaining the pH of sediment suspension at the target level throughout the adsorption experiment is of high importance since the adsorption phenomenon is pH dependent. Due to the heterogeneity of sediment grains and presence of carbonate minerals such as calcite in the solid matrix and significant buffering, this task becomes more challenging when conducting experiments on natural samples. In preliminary experiments few methods such as use of chemical buffers and maintaining a constant gas pressure were tested. The method selected for the adsorption experiments in this study was to use 5mM of HEPES buffer in the electrolyte solution. The electrolyte solution was added to the sediment and the pH of the suspension was adjusted after 1h and again after 12 h of shaking time and prior to addition of As(V). Kanematsu et al. (2011 and 2013) have used 1mM of HEPES in conducting As(V) adsorption isotherm experiments and have demonstrated that HEPES buffer does not affect the data even at low concentrations.

2.5. Sequential Extraction and Desorption Experiments

Three chemical extraction steps were conducted on the sediments sequentially in order to characterize the solid distribution of As and other major elements. The amorphous Fe oxides were extracted by hydoxylamine-hydrochloride for 0.5 h (0.25 M NH_2OH. HC1 in 0.25 M HC1 at 50° C) followed by a 72-h hydoxylamine extraction targeting the more crystalline Fe phases.

The last step was the hot acid total digestion (EPA 3050B). The extracted solutions were analyzed for Al, As, Ca, Fe, and P by ICP-MS.

Desorption experiments were carried out on all nine fresh sediment samples as well as on selected sediments following the completion of adsoprtion isotherm experiments. In order to induce high-pH desorption, sediments were equilibrated with $1.44x10^{-2}$ M $NaHCO_3$ / $2.8x10^{-3}$ M Na_2CO_3 (pH 9.5) for 7 days using the 1:10 ratio.

3. Results

3.1. Arsenic Adsorption Kinetics

Amount of As(V) remaining in solution versus time for different initial concentrations and sediments studied is displayed in Figures 1. Results of the preliminary experiments on S-6, S-7B and S-10 sediments indicate that 144 h is a sufficient equilibrating time to conduct the adsorption experiments on sediments.

Results for un-impacted S-11 and S-12 show a rapid initial adsorption within the first 12 h followed by a more gradual rate afterwards until equilibrium condition reached at 216 h. The gradually slower adsorption observed over time is related to the decrease in the difference between the concentration in solution and surface (Banerjee et al., 2008).

Both sediment demonstrated similar overall patterns however Site 11 exhibits an average of 12 to 22% higher adsorption rate over the course of the experiment. This finding is consistent with the higher maximum sorption capacity determined for S-11 from isotherm experiment results which will be presented in following sections.

The equilibrium adsorption rates decrease with increasing initial aqueous phase As concentration. In case of S-11, maximum adsorption achieved at the three initial As(V) levels of 0.5, 1, and 2.5 mg/L , were 96%, 93%, and 80% respectively. Sediment S-12 achieved smaller equilibrium adsorption rates of 89%, 77% and 54% at the three levels used.

Percentage of the total As(V) adsorption achieved in the first 12 h was 80%, 70%, and 64% for S-11 and 67%, 63%, and 60% for S-12 indicating a decreasing trend with increasing initial concentration. The percentages of total adsorption that occurred after 48h were 6%, 12%, 19% for S-11 and 14%, 17%, 18% for S-12. These result indicate that the As(V) adsorption kinetics become slower with increasing the concentrations in solution and therefore the adequate reaction time needed for reaching equilibrium state in such studies is an important factor at higher initial concentrations.

There are several kinetic models which have been commonly implemented in the literature for fitting adsorption data (Ho and Mckay, 1998; Zhang and Selim 2005; Banerjee et al., 2008; Maji et al., 2008; Oke et al., 2008; Guo et al., 2010; Neupane et al., 2014). These models will be presented below and compared for fitting the data for S-11 and S-12 sediments.

3.1.1. Pseudo-first order k

The pseudo-first order kinetic model has been used in two forms based on the aqueous concentration (Banerjee et al., 2008), and based on the solid sorption capacity (Maji et al., 2008). These two forms are briefly described below and applied to the results.

In the aqueous based model, the adsorption reaction can be hypothesized as

$$C_{aq} + S \xrightarrow{K_{ads}} S - C_s$$

where C_{aq} stands for concentration of adsorbate in solution (eg. As_{aq}), S represents a generic surface site, and S-C_s is the cocnetration of adsorbed species. Given the fact that the concentration of adsorbent is orders of magnitude greater than the solute and remain unchanged, the pseudo-first order reaction can be expressed as

$$\frac{dC_t}{dt} = -K_1' C_t$$

where C_t is the aqueous concentration at time t and K'_1 is the pseudo-first order rate constant (h^{-1}). Integrating and applying the boundary conditions at t=0 and t=t results in the form

$$\ln\left[\frac{C_t}{C_0}\right] = -K_1' t$$

where C_0 is the initial solute concentration at t=0. The model can be fitted using plot of $\ln[C_t/C_0]$ versus time and linear regression. Analysis of the results (Figure 2) indicate that two distinct slopes are present and therefore a piecewise linear regression method was applied to fit the results and determining the cutoff time point where the slope change occurs. The piecewise linear regression method provides good correlation coefficients (R^2>0.98) fitting the data for S-11 and S-12 sediments at the three C_0 levels studied. The average cutoff time point (t_c) is 18.4h for S-11 and 16.6h for S-12. The t_c parameter and the two slopes (kinetic rate constants) derived are presented in Table 2. It can be seen that the rate constants after t_c are one order of magnitude smaller than the rate constants before t_c illustrating the transition from the initially fast kinetic adsorption to the slower and gradual .

The second form of pseudo-first order model based on Lagergren equation and considering the adsorbed concentrations is written as

$$\frac{dq_t}{dt} = K_1'(q_e - q_t)$$

where q_t and q_e are the adsorbed concentration (mg kg^{-1}) at time t and at equilibrium (ie. adsorption capacity). After integrating and applying boundary conditions the equation becomes

$$\ln[q_e - q_t] = \ln[q_e] - K_1' t$$

Therefore a linear plot of $\ln[q_e-q_t]$ versus time would indicate a good fit for this model. However as indicated by others (Ho and Mckay, 1998), this model in most cases does not fit the data well

over the entire range of contact time. In addition, the main disadvantage of this model is that it depends on adsorption capacity ($q_{e)}$ to be known which in most cases is not effectively known and this subsequently introduces uncertainty to the model. In order to fit to data, one needs to either assume or determine the value of equilibrium sorption capacity (q_e) which could become problematic in some cases.

This model was applied to the data in this study using the equilibrium adsorption capacity at the final time point, however both linear and piecewise linear regressions provide poor fits (R^2<0.94)

3.1.2. Pseudo-second order equation

The pseudo-second order equation does not have the disadvantage mentioned for Lagergren equation and could be used to determine the parameters without prior knowledge of sorption capacity required (Ho et al., 2006).

Number of studies have used the pseudo-second order reaction model (Jang et al., 2003; Ho and Ofomaja, 2006; Oke et al., 2008; Guo et al., 2010) to fit adsorption kinetic data. The kinetic rate equation is expressed as

$$\frac{dq_t}{dt} = K_2'(q_e - q_t)^2$$

where $K_2^{'}$ is the rate constant of pseudo-second order adsorption (kg mg-1 h-1) .Applying boundary conditions t = 0 to t = t and $q_t = 0$ to $q_t = q_e$, the integrated and rearranged equation can be written as

$$\frac{t}{q_t} = \frac{1}{q_e}t + \frac{1}{K_2'q_e^2}$$

Therefore, a linear plot of t/q_t versus time would indicate that data follows this kinetic model. Figure 3 shows that fitting the pseudo-second order provides high correlation coefficients (R^2>0.99) in all cases indicating excellent fits to the experimental data.

Term $K_2' q_e^2$ can be regarded as the initial adsorption rate, h (mg kg^{-1} h^{-1}) as $t \rightarrow 0$. Table 3 lists the parameters derived from the pseudo-second order kinetic model. The values of K_2' for As(V) adsorption ranged between 0.07 and 0.006 kg/mg.h at Site 11 and between 0.04 and 0.01 kg/mg.h at Site 12 decreasing with increase of C_0.

3.2. Adsorption Isotherms

The most commonly used adsorption isotherms are the Langmuir and Freundlich equations. The Langmuir equation has a rational basis which and is based on these assumptions: only a monolayer surface coverage is considered, adsorption takes place at independent site, and adsorption sites are equivalent.

The advantage of the Langmuir isotherm over the Freundlich isotherm is the ability to derive a maximum sorption capacity parameter which makes it more appealing for application in soils and sediments adsorption studies. However, the premise of a homogenous adsorbent surface, essential to the Langmuir isotherm, is not a valid assumption for heterogeneous materials such as soils and sediments. On the other hand, the Freundlich model allows for multi-layer adsorption and includes an empirical parameter (n) that accounts for heterogeneity of surface sites with different adsorption energies.

Here, we present the application of these commonly used isotherm equations to model the adsorption data.

3.2.1. Freundlich Isotherm

Freundlich isotherm is one the most commonly empirical models used to fit adsorption data (Lin and Wu, 2001; Badruzzaman et al., 2004; Zhang and Selim, 2006; Boddu et al., 2008) and is expressed as

$$S = K\,C^{n}$$

where K is the Freundlich constant, C and S stand for equilibrium solution (mg L^{-1}) and sorbed (mg kg^{-1}) concentrations. n is a dimensionless parameter representing heterogeneity of the sorption sites. This parameter is usually less than one and accounts for the different adsorption sites. At n=1, the Freundlich equation becomes a linear adsorption model and K is the partition coefficient. The Freundlich equation is generally linearized in order to fit data as follows

$$\log S = n \log C + \log K$$

The adsorption experimental data were fitted with the Freundlich isotherm equation (Figure 4) and the adjusted parameters are presented in Table 4. The generally good fits to the Freundlich isotherm, however, indicate that multiple surface site types are involved in the adsorption reactions. A positive correlation (R^2=0.62) between the derived Freundlich constant and the amorphous Fe content was found.

3.2.2. Langmuir Isotherm

Parameters derived from the Lanmuir equation describe the adsorption affinity (K, L mg^{-1}) and maximum sorption capacity (S_t, mg kg^{-1}).

$$S = S_t \frac{KC}{1 + KC}$$

Conventionally, the Langmuir equation is transformed to a linear form and fitted to the data. There are four distinct methods for linearization of the Langmuir equation (Bolster and Hornberger, 2008). For comparison reasons, all four methods were applied to the data in this study, however none of them provided reasonable fits. As shown by Bolster and Hornberger (2008), linearized forms of the Langmuir equation needlessly limit modeling of adsorption data and therefore their use in soil and sediment studies should be pursued with caution. These

limitations include sensitivity to variability in low levels of S, clumping of data points, overestimation and underestimation of correlation between the transformed linearized variables.

A factor of importance in determining the adsorption maxima by using the Langmuir isotherm is the dependence of determination on the highest experimental values fitted. Lack of an explicit plateau indicating the saturation of surface sites as the solute concentration increases is a common phenomenon in adsorption studies. In this study, two Langmuir fits were obtained with and without the result from the highest initial As(V) concentration (C_0 = 30 mg/L). The resulting fits were compared based on goodness of fit and the percentage increase in the adsorption capacity to determine the best fit to data (Figure 5).

In the case of impacted upstream sites (S-5, S-6, and S-13), by including the highest data point, either the goodness of fit was lowered (R^2<0.9) or the Langmuir model did not fit the data at all. Table 5 lists the parameters derived from both fits and highlights the maximum capacity values accepted.

3.3. Desorption Experiments

Preliminary desorption kinetic experiments on selected sediments from the three major areas of the site showed that similar to adsorption experiments, a minimum equilibrating time of 7 days is needed to reach steady sate in dissolved concentrations of As(V). These experiments were conducted with and without addition of 5mg/L PO_4-P. As expected, presence of PO_4 increased the desorption rates between 13 to 43% (Figure 6).

Desorption experiments conducted on the sediments (S-9, S-10, S-11, and S-13) after the conclusion of isotherm experiments showed that an average of 48 % of the adsorbed As(v) is released back into the solution from the solid phase across the spiked concentration levels. This is in contrast with the significantly smaller rates desorbed from the original sediments as shown

in Table 6. The difference in desorption rates between fresh and spiked sediments could be attributed to the role of different surface sites involved in reversible and irreversible adsorption reactions.

3.4. Sequential Extractions

Percentages of solid phase distribution of Al, As, Ca, Fe and P for the nine studied sediments are presented in Figure 7.

Amorphous and crystalline extractions account for 19 to 36% of the total Fe content. Majority of P extracted from sediments was associated with the amorphous phase and crystalline fraction only represented 3 to 10% of the solid P content.

None of the sediments studied exhibit levels of As greater than the global average concentration of 1-10 mg/kg. This indicates that the due to the inhibiting geochemical factors such as the high pH and significant phosphate competition present at this site, adsorption of As(V) mobilized into the groundwater by the sediments is likely small.

The As/Fe and P/Fe molar ratios for the three extracted fractions are compared in Figure 8. It can be seen that the density of As in the amorphous fraction is generally higher than the crystalline and recalcitrant fractions. This is explained by the known high affinity of amorphous phases for adsorption and accumulation of As and other contaminants. Similar trend is observed for phosphate with significantly P/Fe ratio in the amorphous fraction which is evident by the majority of total solid phase P present in that fraction . Comparison with As/Fe ratios indicate that phosphate is adsorbed or associated with the amorphous phase at a much higher density than As and therefore outcompeting As.

4. Discussion

4.1. Effect of Time

The pseudo-first order kinetic models indicate that adsorption of As(V) on sediments takes place under two distinct phases, initially the reactive sites are occupied with a fast rate and then a more gradual adsorption continues until an equilibrium is reached at about 7 days.

The reaction times used in adsorption studies vary widely (Limousin et al., 2007). Great number of studies have investigated the adsorption of As species on variety of solids such as synthesized and natural pure minerals, synthetic or mineral based adsorbent materials for application in water treatment, and natural soil and sediment samples.

Manning and Goldberg (1996) used 4h reaction time for adsorption of As(V) on pure oxide minerals. Dixit and Hering (2003) used 4-24 h for adsorption of As(III) and As(V) on synthetic HFO, goethite and magnetite. Gimenez et al. (2007) showed that equilibrium for adsorption of As(III) and As(V) on natural iron oxides is reached in less than 2 days. For batch experiments with synthetic iron oxides, Bauer and Blodau (2006) equilibrated As(III) and As(V) solutions for 24 h. Badruzzaman et al. (2004) agitated As(V) and granular ferric hydroxides for 18 days. Kanel et al. (2005) used 12 h reaction time for studying As(III) adsorption on zero-valent iron. Kundu et al. (2004) selected 8 h shaking time for removal of As with hardened Portland cement. Dadwhal et al. (2011) confirmed a 5-day reaction time to be sufficient for reaching equilibrium for adsorption of As(V) on layered double hydroxide adsorbent.

Zhang and Selim (2005) performed batch isotherm experiments on soils for 24 h. Manning and Goldberg (1997) studied As(III) and As(V) adsorption on three soil types by equilibrating the suspensions for 16 h, citing Pierce and Moore (1982) that showed 99% of adsorption taking place within 4 h. Goldberg and Suarez (2013) used 2h of reaction time for studying As(V) adsorption on alluvial sediments. Stollebwerk et al. (2007) conducted batch experiments and

determined that As adsorption on collected oxidized sediments from Bangladesh reaches equilibrium in 2 days. For their batch As(V) adsorption isotherm experiments, Robinson et al. (2011) equilibrated the sediment and solution mixtures for 14 days. Borgnino et al. (2011) reported adsorption of As(V) on clastic sediments reaching equilibrium after 140 h (6 days) Kinetic results in this study show that although a significant amount of total adsorption occurs within the initial 14-19 hours of reaction, the gradual increase in the adsorbed concentration between 48 h and final equilibrium is noticeable (6-19%).

4.2. Effect of Chemical and Physical Properties

Strong positive correlations between As adsorption and Fe, Al, and clay content of soils have been reported (Smedley and Kinniburgh, 2002).

In order to investigate any relations between the chemical and physical characteristics of the sediments and the adsorption capacity values derived from the Langmuir models, univariate linear regression analyses were carried out. The factors studied were sediments particle size distribution, natural pH, Surface area measurement (BET), concentration of dissolved As(V) at each sample site, solid phase distribution of Al, As, Ca, Fe and P. No statistically significant relation among all sediments studied was found. Adsorption capacity increases with distance towards downstream and the un-impacted sediments have the highest Langmuir S_t.

General relationships between the adsorption capacity of sediments and parameters such as amorphous Al and Fe oxide content, and BET surface area exist among the downstream and un-impacted sites (Figure 9). However these factors do not adequately describe the variation of adsorption capacity values across all sites.

These results indicate that predicting the adsorption capacity of heterogamous phases such as sediments may not be solely possible based on general chemical and physical characteristics, and might require incorporation of additional mineralogical data and spectroscopic studies.

4.3. Rates of Desorption

Comparison between the rates of desorption from fresh sediments and sediments spiked with As(V) indicate that the majority of solid phase As is present in non-reactive sites further suggesting that the attenuation of mobile As in the plume by the sediments have been relatively insignificant. The desorption experiments were conducted 7 days after the conclusion of adsorption experiments. Studies have shown that the adsorbed species diffuse into the solid matrix of sorbent phases over time. Only a weak correlation (R^2= 0.55) between the amount of As desorbed from sediments and solid phases associated with the amorphous Fe oxides exists.

4.4. Adsorption Isotherms

Arsenate adsorption on environmental surfaces is more favorable in the pH range 4 to 7 (Dixit and Hering, 2003) and tends to be limited at higher pH values due to increased repulsive forces between the negatively charged As oxyanion species and the predominantly negatively charged solid particles. Several studies on soils and sediments have shown adsorption maxima near pH 7 (Stollenwerk et al., 2003), therefore the adsorption experiments in this study were conducted at pH 7 in order to obtain estimations for the maximum sorption capacities.

The maximum sorption capacity is the most important finding from isotherm experiments that can be potentially incorporated in the surface complexation and reactive transport models. In this context, Langmuir isotherm is therefore preferred over the Freundlich equation as it includes the S_t fitting parameter.

One difficulty in conducting the adsorption isotherm experiments and interpreting the data with a model such as Langmuir is making an appropriate distinction between the monolayer adsorption capacity of the sediments and multilayer retention resulted from surface precipitation occurring at higher concentrations of adsorbate. Results of this study show that the Langmuir equation is very sensitive to the highest C_0 used in the experiments as this parameter often controls the value derived for S_t. Therefore it is important to have a basis for selecting the range of aqueous concentrations to be studied in an adsorption in order to avoid possible overestimation or underestimation of adsorption capacities.

There have been several modifications to the Langmuir equation to account for the effects of pH, competition for sorption sites, pre-adsorbed solutes and heterogeneity of sorbent phases (Jeppu et al., 2012; Zhou et al., 2005; Bradl, 2004; Rau et al., 2003; Turiel et al., 2003). The Langmuir-Freundlich isotherm includes an index of heterogeneity (n) that can vary from 0 to 1 depending on the heterogeneity of the sorbent medium. However, the Langmuir-Freundlich equation is too flexible and different sets of fitting parameters (St, K, n) can describe the experimental data.

5. Conclusions

The pseudo-first order equation is not capable of fitting the data over the entire range as indicated by other studies as well (Guo et al., 2010; Banerjee et al., 2008; Oke et al., 2008), however, piecewise linear regression was applied to fit the plots of ln $[C/C_0]$ versus time in order to estimate the first order reaction rate (K_1) for two distinct stages of reaction and describe the biphasic behavior of solute adsorption. Pseudo-second order kinetic model was capable of providing the most accurate fit to experimental data in this study without requiring a pre-determined equilibrium adsorption maximum.

The highest level of adsorption takes place at Site 10 with S_t value of 97 mg/kg which is located in the un-impacted zone of the study site. Only poor correlations exist between the observed maximum sorption capacity and sediment chemical compositions such as Fe and Al content or physical properties such as BET surface area. Sensitivity of the Langmuir model fits with respect to the highest concentration values was evaluated

The lower rates of desorption from fresh sediments than the sediments loaded with As(V) indicate that the existing solid phase As on the sediments are mostly associated with non-reactive or irreversible surface sites as opposed to freshly adsorbed As occupying more reactive sites.

Figures

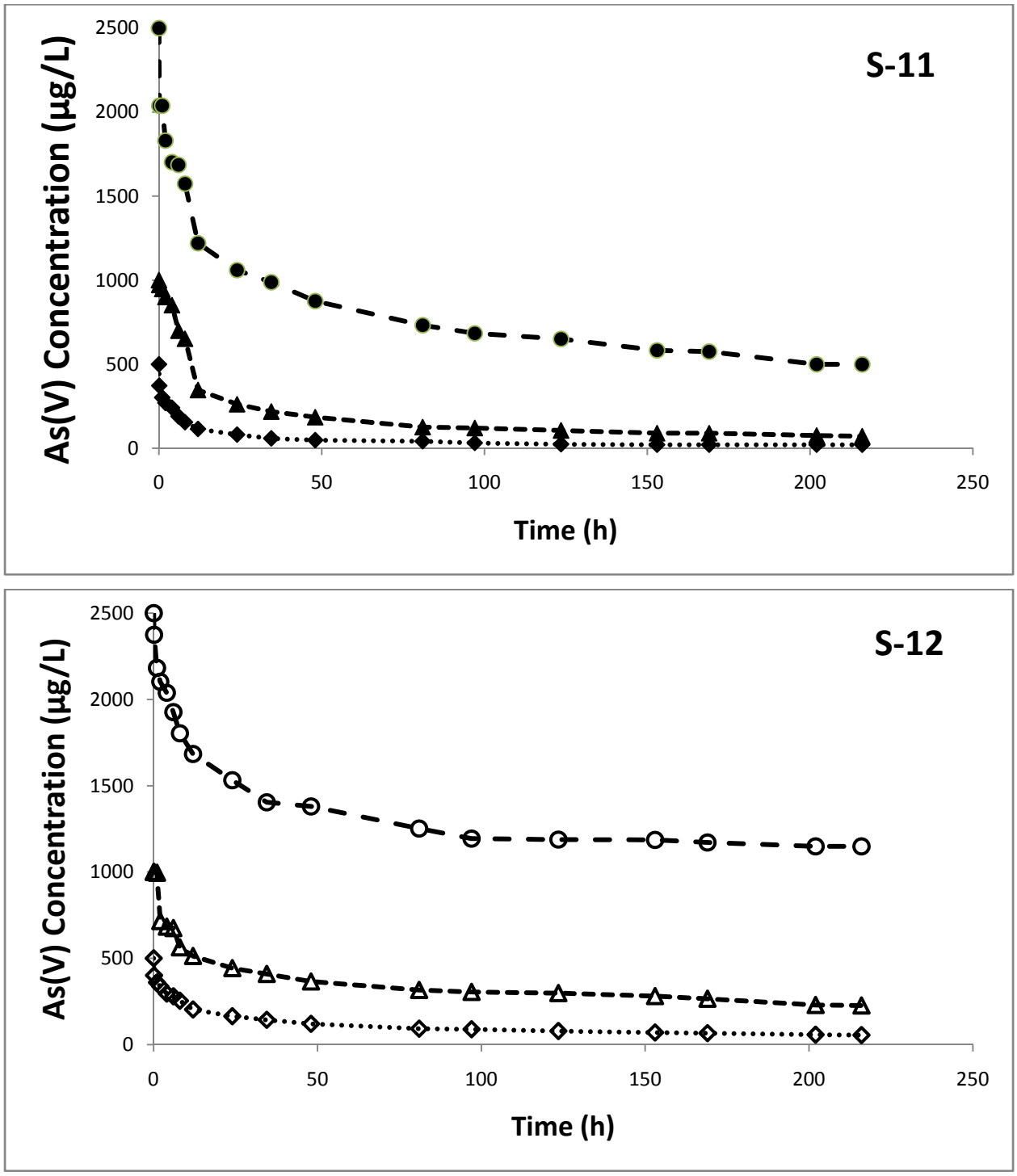

Figure 1. As(V) concentration remaining in solution versus time for S-11 and S-12 with different initial concentrations (C_0) of 0.5, 1, and 2.5 mg/L

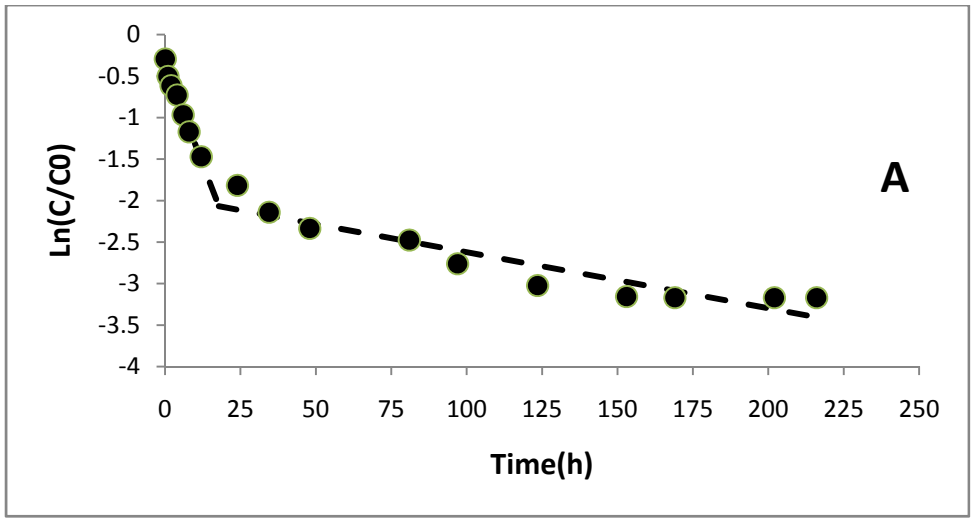
Ln(C/C0)
0
-0.5
-1
-1.5
-2
-2.5
-3
-3.5
-4
0
25
50
75
100
125
150
175
200
225
250
Time(h)
A

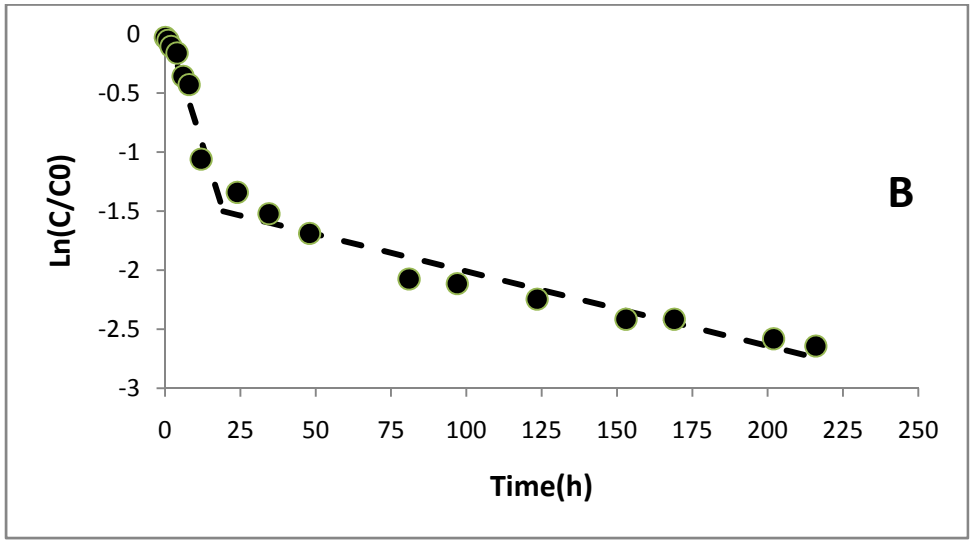
Ln(C/C0)
0
-0.5
-1
-1.5
-2
-2.5
-3
0
25
50
75
100
125
150
175
200
225
250
Time(h)
B

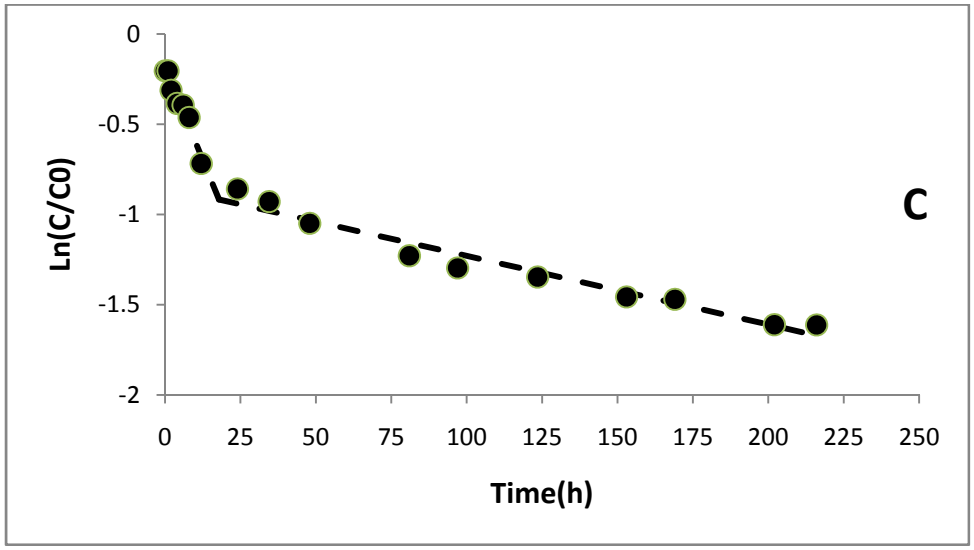
Ln(C/C0)
0
-0.5
-1
-1.5
-2
0
25
50
75
100
125
150
175
200
225
250
Time(h)
C

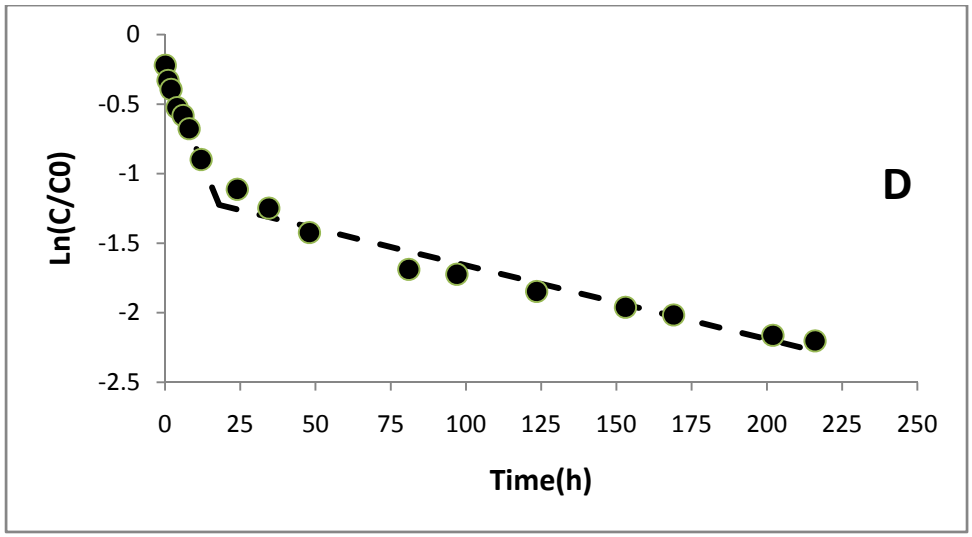
0
-0.5
-1
-1.5
-2
-2.5
Ln(C/C0)
0
25
50
75
100
125
150
175
200
225
250
Time(h)
D

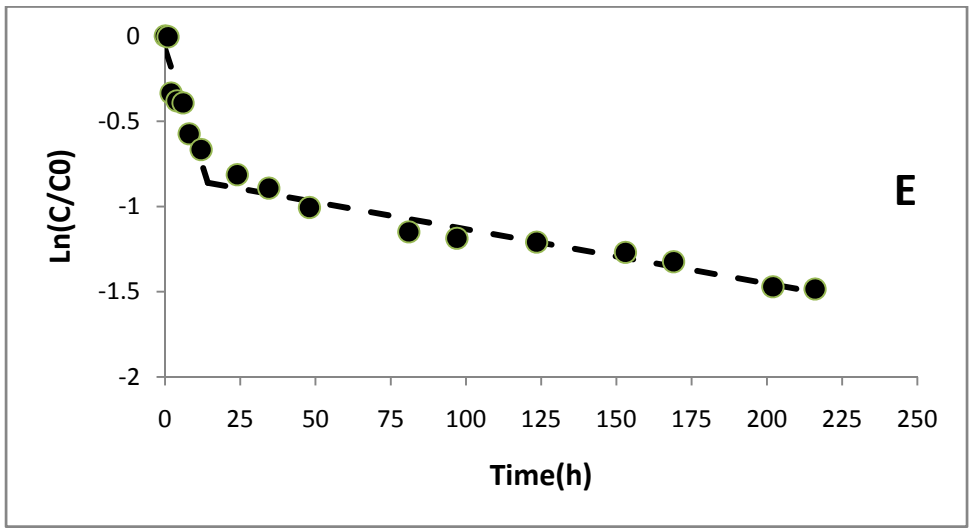
0
-0.5
-1
-1.5
-2
Ln(C/C0)
0
25
50
75
100
125
150
175
200
225
250
Time(h)
E

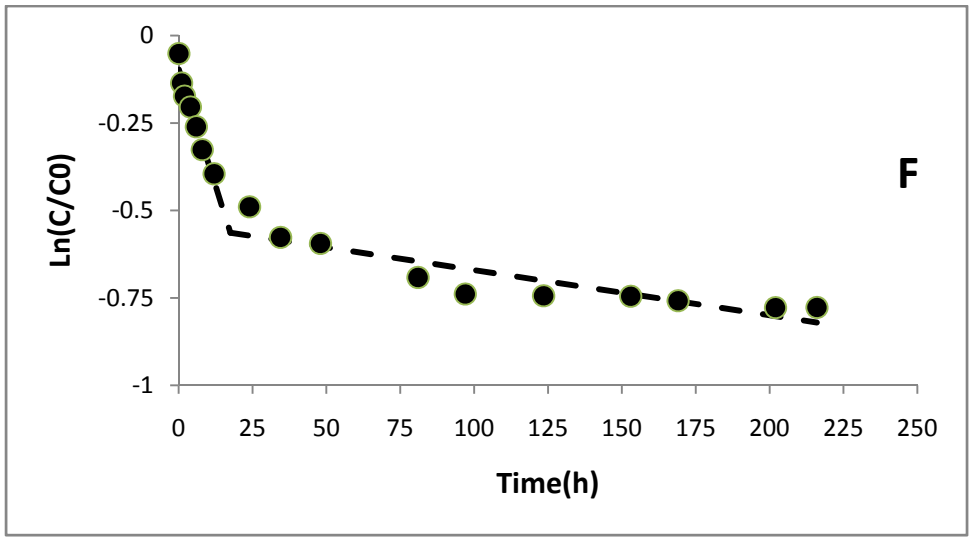
0
-0.25
-0.5
-0.75
-1
Ln(C/C0)
0
25
50
75
100
125
150
175
200
225
250
Time(h)
F

Figure 2. Plots of Ln(C/C0) versus time for S-11 with (A) C_0=0.5 mg/L, (B) C_0= 1 mg/L , (C) C_0=2.5 mg/L, and for S-12 with (D) C_0= 0.5 mg/L, (E) C_0=1 mg/L , (F) C_0=2.5 mg/L. Dashed lines represent piecewise linear regression fits.

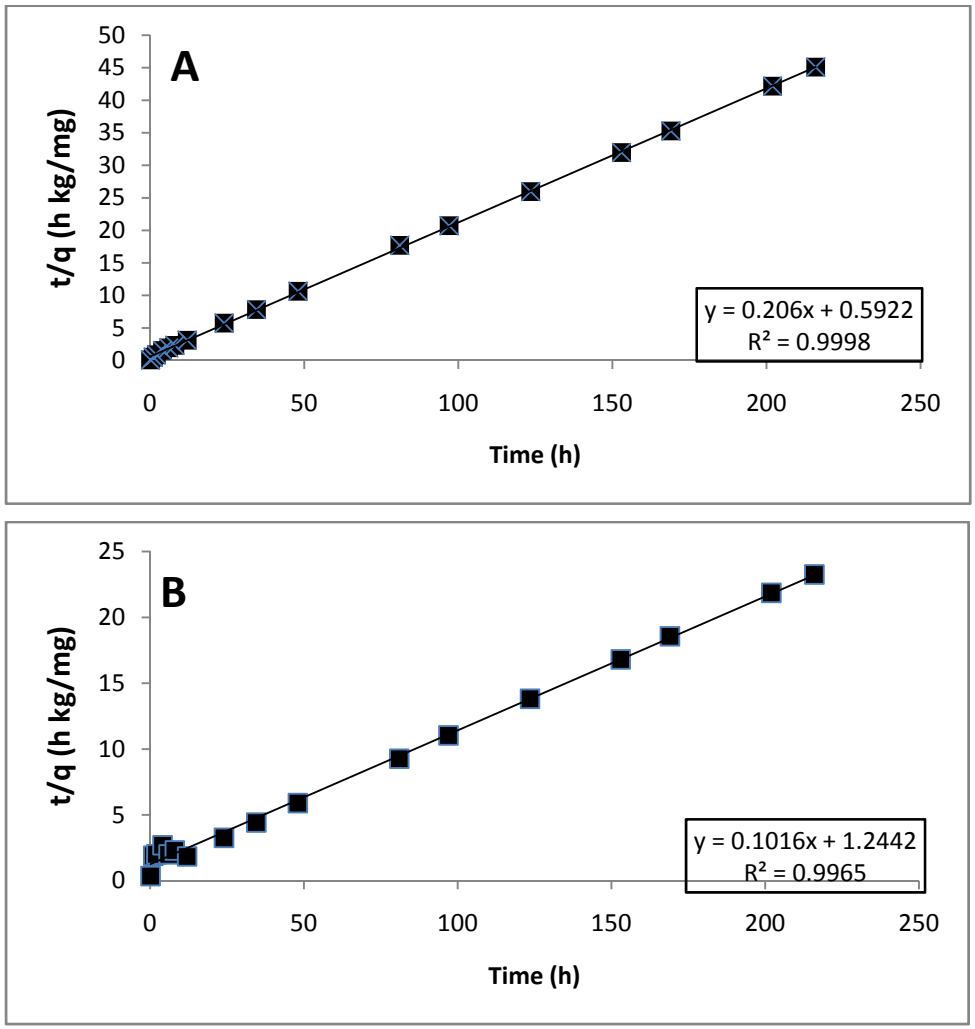

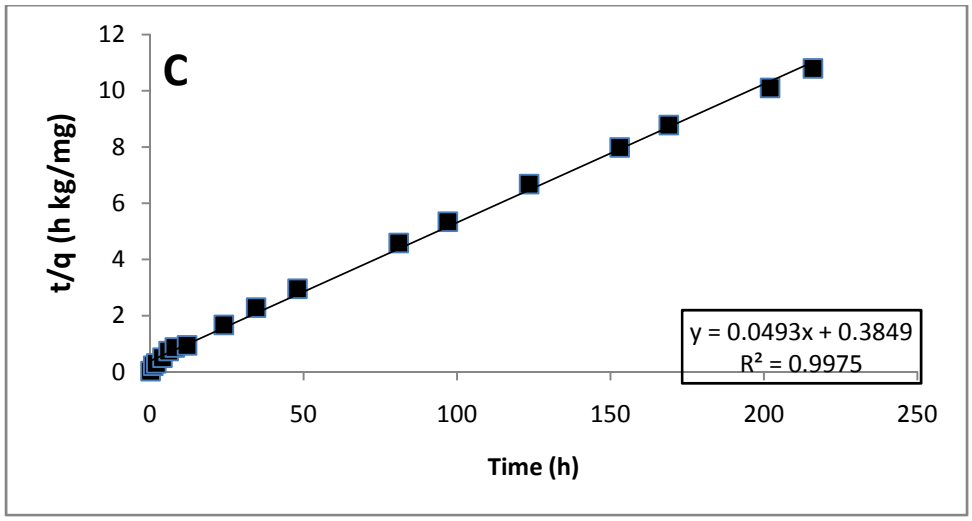
C
t/q (h kg/mg)
Time (h)
y = 0.0493x + 0.3849
R² = 0.9975
0
2
4
6
8
10
12
0
50
100
150
200
250

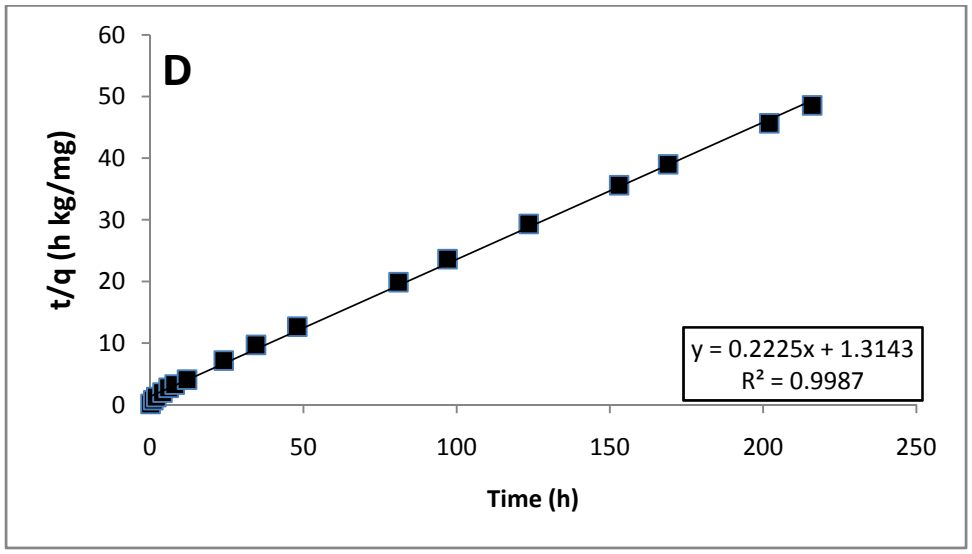
D
t/q (h kg/mg)
Time (h)
y = 0.2225x + 1.3143
R² = 0.9987
0
10
20
30
40
50
60
0
50
100
150
200
250

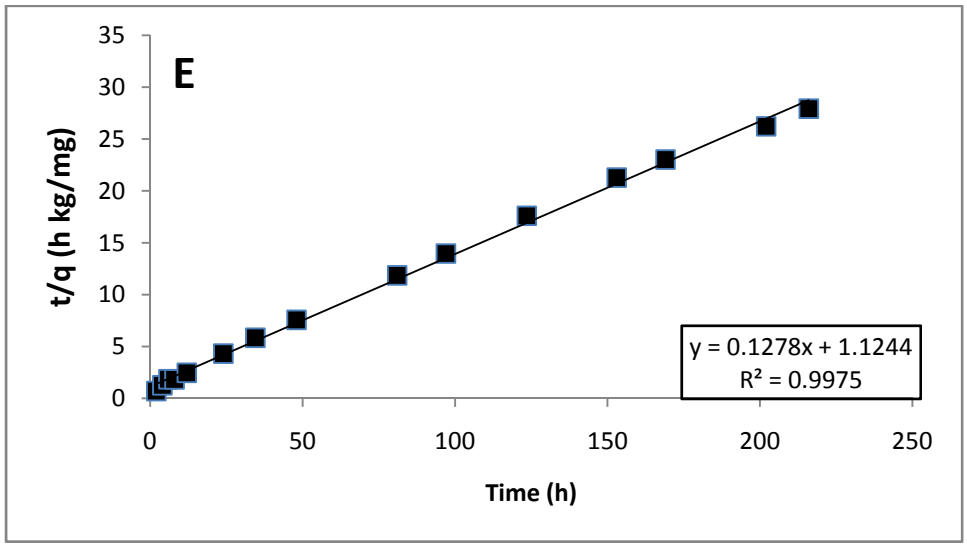
E
t/q (h kg/mg)
Time (h)
y = 0.1278x + 1.1244
R² = 0.9975
0
5
10
15
20
25
30
35
0
50
100
150
200
250

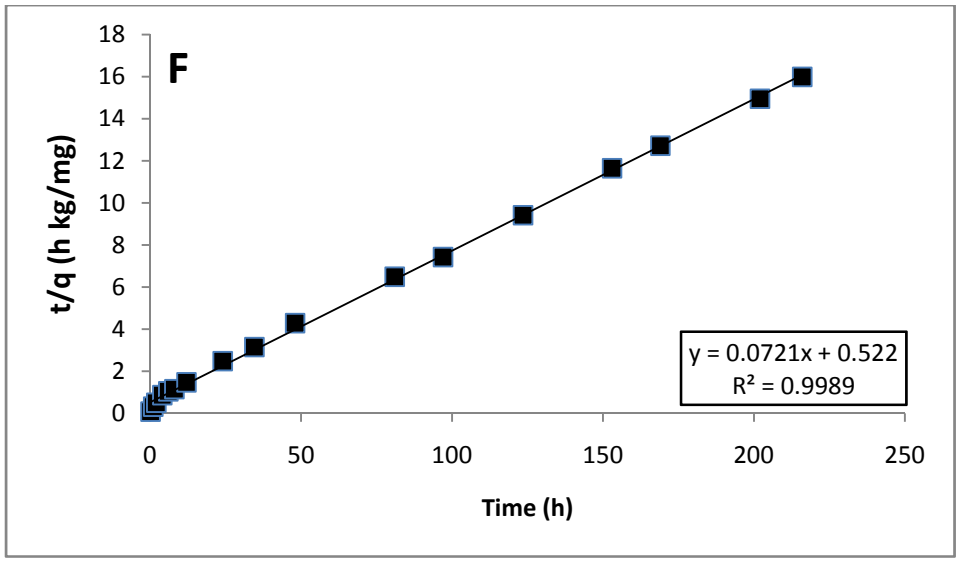

Figure 3. Plots of t/q versus time for S-11 with (A) C_0=0.5 mg/L, (B) C_0= 1 mg/L , (C) C_0=2.5 mg/L, and for S-12 with (D) C_0= 0.5 mg/L, (E) C_0=1 mg/L , (F) C_0=2.5 mg/L. Lines represent linear regression fits.

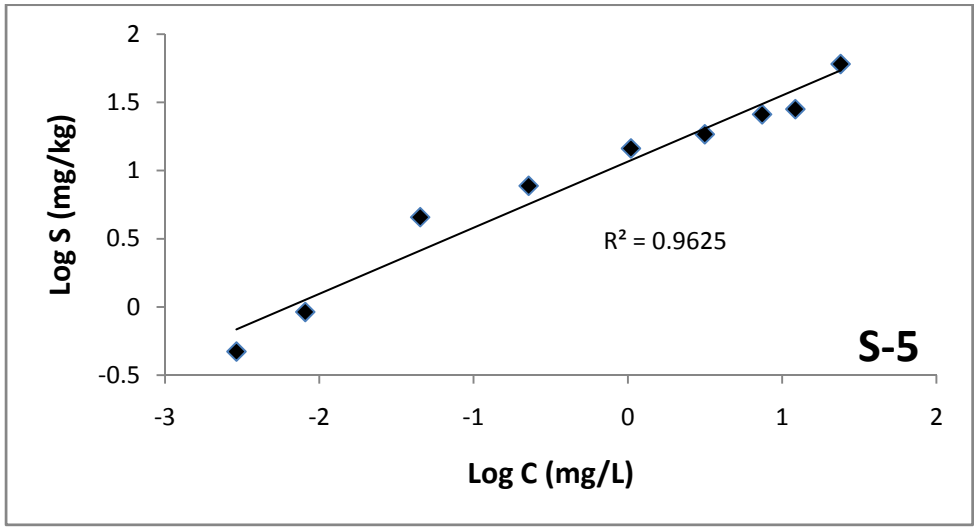

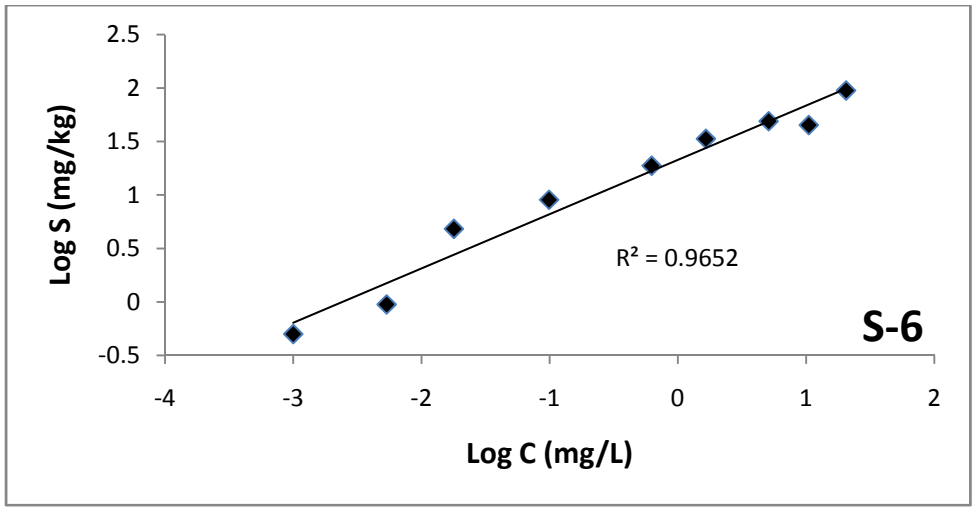
Log S (mg/kg)
Log C (mg/L)
R² = 0.9652
S-6

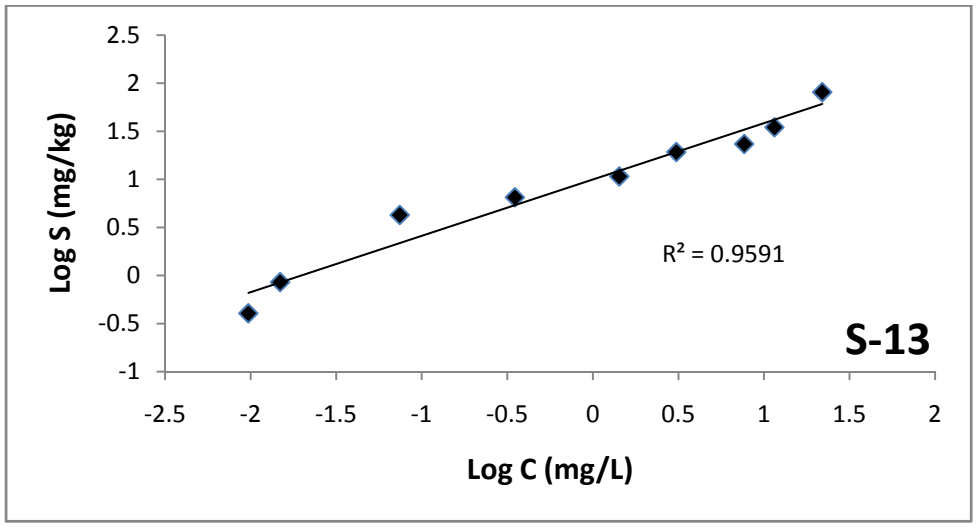
Log S (mg/kg)
Log C (mg/L)
R² = 0.9591
S-13

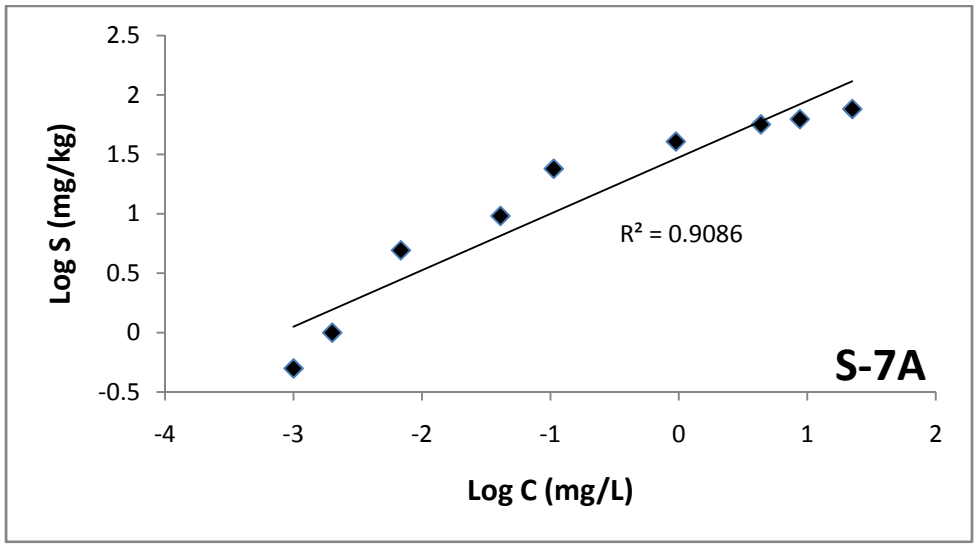
Log S (mg/kg)
Log C (mg/L)
R² = 0.9086
S-7A

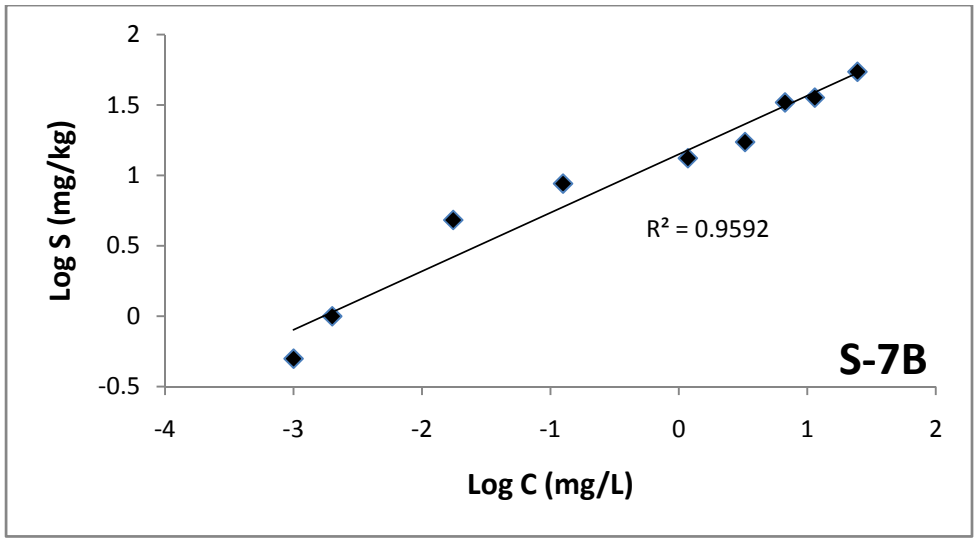
Log S (mg/kg)
2
1.5
1
0.5
0
-0.5
-4
-3
-2
-1
0
1
2
Log C (mg/L)
R² = 0.9592
S-7B

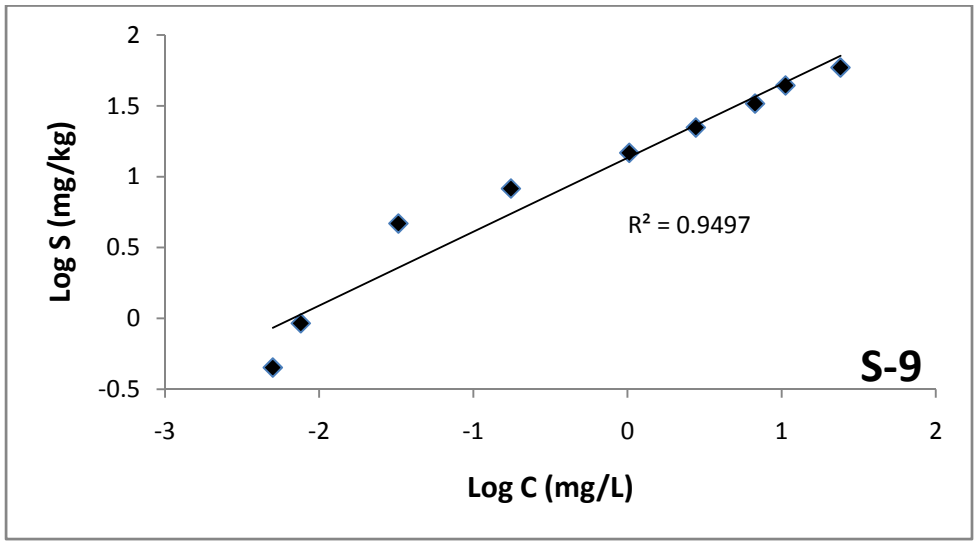
Log S (mg/kg)
2
1.5
1
0.5
0
-0.5
-3
-2
-1
0
1
2
Log C (mg/L)
R² = 0.9497
S-9

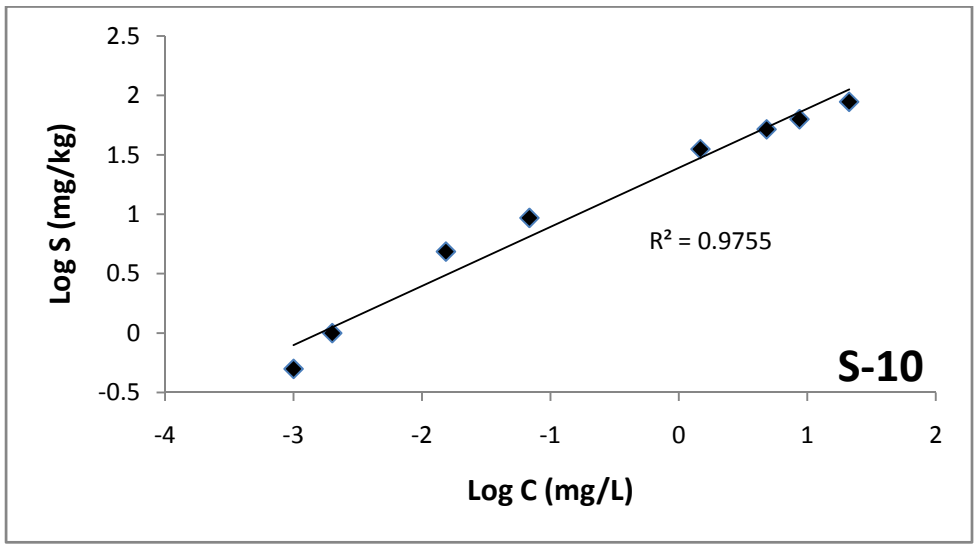
Log S (mg/kg)
2.5
2
1.5
1
0.5
0
-0.5
-4
-3
-2
-1
0
1
2
Log C (mg/L)
R² = 0.9755
S-10

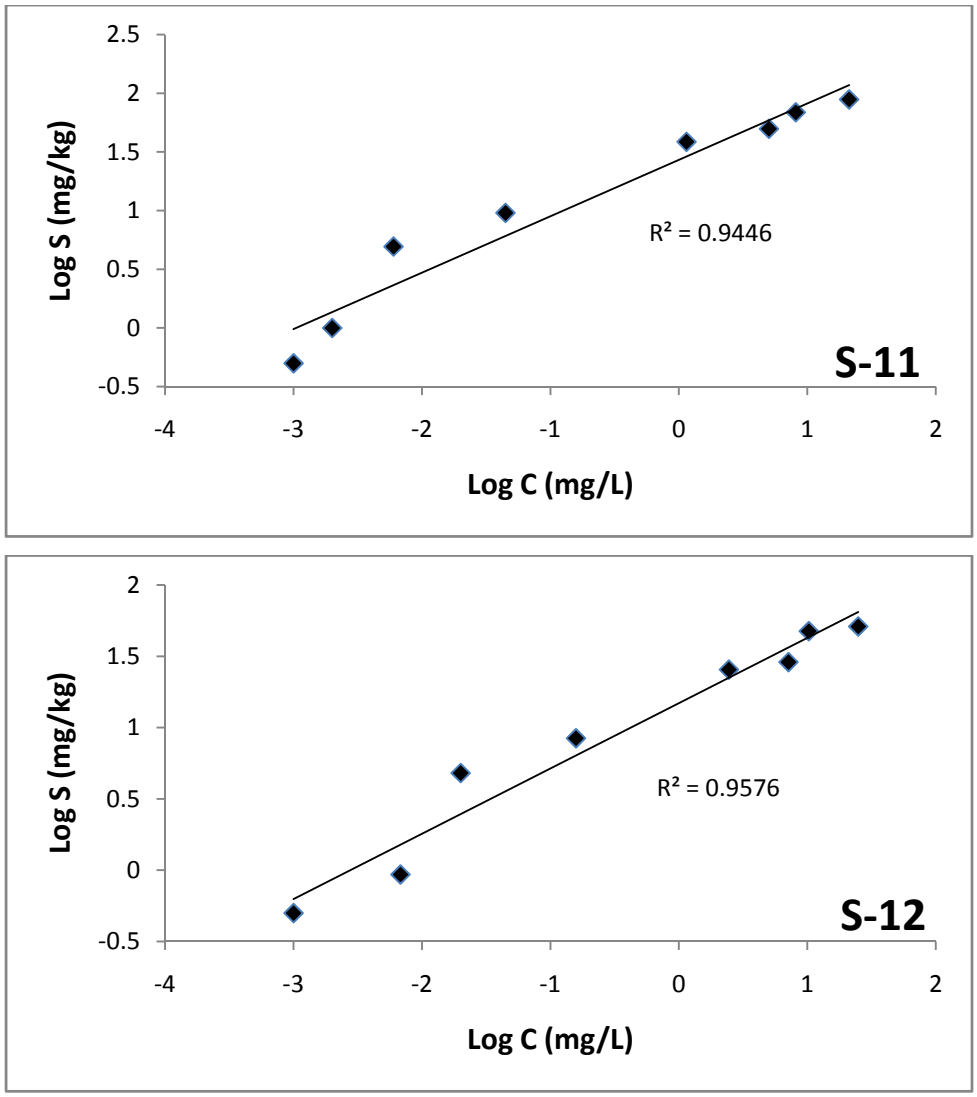

Figure 4. Plots of Freundlich isotherm model fits to adsorption data.

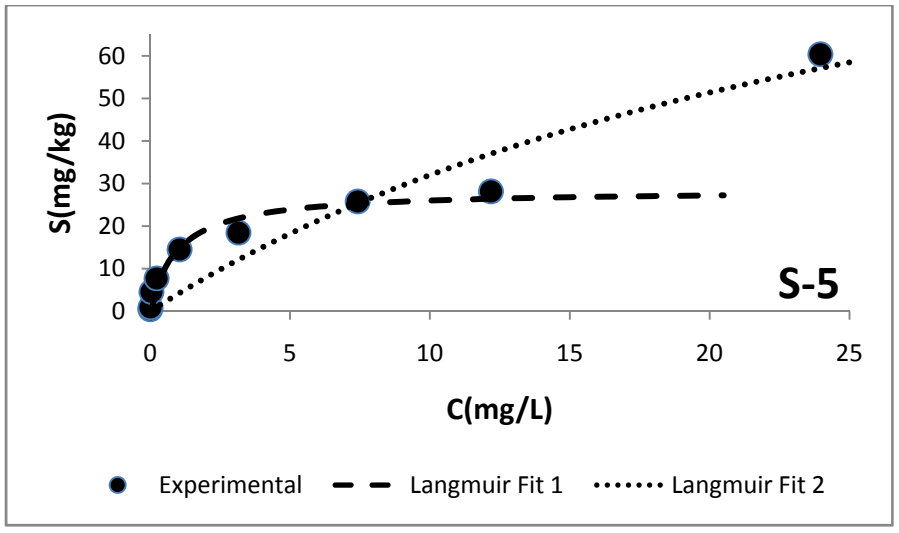

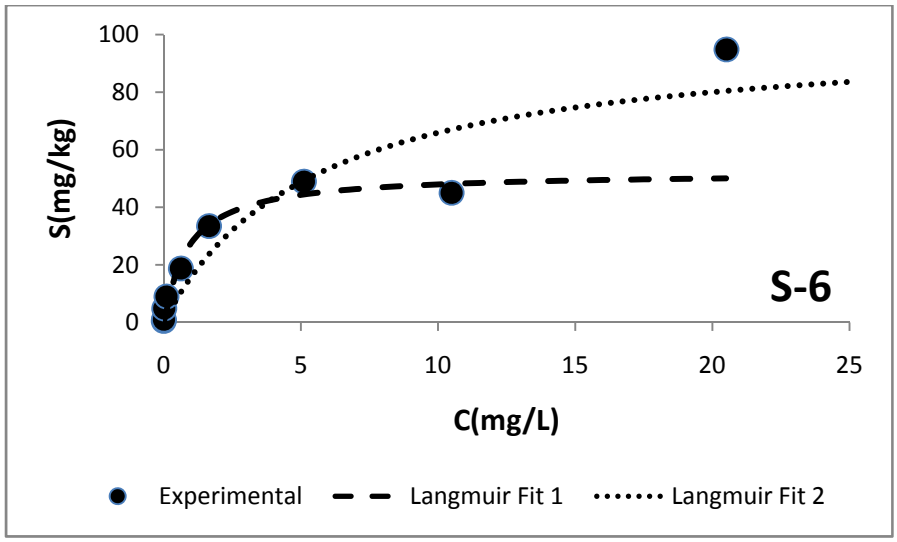
S(mg/kg)
100
80
60
40
20
0
0
5
10
15
20
25
C(mg/L)
S-6
Experimental
Langmuir Fit 1
Langmuir Fit 2

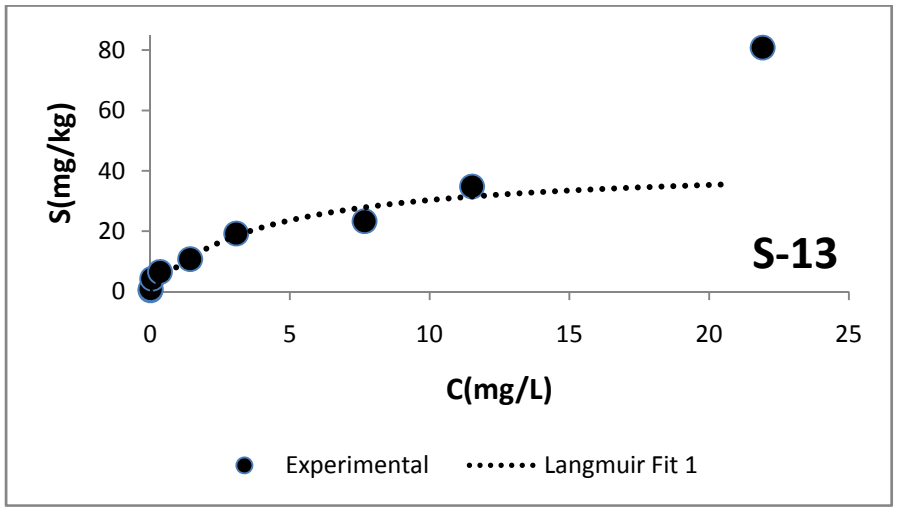
S(mg/kg)
80
60
40
20
0
0
5
10
15
20
25
C(mg/L)
S-13
Experimental
Langmuir Fit 1

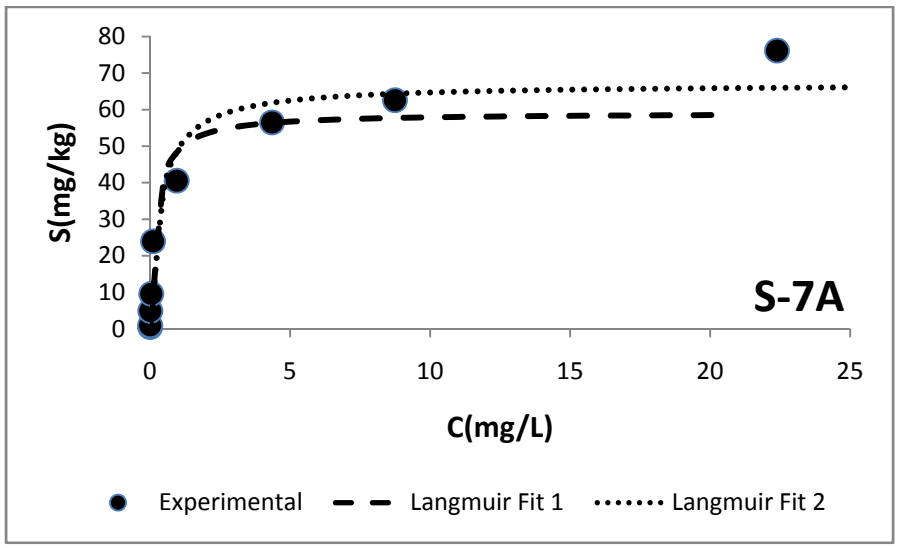
S(mg/kg)
80
70
60
50
40
30
20
10
0
0
5
10
15
20
25
C(mg/L)
S-7A
Experimental
Langmuir Fit 1
Langmuir Fit 2

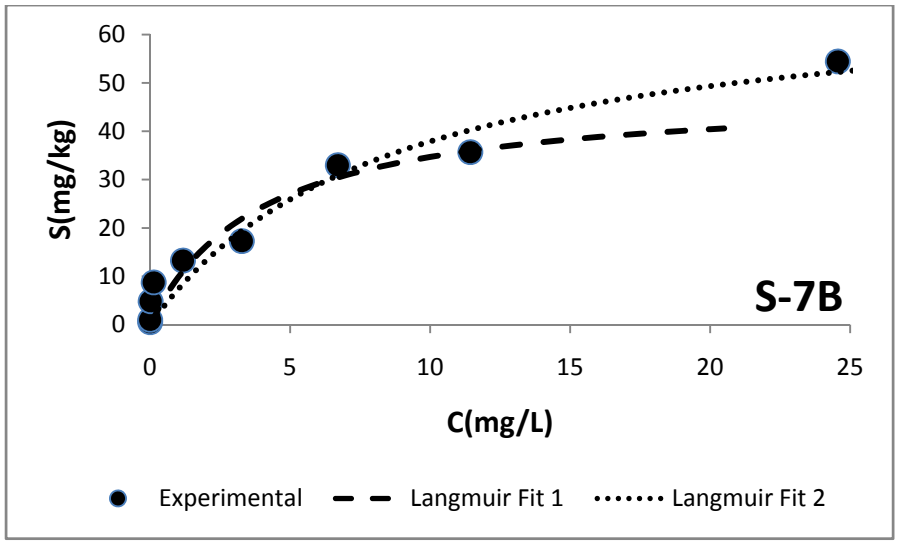
S(mg/kg)
C(mg/L)
S-7B
Experimental
Langmuir Fit 1
Langmuir Fit 2

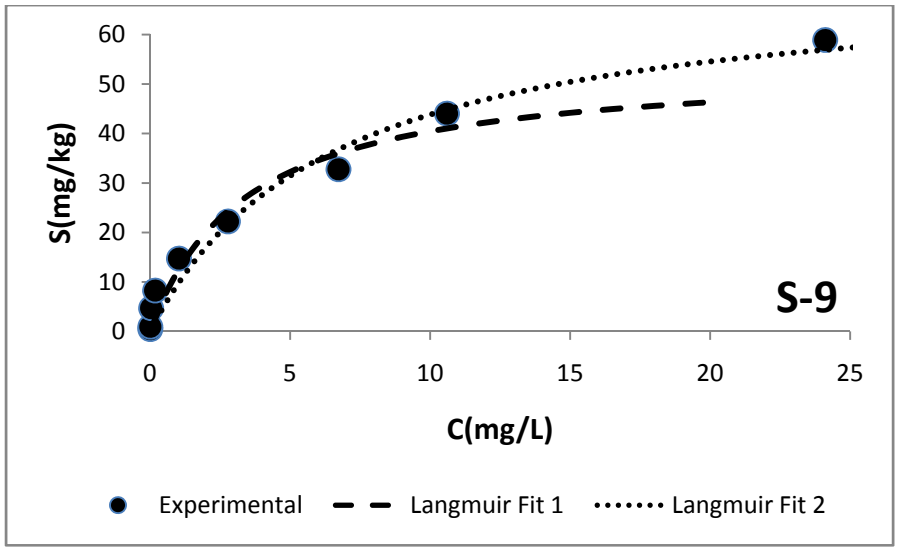
S(mg/kg)
C(mg/L)
S-9
Experimental
Langmuir Fit 1
Langmuir Fit 2

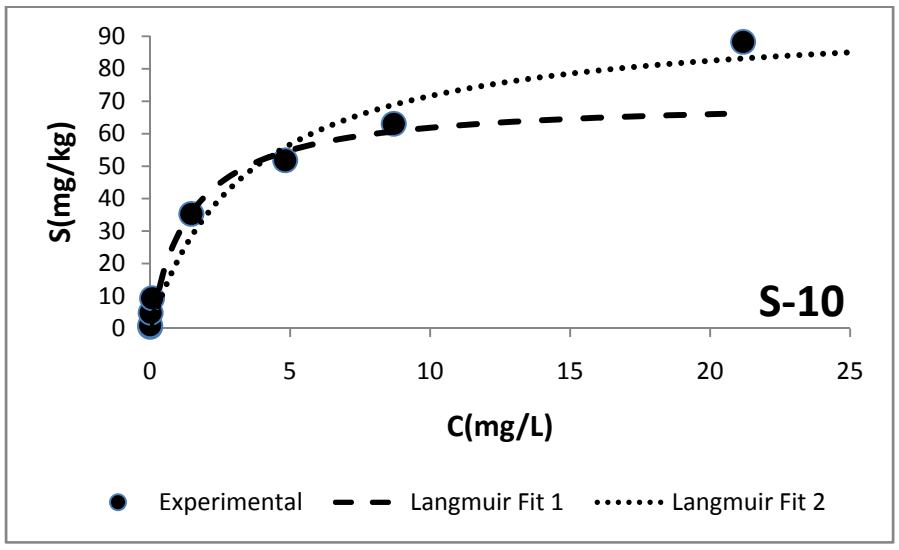
S(mg/kg)
C(mg/L)
S-10
Experimental
Langmuir Fit 1
Langmuir Fit 2

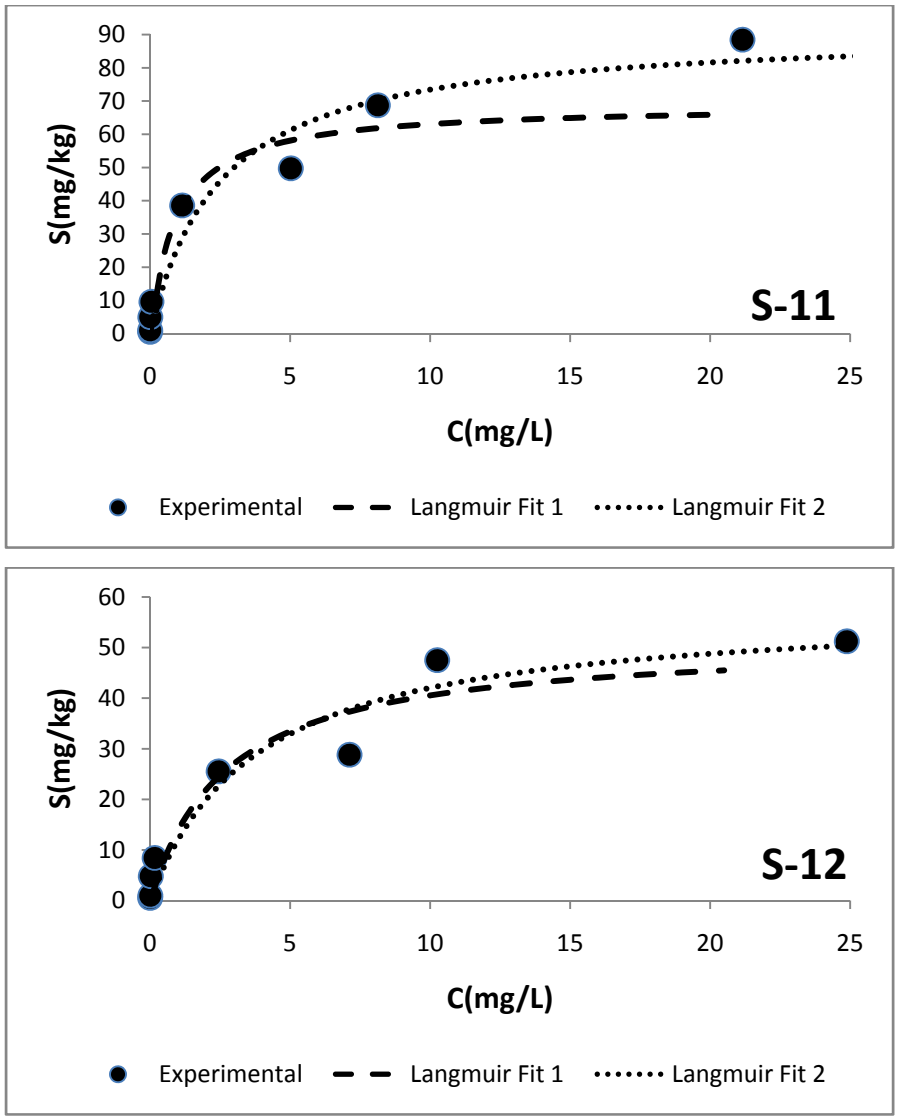

Figure 5. Langmuir isotherm fits to adsorption data. Fit 1 (dashed line) excludes the highest data point, Fit 2 (dotted line) includes all data points.

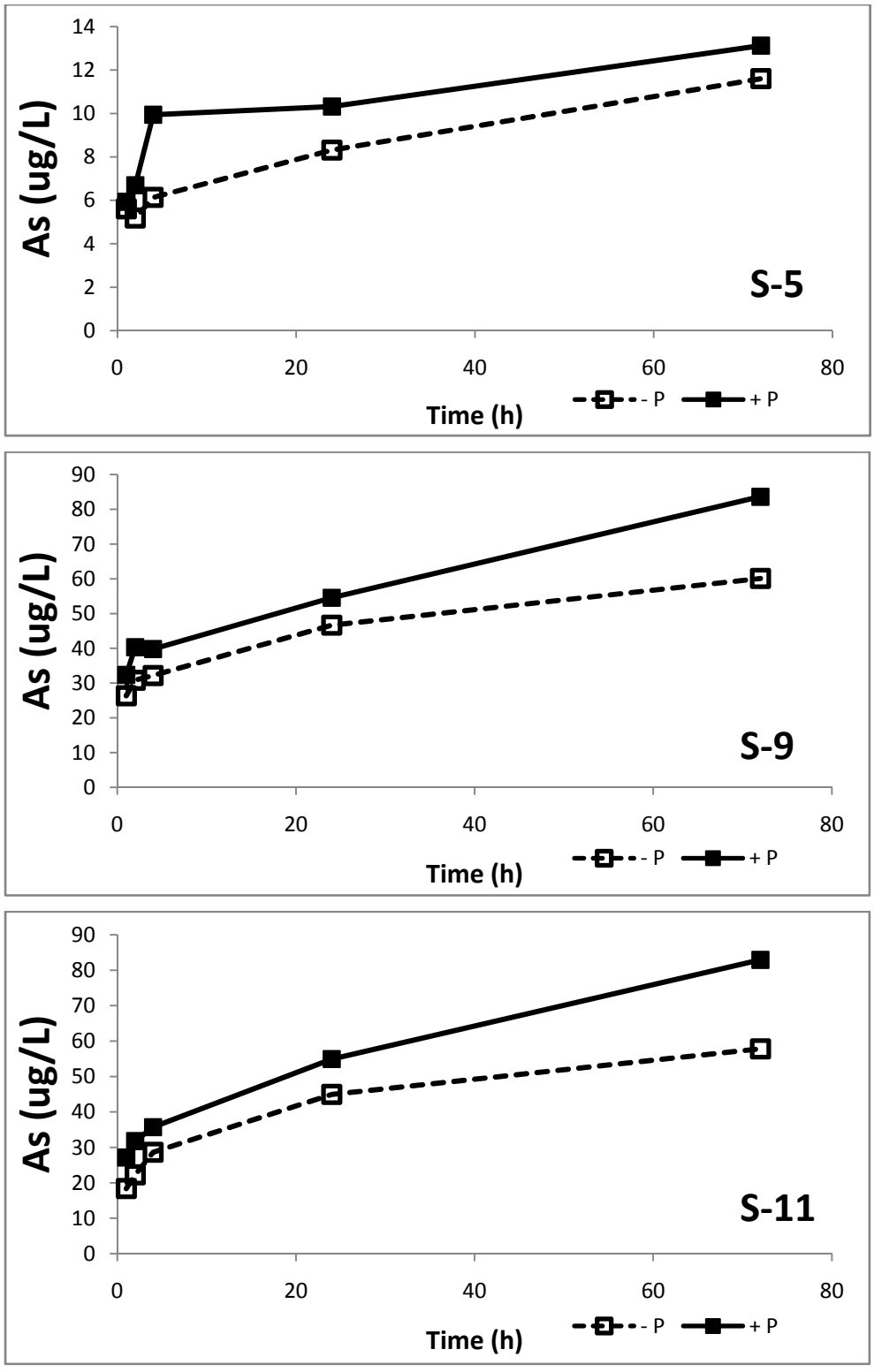

Figure 6. Desorption of As over time by equilibrating sediments with pH 9.5 $NaHCO_3/Na_2CO_3$ solution. Closed markers indicate presence of 5 mg/L PO_4-P in the solution.

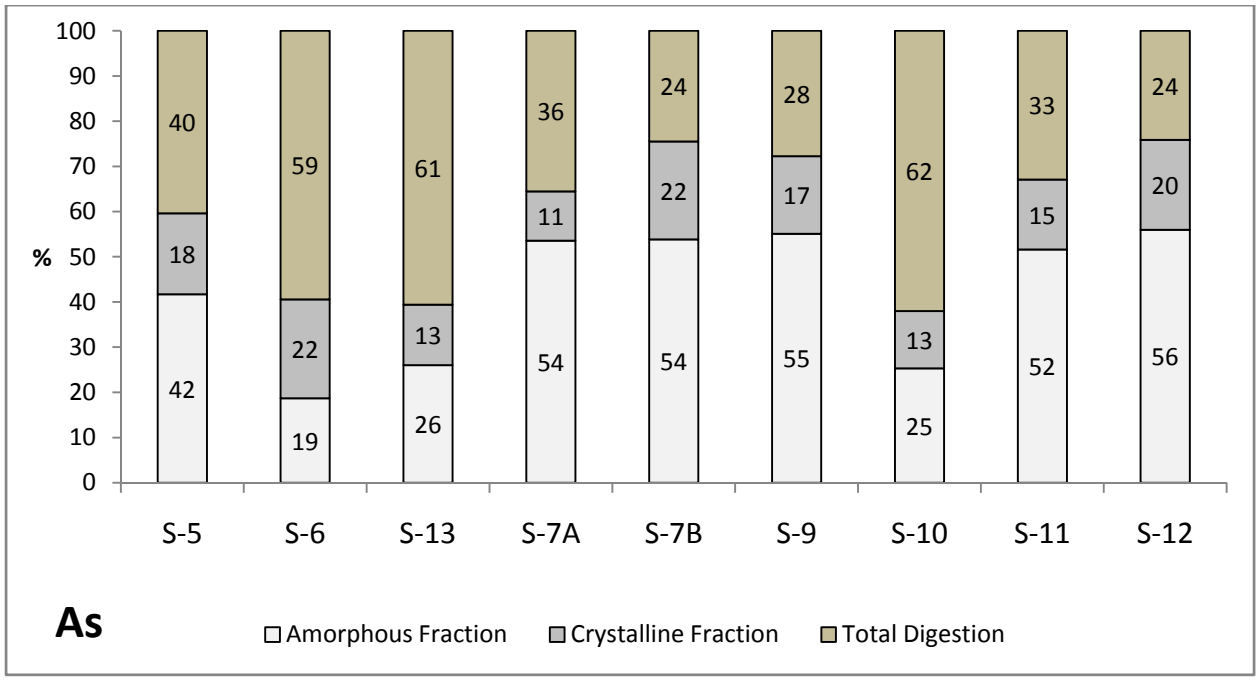
100
90
80
70
60
%
50
40
30
20
10
0
40
18
42
59
22
19
61
13
26
36
11
54
24
22
54
28
17
55
62
13
25
33
15
52
24
20
56
S-5
S-6
S-13
S-7A
S-7B
S-9
S-10
S-11
S-12
As
Amorphous Fraction
Crystalline Fraction
Total Digestion

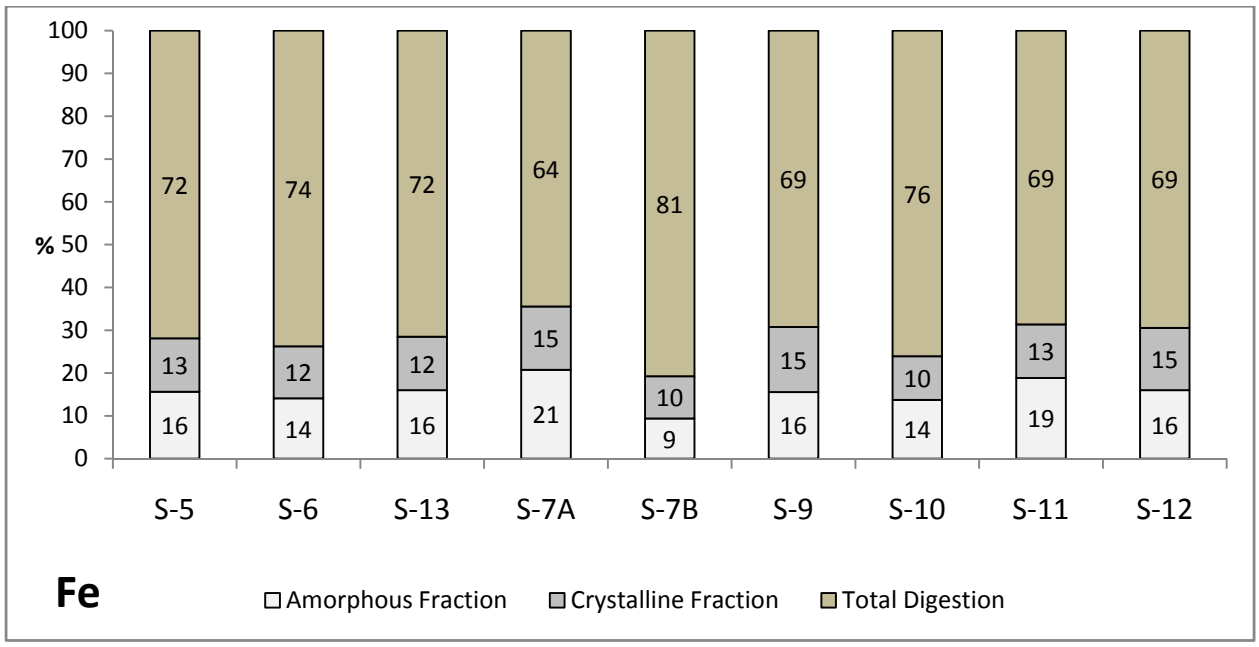
100
90
80
70
60
%
50
40
30
20
10
0
72
13
16
74
12
14
72
12
16
64
15
21
81
10
9
69
15
16
76
10
14
69
13
19
69
15
16
S-5
S-6
S-13
S-7A
S-7B
S-9
S-10
S-11
S-12
Fe
Amorphous Fraction
Crystalline Fraction
Total Digestion

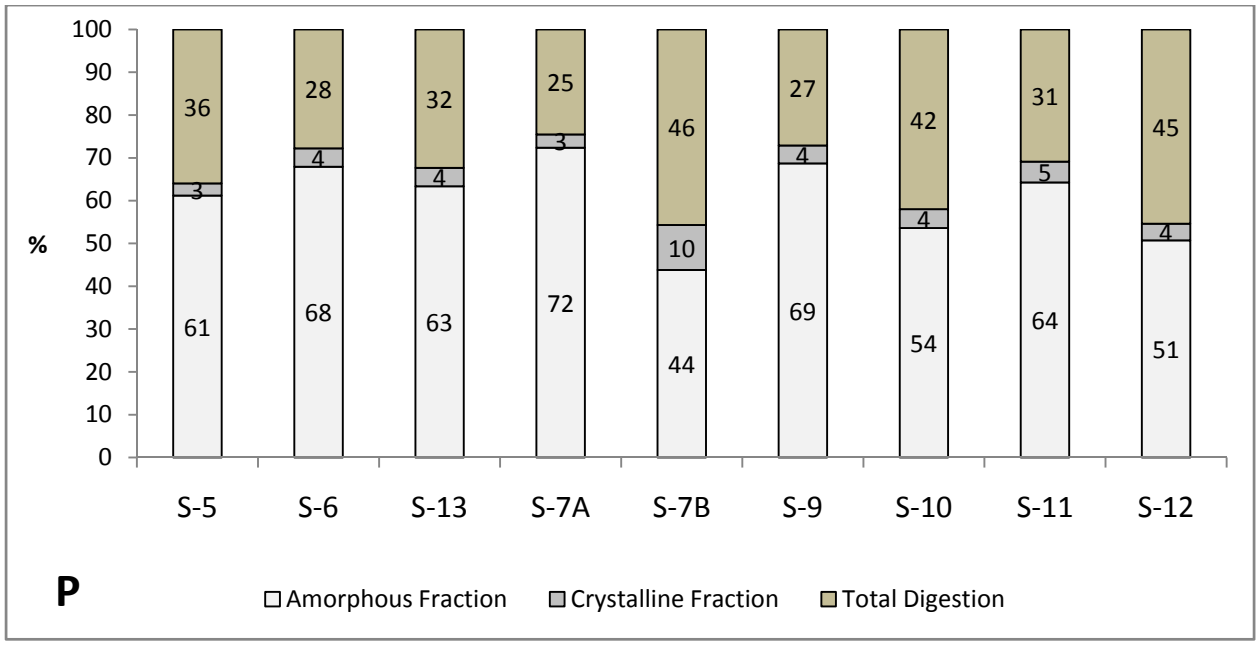
100
90
80
70
60
50
40
30
20
10
0
%
36
3
61
28
4
68
32
4
63
25
3
72
46
10
44
27
4
69
42
4
54
31
5
64
45
4
51
S-5
S-6
S-13
S-7A
S-7B
S-9
S-10
S-11
S-12
P
Amorphous Fraction
Crystalline Fraction
Total Digestion

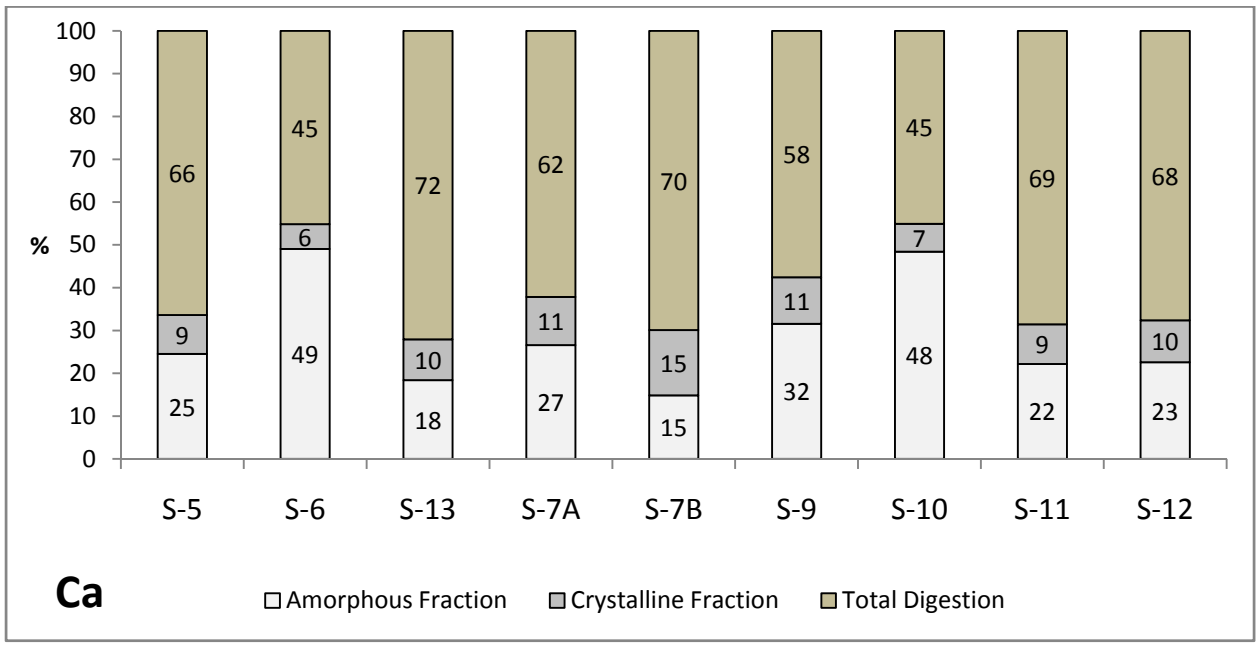
100
90
80
70
60
50
40
30
20
10
0
%
66
9
25
45
6
49
72
10
18
62
11
27
70
15
15
58
11
32
45
7
48
69
9
22
68
10
23
S-5
S-6
S-13
S-7A
S-7B
S-9
S-10
S-11
S-12
Ca
Amorphous Fraction
Crystalline Fraction
Total Digestion

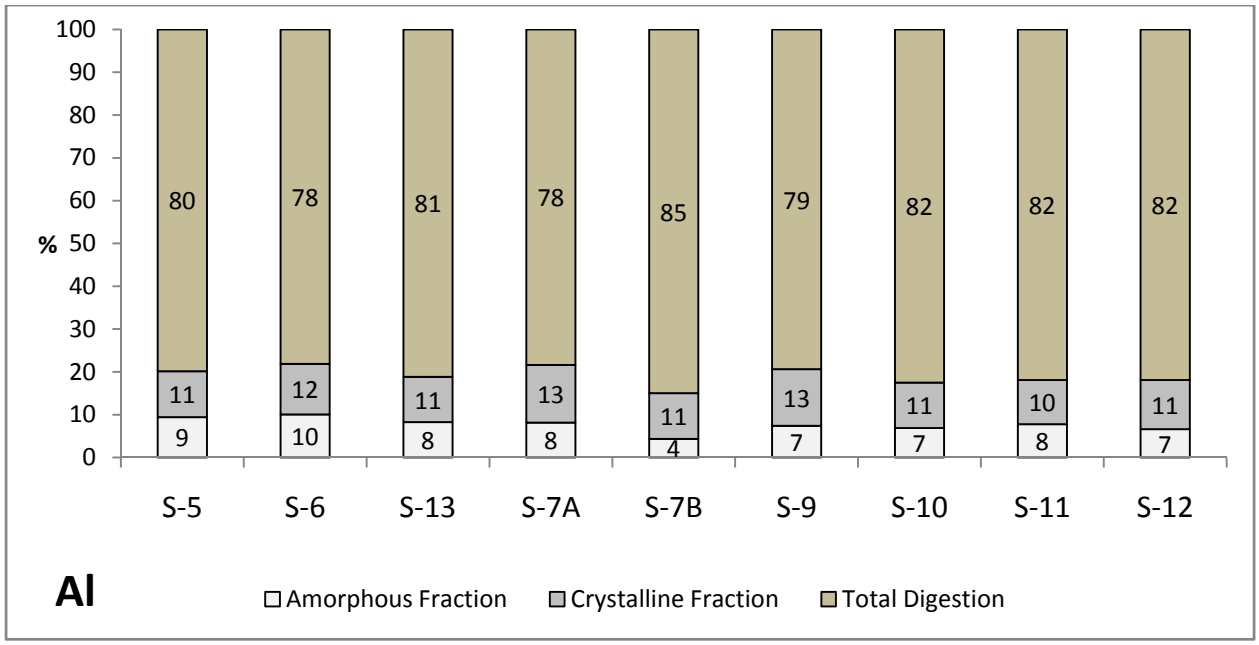

Figure 7. Solid phase distribution (%) of As, Fe, P, Ca, and Al among the three extracted phases (amorphous, crystalline and recalcitrant).

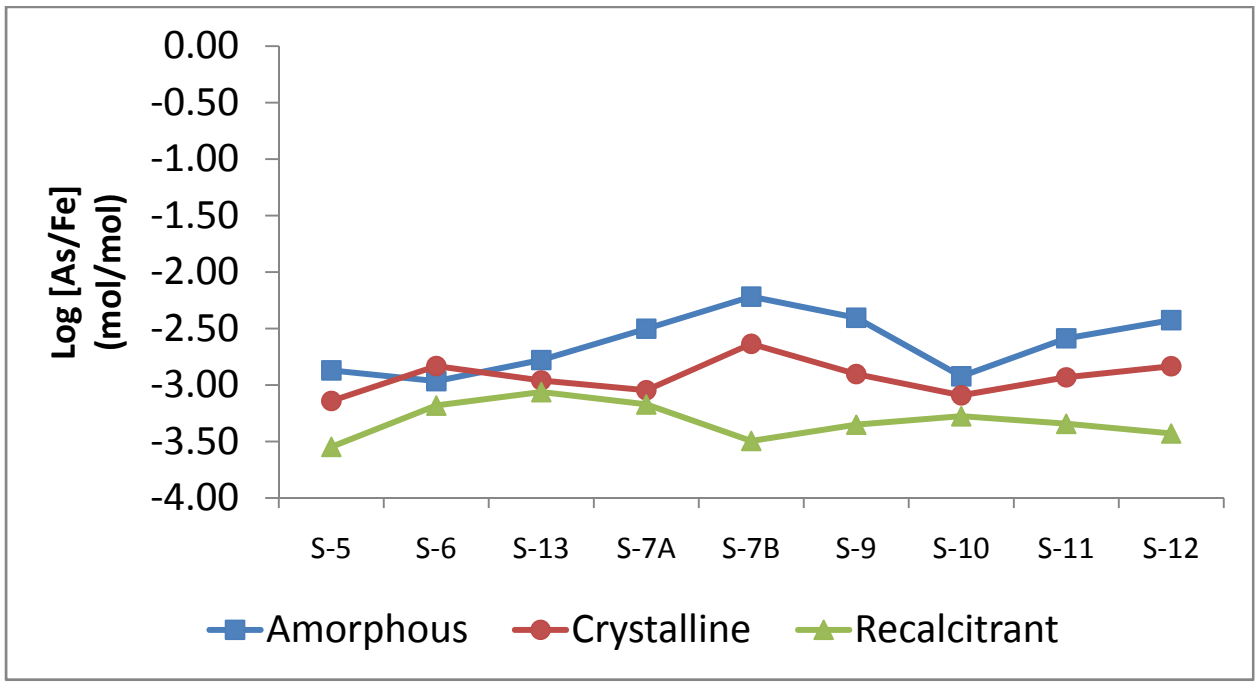

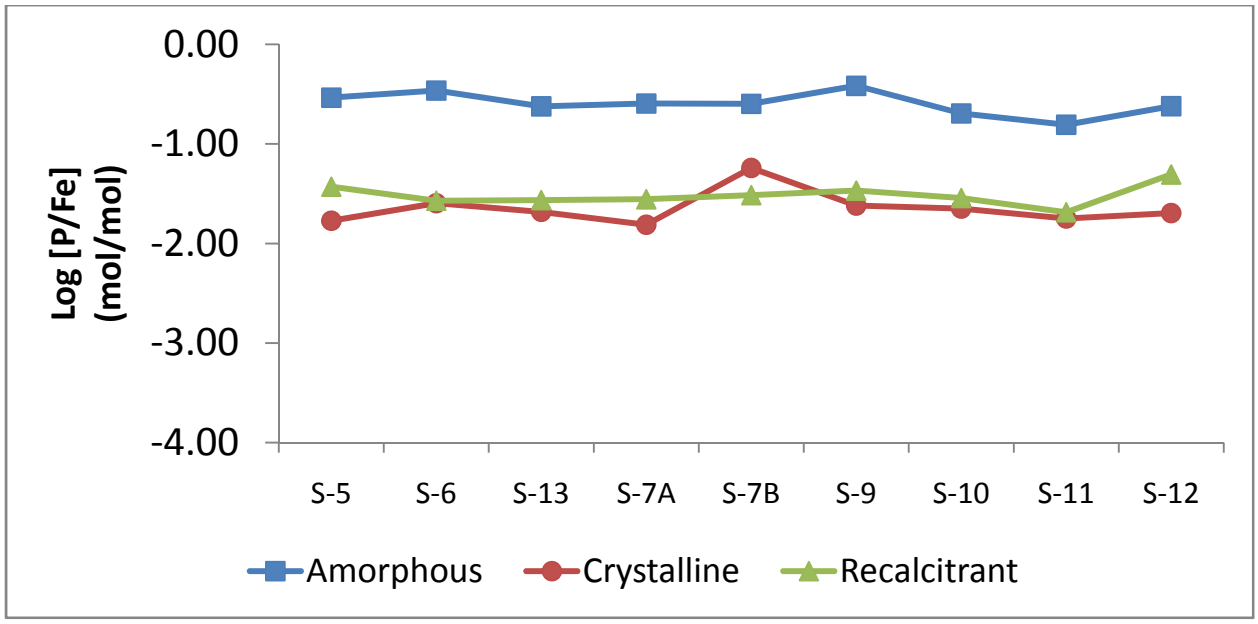

Figure 8. Molar ratios of As/Fe and P/Fe extracted from the different solid phases.

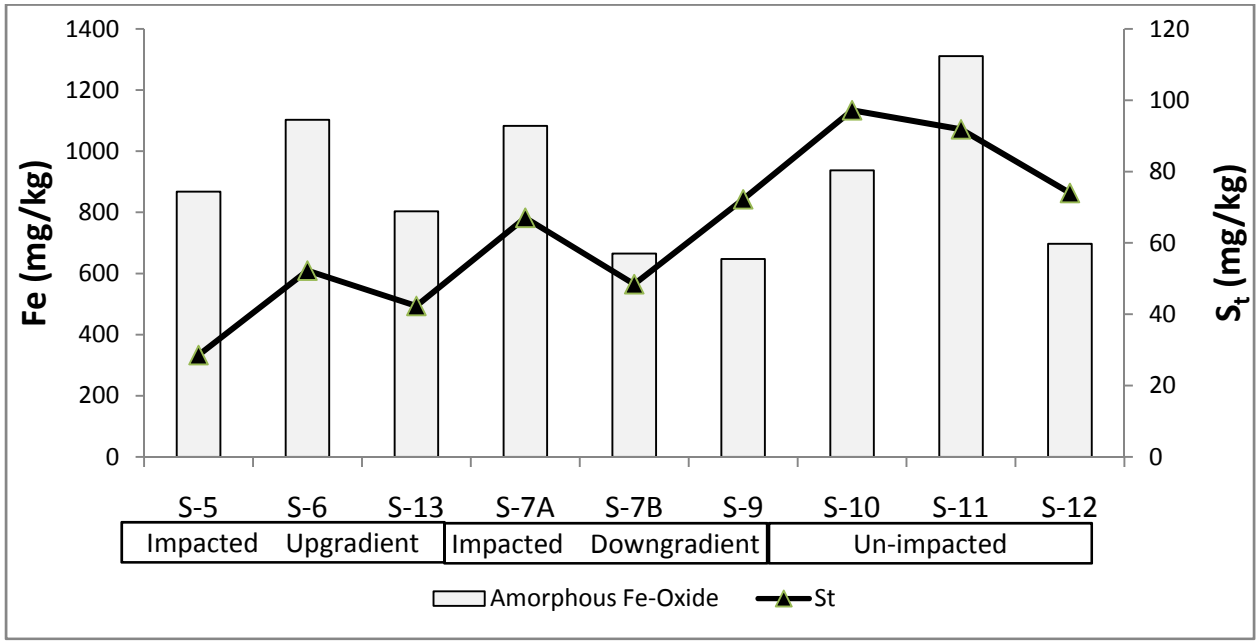

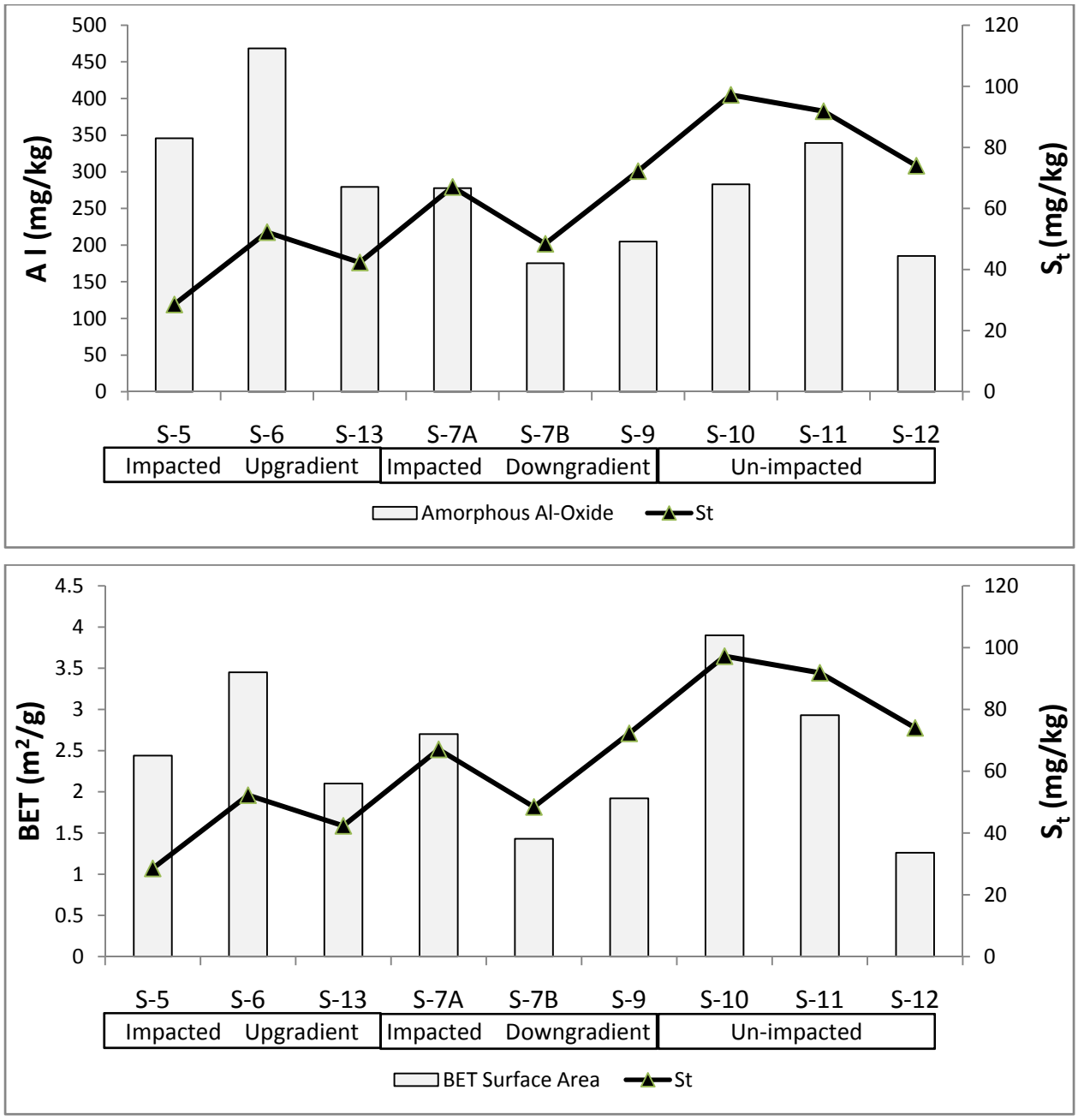

Figure 9. Comparison between the Langmuir St parameter and adsorptive chemical and physical characteristics of sediments (amorphous Fe, amorphous Al, and BET surface area). Bars represent the sediment characteristics and lines with markers represent the St parameter.

Tables

Table 1. Chemical and physical properties of sediments

Sediment	Depth	pH	Surface Area (m^2/g)	Clay (%)	Sand (%)	Silt (%)	USDA Classification	Water Content (%)	Organic Content (%)	Notes
Impacted Upgradient										
S-5	23-27.5	9	2.44	6.19	89.81	4.00	sand	22.1	2.3	brown fine sand
S-6	29-37	9.2	3.45	12.39	69.78	17.84	sandy loam	11.2	1.7	gray sandy till
S-13	34-44	9.1	2.1	4.15	94.57	1.28	sand	21.6	2.4	brown fine to medium sand
Impacted Downgradient										
S-7A	43-49	8.3	2.7	9.51	78.48	12.01	sandy loam	22.2	2.1	brown fine sand
S-7B	49-58	8.3	1.43	4.18	92.54	3.28	sand	9.7	2.1	brown coarse sand
S-9	47-56	8.1	1.92	7.50	88.50	4.00	loamy sand	22.5	2.2	brown fine to coarse sand
Un-impacted										
S-10	51-58	8.7	3.9	9.50	88.50	2.00	loamy sand	21.9	1.7	gray fine to medium sand
S-11	46-56	7.7	2.93	5.20	92.50	2.30	sand	15.4	2.4	brown fine to medium sand
S-12	48-58	7.7	1.26	6.85	90.66	2.49	sand	22.5	2.3	brown fine to medium sand

Table 2. Pseudo-first order kinetic model parameters obtained from piecewise linear regression.

Sediment	C_0 = 0.5 mg/L				C_0 = 1 mg/L				C_0 = 2.5 mg/L			
	R^2	t_c (h)	$K'_{1<tc}$ (h^{-1})	$K'_{1>tc}$ (h^{-1})	R^2	t_c (h)	$K'_{1<tc}$ (h^{-1})	$K'_{1>tc}$ (h^{-1})	R^2	t_c (h)	$K'_{1<tc}$ (h^{-1})	$K'_{1>tc}$ (h^{-1})
S-11	0.9832	17.83	0.0950	0.0068	0.9880	19.34	0.0813	0.0063	0.9915	17.92	0.0405	0.0038
S-12	0.9914	18.00	0.0533	0.0053	0.9885	14.19	0.0554	0.0032	0.9892	17.52	0.0268	0.0013

Table 3. pseudo-second order kinetic model parameters obtained from linear regression.

Sediment	C_0 = 0.5 mg/L				C_0 = 1 mg/L				C_0 = 2.5 mg/L			
	R^2	h (mg/kg.h)	K'_2 (kg/mg.h)	q_e (mg/kg)	R^2	h (mg/kg.h)	K'_2 (kg/mg.h)	q_e (mg/kg)	R^2	h (mg/kg.h)	K'_2 (kg/mg.h)	q_e (mg/kg)
S-11	0.9998	1.69	0.0717	4.85	0.9965	0.80	0.0083	9.84	0.9975	2.60	0.0063	20.28
S-12	0.9987	0.76	0.0377	4.49	0.9975	0.89	0.0145	7.82	0.9989	1.92	0.0100	13.87

Table 4. Freundlich adsorption isotherm model parameters.

	Freundlich Parameters		
	$K(mg/kg)(L/mg)^n$	n	R^2
S-5	11.64	0.4852	0.9625
S-6	21.29	0.5077	0.9652
S-13	9.96	0.586	0.9591
S-7A	29.77	0.4745	0.9086
S-7B	14.16	0.4157	0.9592
S-9	13.58	0.5209	0.9497
S-10	24.58	0.4972	0.9755
S-11	27.04	0.4808	0.9446
S-12	14.83	0.4579	0.958

Table 5. Langmuir adsorption isotherm parameters. Fit 1 does not include the highest data point (C_0=30mg/L); Fit 2 includes all data point. Accepted fits are highlighted.

Sediment	Langmuir Parameters						S_t Increase(%)
	Fit 1			Fit 2			
	K(L/mg)	S_t(mg/kg)	R^2	K(L/mg)	S_t(mg/kg)	R^2	
S-5	1.03	28.53	0.962	0.03	130.43	0.895	357
S-6	1.12	52.23	0.976	0.18	101.76	0.879	95
S-13	0.25	42.31	0.948	-	-	-	-
S-7A	4.71	59.13	0.975	2.74	67.05	0.956	13
S-7B	0.25	48.42	0.949	0.12	70.64	0.917	46
S-9	0.29	54.24	0.917	0.15	72.23	0.969	33
S-10	0.69	70.79	0.983	0.28	97.20	0.974	37
S-11	1.07	68.94	0.969	0.40	91.84	0.956	33
S-12	0.37	51.48	0.91	0.26	74.12	0.94	43

Table 6. Arsenic desorption rates from original and As-loaded sediments (before and after adsorption experiments)

Sediment	Desorbed from fresh samples		Desorbed from As-loaded sediments (% of adsorbed)							
	(mg/kg)	(% of Amorphous phase)	C_0 (mg/L)							
			0.05	0.1	0.5	1	2.5	5	10	15
S-5	0.07	4.3	-	-	-	-	-	-	-	-
S-6	0.26	16.3	-	-	-	-	-	-	-	-
S-13	0.08	4.4	-	-	-	-	68.9	42.4	41.9	38.3
S-7A	0.99	21.6	-	-	-	-	-	-	-	-
S-7B	0.50	9.2	-	-	-	-	-	-	-	-
S-9	0.47	13.7	50.2	52.3	48.3	49.2	-	52.0	39.1	35.5
S-10	0.25	16.4	32.9	34.1	49.1	42.4	-	56.5	57.2	52.7
S-11	0.46	10.0	68.1	42.4	44.7	38.7	-	53.8	60.4	48.7
S-12	0.32	9.1	-	-	-	-	-	-	-	-

References

Antelo, J., Avena, M., Fiol, S., López, R., & Arce, F. (2005). Effects of pH and ionic strength on the adsorption of phosphate and arsenate at the goethite-water interface. *Journal of Colloid and Interface Science*, *285*(2), 476–86.

Badruzzaman, M., Westerhoff, P., & Knappe, D. R. (2004). Intraparticle diffusion and adsorption of arsenate onto granular ferric hydroxide (GFH). *Water research*, *38*(18), 4002-4012.

Banerjee, K., Amy, G. L., Prevost, M., Nour, S., Jekel, M., Gallagher, P. M., & Blumenschein, C. D. (2008). Kinetic and thermodynamic aspects of adsorption of arsenic onto granular ferric hydroxide (GFH). *Water Research*, *42*(13), 3371–3378.

Bauer, M., & Blodau, C. (2006). Mobilization of arsenic by dissolved organic matter from iron oxides, soils and sediments. *Science of the Total Environment*, *354*(2), 179-190.

Boddu, V. M., Abburi, K., Talbott, J. L., Smith, E. D., & Haasch, R. (2008). Removal of arsenic (III) and arsenic (V) from aqueous medium using chitosan-coated biosorbent. *Water Research*, *42*(3), 633–42. doi:10.1016/j.watres.2007.08.014

Bolster, C. H., & Hornberger, G. M. (2008). On the Use of Linearized Langmuir Equations. *Soil Science Society of America Journal*, *72*(6), 1848. doi:10.2136/sssaj2006.0304

Borgnino, L., De Pauli, C. P., & Depetris, P. J. (2012). Arsenate adsorption at the sediment–water interface: sorption experiments and modelling. *Environmental Earth Sciences*, *65*(2), 441-451.

Dadwhal, M., Sahimi, M., & Tsotsis, T. T. (2011). Adsorption isotherms of arsenic on conditioned layered double hydroxides in the Presence of various competing ions. *Industrial and Engineering Chemistry Research*, *50*, 2220–2226.

Hiemstra, T., & Van Riemsdijk, W. H. (1999). Surface structural ion adsorption modeling of competitive binding of oxyanions by metal (hydr) oxides. *Journal of Colloid and Interface Science*, *210*(1), 182-193.

Ho, Y. S., & Mckay, G. (1998). A Comparison of Chemisorption Kinetic Models Applied To Pollutant Removal on Various Sorbents. *Process Safety and Environmental Protection*, *76*(November), 332–340.

Ho, Y. S., & Ofomaja, A. E. (2006). Pseudo-second-order model for lead ion sorption from aqueous solutions onto palm kernel fiber. *Journal of hazardous materials*, *129*(1), 137-142.

Jang, M., Shin, E. W., Park, J. K., & Choi, S. I. (2003). Mechanisms of Arsenate Adsorption by Highly-Ordered Nano-Structured Silicate Media Impregnated with Metal Oxides. *Environmental Science and Technology*, *37*(21), 5062–5070.

Jeppu, G. P., & Clement, T. P. (2012). A modified Langmuir-Freundlich isotherm model for simulating pH-dependent adsorption effects. *Journal of Contaminant Hydrology*, *129-130*, 46–53.

Kapaj, S., Peterson, H., Liber, K., & Bhattacharya, P. (2006). Human health effects from chronic arsenic poisoning–a review. *Journal of Environmental Science and Health Part A*, *41*(10), 2399-2428.

Lakshmipathiraj, P., Narasimhan, B. R. V., Prabhakar, S., & Raju, G. B. (2006). Adsorption of arsenate on synthetic goethite from aqueous solutions. *Journal of Hazardous Materials*, *136*(2), 281-287.

Lin, T. F., & Wu, J. K. (2001). Adsorption of arsenite and arsenate within activated alumina grains: equilibrium and kinetics. *Water research*, *35*(8), 2049-2057.

Giménez, J., Martínez, M., de Pablo, J., Rovira, M., & Duro, L. (2007). Arsenic sorption onto natural hematite, magnetite, and goethite. *Journal of Hazardous Materials*, *141*(3), 575-580.

Goldberg, S., & Johnston, C. T. (2001). Mechanisms of arsenic adsorption on amorphous oxides evaluated using macroscopic measurements, vibrational spectroscopy, and surface complexation modeling. *Journal of colloid and Interface Science*, *234*(1), 204-216.

Guo, H., Li, Y., & Zhao, K. (2010). Arsenate removal from aqueous solution using synthetic siderite. *Journal of Hazardous Materials*, *176*(1-3), 174–80.

Maji, S. K., Pal, A., & Pal, T. (2008). Arsenic removal from real-life groundwater by adsorption on laterite soil. *Journal of Hazardous Materials*, *151*(2-3), 811–20.

Manning, B. A., & Goldberg, S. (1996). Modeling Competitive Adsorption of Arsenate with Phosphate and Molybdate on Oxide Minerals. *Soil Science Society of America Journal*.

Manning, B. A., & Goldberg, S. (1997). ARSENIC (III) AND ARSENIC (V) ADSORPTION ON THREE CALIFORNIA SOILS. *Soil Science*, *162*(12), 886-895.

Masel, R. I. (1996). *Principles of adsorption and reaction on solid surfaces* (Vol. 3). John Wiley & Sons.

Neupane, G., Donahoe, R. J., & Arai, Y. (2014). Kinetics of competitive adsorption/desorption of arsenate and phosphate at the ferrihydrite–water interface. *Chemical Geology*, *368*, 31–38.

Oke, I. a., Olarinoye, N. O., & Adewusi, S. R. a. (2008). Adsorption kinetics for arsenic removal from aqueous solutions by untreated powdered eggshell. *Adsorption*, *14*(1), 73–83.

Radu, T., Kumar, A., Clement, T. P., Jeppu, G., & Barnett, M. O. (2008). Development of a scalable model for predicting arsenic transport coupled with oxidation and adsorption reactions. *Journal of Contaminant Hydrology*, *95*(1-2), 30–41.

Robinson, C., Brömssen, M. Von, Bhattacharya, P., Häller, S., Bivén, A., Hossain, M., … Thunvik, R. (2011). Dynamics of arsenic adsorption in the targeted arsenic-safe aquifers in Matlab, south-eastern Bangladesh: Insight from experimental studies. *Applied Geochemistry*, *26*(4), 624–635.

Sherman, D. M., & Randall, S. R. (2003). Surface complexation of arsenic (V) to iron (III)(hydr) oxides: structural mechanism from ab initio molecular geometries and EXAFS spectroscopy. *Geochimica et Cosmochimica Acta*, *67*(22), 4223-4230.

Sohn, S., & Kim, D. (2005). Modification of Langmuir isotherm in solution systems - Definition and utilization of concentration dependent factor. *Chemosphere*, *58*, 115–123.

Smedley, P. L., & Kinniburgh, D. G. (2002). A review of the source, behaviour and distribution of arsenic in natural waters. *Applied Geochemistry*, *17*(5), 517–568.

Stollenwerk, K. G. (2003). Geochemical processes controlling transport of arsenic in groundwater: a review of adsorption. In *Arsenic in ground water* (pp. 67-100). Springer US.

Stollenwerk, K. G., Breit, G. N., Welch, A. H., Yount, J. C., Whitney, J. W., Foster, A. L., … Ahmed, N. (2007). Arsenic attenuation by oxidized aquifer sediments in Bangladesh. *The Science of the Total Environment*, *379*(2-3), 133–50.

USDA-SCS, 1972. Soil Survey Laboratory Methods and Procedures for Collecting Soil Samples. US Government Printing Office, Washington DC.

Zhang, H., & Selim, H. M. (2005). Kinetics of arsenate adsorption-desorption in soils. *Environmental Science & Technology*, *39*(16), 6101–8.

Zhang, H., & Selim, H. M. (2006). Modeling the Transport and Retention of Arsenic (V) in Soils. *Soil Science Society of America Journal*, *70*(5), 1677.

Chapter 3. Arsenic Mobilization in an Oxidizing Alkaline Groundwater: Experimental Studies, Comparison and Optimization of Geochemical Modeling Parameters

Abstract

Arsenic (As) mobilization and contamination of groundwater affects millions of people worldwide. Progress in developing effective in-situ remediation schemes requires the incorporation of data from laboratory experiments and field samples into calibrated geochemical models.

In an oxidizing aquifer where leaching of high pH industrial waste from unlined surface impoundments led to mobilization of naturally occurring As up to 2 mg/L, sequential extractions of solid phase As as well as, batch sediment microcosm experiments were conducted to understand As partitioning and solid-phase sorptive and buffering capacity. These data were combined with field data to create a series of geochemical models of the system with modeling programs PHREEQC and FITEQL. Different surface complexation modeling approaches, including component additivity (CA), generalized composite (GC), and a hybrid method were developed, compared and fitted to data from batch acidification experiments to simulate potential remediation scenarios. Several parameters strongly influence the concentration of dissolved As including pH, presence of competing ions (particularly phosphate) and the number of available sorption sites on the aquifer solids. Lowering the pH of groundwater to 7 was found to have a variable, but limited impact (<63%) on decreasing the concentration of dissolved As. The models indicate that in addition to lowering pH, decreasing the concentration of dissolved phosphate and/or increasing the number of available sorption sites could significantly decrease the As solubility to levels below 10 μg/L. The hybrid and GC modeling results fit the experimental data well (NRMSE<10%) with reasonable effort and can be implemented in further

studies for validation.

1. Introduction

Arsenic (As), considered one of the most serious inorganic contaminants in drinking water can adversely impact human health and is recognized as a prominent environmental cause of cancer mortality worldwide (Smedley and Kinniburgh, 2002; Welch at al., 2000; Smith et al., 1992). Arsenic is a ubiquitous trace element in the environment and can be mobilized from solid phases through a combination of natural processes such as weathering reactions, biological activity and volcanic emissions as well as through a range of anthropogenic activities. Following the World Health Organization (WHO) guideline in 1993, the US Environmental Protection Agency (US-EPA) limit for As in drinking waters was reduced from 50 to 10 μg/L (ppb) in January 2001 (EPA, 2002).

While use of As containing compounds has decreased in recent decades and elevated levels of As in groundwater can generally be attributed to naturally occurring sources, anthropogenic activities such as agricultural and mining operations, industrial processes and associated waste disposals can still cause or facilitate favorable conditions for mobilization of As from geologic sources into groundwater. Arsenic is the second most common contaminant of concern in National Priorities List (NPL), occurring at 47% of all Superfund sites in the US (EPA, 2002). High levels of As in the groundwaters of Bangladesh and West Bengal originate from natural sources with mobilization stimulated by anthropogenic inputs of natural organic matter (NOM) (Neumann et al., 2009; Harvey et al., 2006).

Arsenic speciation and fate is controlled by the pH and redox potential (Eh) of the system, the presence of ligands such as NOM and competing ions, and the mineral present at the site.

Arsenic in groundwater is primarily present as oxyanions of As(V) (arsenate, with pKa's of 2.2, 6.9 and 11.5) or As(III) (arsenite, with pKa's of 9.3 and 14.2)

Arsenic mobilization from solid to aqueous phases can occur in both reducing and oxidizing environments. Most studies have focused on reducing conditions, under which both As and Fe may be reduced and mobilized by microbial activity, as is occurring in Bangladesh (Radloff et al., 2011; Ravenscroft et al., 2009;Van Geen et al., 2006; Zheng et al., 2004; Anawar et al., 2002), Vietnam (Thi Hoa Mai et al., 2014; Larsen et al., 2008; Postma et al., 2007; Berg et al., 2001), Cambodia (Lawson et al. 2013; Omoregie et al., 2013; Quicksall et al., 2008; Rowland et al., 2007; Polya et al., 2005), West Bengal, India (Neidhardt et al. 2014; Lawson et al. 2013; Islam et al. 2004; McArthur et al., 2004).

Fewer studies have addressed oxidizing conditions, in which As(V) may be mobilized by desorption at high pH (Currel et al. 2011; Scanlon et al., 2009; Bhattacharya et al., 2006; Smedley et al., 2005).

Adsorption and coprecipitation on solid phases has been recognized as the principal factor in controlling As mobility in the environment (Wang et al., 2006). Sorption of As on Fe (III) (hydr)oxides is known as the most important process for limiting As solubility and has been investigated extensively. Due to their abundance in natural systems, high surface area and ability to adsorb As in large capacities, ferrihydrite (also referred to as amorphous hydrous ferric oxides or HFO) appears to be the most important solid phase responsible for removing As from the groundwater (Appelo and De Vet, 2003; Stollenwerk, 2003). The mechanism for specific adsorption has been described as ligand exchange reactions between ions in solution and surface functional groups leading to formation of both monodentate and bidentate inner-sphere complexes (Appelo and Postma, 2005; Sherman and Randall, 2003; Wilkie and Hering, 1996).

Efficiency of As adsorption onto Fe (III) oxides depends on a variety of factors such as the amounts and sorption capacity of minerals present, pH, concentrations and oxidation state of As, and concentration of other dissolved species that compete with As for adsorption sites (Stollenwerk et al., 2007). Ferrihydrite which has an amphoteric surface has strong affinity for adsorption of arsenate in pH range of 4-8. Adsorption studies at varying pH levels on ferrihydrite have shown that arsenate adsorption is higher at low pH values due to the net positive charge of the surface attracting negatively charged As(V) species (Raven et al., 1998). At high pH, arsenate adsorption becomes limited due to increased repulsion between the both negatively charged arsenate species and surface sites while arsenite can be retained in much larger amounts at such pH values due to its neutral charge (Masue et al., 2007; Dixit and Hering, 2003). Arsenic sorption can significantly be limited by presence of competing anions such as phosphate, silicates, bicarbonate and sulfate (Neupane et al., 2014; Kanematsu et al., 2012; Kanel et al., 2005; Dixit and Hering, 2003; Hongshao and Stanforth, 2001; Manning and Goldberg, 1996).

Efforts at applying geochemical modeling to simulate contamination and remediation scenarios in natural systems is challenging due to the complexity of interactions between groundwater and the solid matrix of the aquifer (Sharif et al., 2011). The majority of studies available on adsorption and surface complexation of trace contaminants have been conducted on pure mineral phases under controlled laboratory conditions. However, applicability of these findings to an environmental setting is limited due to the heterogeneous nature of aquifer media and the interactions among the various solid compositions.

Surface Complexation Models (SCM) for retention of trace elements such as As on natural heterogeneous solid phases can be categorized by two main approaches: (1) component

additivity (CA) and (2) generalized composite (GC) (Davis et al., 1998). In the CA approach, it is assumed that the overall retention of solutes on a complex mineral assemblage can be described by combining the sorption results on the individual specific solid phases composing the sorbent mixture. This is possible by using databases developed from independent adsorption studies on the individual pure phases. The modeler needs to first adequately analyze the studied solid phase to characterize the composition of mineral mixture. Therefore in the CA approach the emphasis is usually on collecting mineralogical data for appropriate identification and quantification of solid phases responsible for sorption, without fitting the constants with experimental data.

In the GC approach, a generic solid surface is defined and assumed to represent the sorptive behavior of the entire mineral assemblage and site-specific surface characteristics are determined by conducting variety of experiments and fitting of data. Therefore, the GC approach focuses on investigating the site-specific holistic sorption characteristics of solid phases as a function of pH, concentration of adsorbing ion, and influence of competing ions. The stoichiometry and surface complex formation constants are then determined by statistical methods and fitting the experimental data.

While the CA approach seems to be more sound in theory, applying it to heterogeneous solid surfaces has limitations. First, in many situations sufficiently characterizing the composition of the sediments may not be possible or practical. Second, due to heterogeneity of natural sediment surfaces, the different mineral phases could interact and behave very differently than expected based on the findings from studies of isolated pure phases under controlled conditions. Presence of secondary minerals, impure mixture of phases, interactions with NOM, organic coating and clay minerals makes application of SCMs to natural sediments more challenging. (Biswas et al.,

2014; Jessen et al., 2012; Hiemstra et al., 2010). Because of the difficulty in describing the actual surface charge of complex solid mixtures, applying the pH-dependent electrostatic correction terms required in the commonly used SCMs is not accurate for describing the adsorption on natural particles (Davis et al., 1998).

Also, the surface complexation mass-action reaction constants that are usually adopted from reference databases are developed from adsorption studies with constant background electrolyte concentrations in solution and will have limitations when applied to adsorption of solutes from the more complex natural groundwater systems. The intrinsic surface acidity constants are derived from titration experiments in simple electrolyte solutions and based on the assumption that only the surface functional groups control the aid-base reactions. However in natural systems, presence of various ions in solution and dissolution of phases such as carbonates invalidate this assumption.

Sharif et al. (2011) signified the inherent uncertainty in using the CA approach and the need for properly determining the surface properties rather than relying on default site characteristics from literature. Jessen et al. (2012) showed that a site-specific developed GC model produced more satisfying results than using the default SCM models from literature.

On the other hand, successful application of the GC approach for a complex natural system with various competing ions and across a wide pH range requires an extensive series of adsorption studies in order to obtain an internally consistent and comprehensive set of reactions and constants. Therefore, developing a GC model for the purpose of practical application at a specific contaminated site can involve substantial laboratory studies. Another difficulty for implementing the GC method for natural sediments is the accurate determination of acidity constants for surface functional groups. Due to heterogeneity and possible dissolution of other phases (eg.

carbonates), interpretation of acid-base titrations data for determining the surface charge of sediments become very complex. In most cases in order to achieve simplicity, the GC approach is applied without explicit representation of an electrostatic term (Sracek et al., 2004; Davis et al., 1998). Consequently the simplified model does not make electrostatic corrections to intrinsic complexation constants to account for changes in surface charge due to adsorption of ions.

Site specific GC has been successfully applied for uranium adsorption modeling purposes (Hyun et al., 2009; Bond et al., 2007; Davis et al., 2004), but applications for modeling As adsorption are rare. For example in a study on adsorption of As on oxidized sediments in Bangladesh (Stollenwerk et al., 2007) which was also shown promising for application in a different aquifer (Jessen et al., 2012).

As mentioned above, both the CA and GC approaches have certain difficulties for application in an impacted natural environment and in a timely efficient manner. Using laboratory and field data with the easily-accessible geochemical modeling tools PHREEQC and FITEQL, the current study aims at both comparing CA and GC approaches and also evaluating the effectiveness a hybrid CA/GC modeling approach for practical application with the purpose of achieving engineering solutions. We test the hypothesis that a hybrid CA/GC approach to modeling can be an effective, efficient choice to guide As remediation efforts.

2. Materials and Methods

2.1. Site Description

The study site (Figure 1), located in New England, USA, is a former manufacturing facility at which approximately 5000 gallons per week of hydroxide-containing waste sludge were disposed in unlined surface impoundments during the second half of the 1970's. The high pH waste sludge is believed to have contained phosphate-based detergents and chelating agents as

well as copper and other plating metals. Waste disposal in the impoundments ended in the early 1980's and the impoundments were closed in early 1990's by removing the sludge and capping with low permeability cover material.

The As(V) concentrations in the most affected areas of the site range from 140 µg/L to 800 µg/L. The source of arsenic in the groundwater is attributed mainly to the desorption and leaching from native solid phases into groundwater due to increased pH and phosphate concentrations while some portion may also derive from the waste solids. An association between an alkaline ground water (pH > 8) and high arsenic has historically been found in several areas of the United States, including eastern New England where 20-30% of private wells exceed the As drinking water standard (Ayotte et al. 2003, 2006; Welch at al., 2000; Robertson, 1989).

In previous ground water samples, arsenic was present mainly as the oxidized form As(V). Oxidizing conditions at the site were evident by the Eh value ranges of samples and low Fe(II). The sampling results from 2011-2012 show dissolved oxygen (DO) ranging from 0.4 to 4.7 mg/L in impacted sites and 8.4 mg/L as background. The ORP measurements were between 60 to 130 mV in all samples indicating oxidizing conditions. X-ray diffraction (XRD) and scanning electron microscopy (SEM) analyses of the sediments showed that the mineralogical composition is dominated mainly by quartz and feldspars.

2.2. Sampling Locations

Multiple co-located sediment and groundwater sampling locations were selected within and downstream of the former impoundment area where As(V) and pH values have been elevated. Site 2 is located beneath the former surface impoundments of waste materials and where the high pH conditions occurred. The sediment in this site consisted of a brown sandlens within the till formation. Sediment at Site 4, which has the highest groundwater As(V) concentration, is gray

till and based on screening tests with HCl, calcite is present in the soil matrix. Soil from Site 6 was also grey till with evidence of calcite. Site 7 is located further downgradient within the known As(V) plume where the aquifer soil consists of sand and gravel. The pH has been elevated (i.e., > 8) at this location and As(V) concentrations are the second highest following Site 4. Site 8, characterized as a sand and gravel aquifer, is located downgradient, beyond the portion of the aquifer that has been impacted by the As(V) plume. The flow path indicates that over time, the plume could eventually reach site 8.

2.3. Sample Collection

Sediment and groundwater samples were collected in 2013-2014 and shipped in coolers to UCLA. Soil borings were advanced with the drive and wash technique using 3-inch diameter steel casing and a two-foot long split spoon sampler ahead of the casing to collect undisturbed soil sample. Sediments collected from adjacent depth intervals were transferred to clean stainless steel containers, mixed thoroughly to form a composite sample, placed in glass screw-top jars. All samples were refrigerated (4° C) in dark prior to and between experiments. Sample collection intervals and soil descriptions are provided in Table 1.

Borings A, C, D, E and F were advanced adjacent to monitoring wells screened at the same interval as the soil samples. Groundwater samples were collected from these wells using low-flow sampling techniques. The wells were purged using a peristaltic pump with dedicated LDPE tubing. Pumping rates were controlled to minimize drawdown to approximately 1 foot or less. Temperature, pH and specific conductance were monitored during purging until these parameters stabilized. Groundwater samples were collected in clean, unpreserved 250 ml plastic bottles and refrigerated until use.

2.4. Materials

All solutions used in experiments were prepared with nanopure Milli-Q (18 MΩ-cm) water. Before use, all polypropylene tubes and glass volumetric flasks were filled with 1.2 N HCl and stored overnight prior to washing five times with Milli-Q water. All experiments were conducted in room temperature and in contact with the atmosphere.

2.5. Analytical Methods

The pH of the solutions was measured using an AB15 Plus pH meter, calibrated using commercial pH 4.0, 7.0, and 10.0 buffer solutions. Filtered solutions from adsorption isotherm experiments were analyzed for total As by Graphite Furnace Atomic Absorption Spectrometry (GFAAS). The instrument was calibrated daily and prior to use with 5 standard solutions made in the same matrix as the analyzed solution (linear dynamic range; 10-100 μg/L). The analyses were conducted in triplicates with palladium-magnesium nitrate matrix modifiers and the relative standard deviations of measurements were below 5%. The filtered solutions from sequential extractions and acidification experiments were analyzed for As and other elements by Inductively Coupled Plasma Mass Spectrometry (ICP-MS).

2.6. Sequential Extractions/Total Digestion

Oxalate and PO_4 extractable steps from the procedure specified in Keon et al. (2001) and total digestion (EPA method 3050B) were were implemented sequentially for the extraction of solid phase As. PO_4-extractable fraction represents the strongly-adsorbed As that is removed by anion exchange of PO_4^{3-} for AsO_4^{3-}. Oxalate-extraction step targets As coprecipitated with amorphous Fe oxides and the removal process is cited as ligand promoted complexation and dissolution of Fe, Al and Mn oxyhydroxides. Arsenic associated with crystalline Fe oxides, silicates and sulfides in addition to residual and recalcitrant fractions are pooled in the total digestion (TD) step. Table 2 summarizes the extractants and procedures used. Sediment to extractant ratio of 5 g

to 25 mL was used for all samples in duplicates. Separate extractions using hydroxylamine hydrochloride (0.25 M NH_2OH. HC1 in 0.25 M HC1, at 50° C for 0.5 h) were also conducted on sediments as an alternative method of dissolution of poorly crystalline iron oxides. Samples were shaken in polypropylene centrifuge tubes for the specified time durations prior to being centrifuged for 25 minutes at 7800 rpm. Supernatants were filtered with 0.45μm filters and preserved with concentrated HCl (0.2% v/v) prior to being analyzed by GFAAS.

2.7. Batch Adsorption Experiments

For adsorption isotherm experiments, sediments were mixed with 0.1M NaCl background electrolyte solutions in polypropylene centrifuge tubes (1:10 sediment/solution ratio) and adjusted to pH 7 before addition of As(V) ($Na_2HAsO_4.7H_2O$, Sigma-Aldrich, ACS reagent grade) to final concentrations ranging from 50 to 10,000 μg/L. Sample tubes were stored at room temperature and allowed to equilibrate on a rotary mixer at 8 RPM continuously for 7 days. Solutions were centrifuged, filtered (0.45 μm) and preserved with concentrated HCl (0.2% v/v) prior to total As analysis by GFAAS. The concentration of adsorbed As was calculated by conducting mass balance between the initial spiked concentration and the final concentration in filtered supernatant.

The Langmuir isotherm is a very commonly used empirical adsorption model with the physical basis that solids have a limited sorption capacity which could be reached at high concentrations of solutes. In comparison to other common models such as Freundlich, application of the Langmuir isotherm in soils and sediments studies has the advantage of providing an adjustable parameter that accounts for the maximum sorption capacity of sorbents. The Langmuir equation is as expressed as

$$S = S_t \frac{KC}{1 + KC}$$

where S is the adsorbed concentration (mg/kg), S_t is the maximum sorption capacity (mg/kg), K is a parameter representing the binding affinity (L/mg), and C is the equilibrium concentration in the solution phase (mg/L).

2.8. Batch Acidification Experiments

Batch acidification experiments were conducted to test the hypothesis that lowering the pH to practically achievable levels (pH 7) in the field would re-establish a sorptive environment for As(V) and decrease the dissolved concentrations significantly. Oxic groundwater samples from Sites 4, 6, 7 and 8 were shaken and mixed with the corresponding site's sediment in triplicates using 1g:10mL solid to solution ratio. Sets of the samples from each site were acidified to lower pH target levels and one set served as the control with no acidification. Samples were capped and continuously mixed with orbital shaker during the experiment. pH values were recorded before and after the initial mixture and also as the acidification progressed by adding increments of 1N HCl. pH values were measured and adjusted daily to keep at the target values.

Following the stabilization of the pH levels (12 days), the triplicate suspensions were centrifuged, supernatant filtered (0.45 μm) and preserved by adding concentrated HCl to 0.2% v/v.

2.9. Acid Titrations

In order to further understand the buffering behavior of aquifer systems, acid titrations were conducted for Sites 4 and 7 in batch setting. For each site, three sets of conditions were studied in duplicate: (1) suspensions of sediment and 0.1 M NaCl electrolyte solution; (2) suspensions of sediment and corresponding groundwater; (3) groundwater alone. Suspensions were mixed at solid/solution ratio of 1:10. The titrations were performed with incremental addition of 0.1 N HCl under continuous N_2 atmosphere and stirring.

2.10. BET Surface Area

Surface areas of samples were measured by N_2 and Kr adsorption isotherm using Micromeritics ASAP 2020 instrument by Brunauer–Emmett–Teller (BET) method.

2.11. Geochemical Modeling

The geochemical modeling computer program, PHREEQC Interactive Version 3 (Parkhurst and Appelo, 2013) was used for calculating chemical equilibrium speciation, mineral saturation indices, and to simulate the adsorption of As and other solutes using surface complexation modeling (SCM). TheMinteq.v4 (Allison et al., 1990) database was selected and used with certain modifications and additions as necessary.

Four different types of models were constructed for predicting and fitting the acidification experimental data in each sampling site. The models are described below and Table 3 presents the comparison among the model development parameters and assumptions.

2.11.1. Component Additivity-Electrostatic Models

Two of the models followed the CA approach and used electrostatic correction terms for describing the electrical double layer (referred to hereafter as CA-Oxalate and CA-Hydroxylamine model). For the electrostatic models, HFO was assumed to be the main reactive surface site assigned for adsorption of As and other solutes, in accordance with the internally consistent database of Diffuse Double Layer (DDL) model (Dzombak and Morel, 1990). The selected SCM accounts for ligand exchange reactions between solutes and surface hydroxyl groups and also the pH dependent surface charge of sorbent sites.

The method used for estimating the surface site concentration is the major distinction between the electrostatic models. Total sorption sites were calculated in these two models, using the Fe concentrations released from chemical extractions of amorphous iron minerals by oxalate and

hydroxylamine hydrochloride extractants. The calculations for total binding sites in CA models were conducted considering the assumed density of 0.2 mol of weak adsorption sites per mol of Fe.

The published surface reaction stoichiometries and complexation constants for HFO were used in these models without fitting to predict the data. The thermodynamic reactions and constants for surface complexation of major competing ions with HFO were incorporated in the model from reference sources (Dzombak and Morel ,1990; Allison, 1990; Swedlund and Webster, 1999; Appelo et al., 2002). Table 4 lists the intrinsic reaction constants for adsorption of As and other ions on HFO included in the PHREEQC input.

2.11.2. Generalized Composite-NEM Model

This model followed the GC approach strictly, without including the electrostatic factor (non-electrostatic model, referred to hereafter as the GC-BET model). The BET surface area measurements were used to calculate surface site concentrations using the 3.84μmol/m^2 site density in the GC model without including the electrostatic energy terms (Davis et al., 1998). This estimation method normalizes the contributions of all active sorbent phases to a defined average generic site.

In this model, the complexity introduced by the DDL theory is not considered and the pH dependence of adsorption is incorporated into the surface reaction constants fitted to the experimental data.

2.11.3. Hybrid Model

The hybrid CA/GC model (referred to hereafter as the Hybrid-Isotherm model) is similar to the CA models in terms of representation of electrostatic energy terms, however it uses a more

generalized method for estimating the sorbent site density and the surface reaction constants for As(V) and phosphate are fitted to experimental data.

The Langmuir-derived S_t parameter (mg As/kg sediment) values determined from the adsorption isotherm experiments were used to calculate the amount of surface sites in the hybrid model. The hybrid model uses HFO with the surface acidity constants and electrostatic correction terms of DDL model, as a surrogate site for adsorption of solutes.

2.11.4. Model Application

Models were run in PHREEQC to simulate the concentration of major parameters as a function of pH for comparison with the acidification experimental data (Input descriptions are available in the supplementary materials). The groundwater monitoring data and the acidification experiment control samples from current study were used to compile the solution input variables in the models. The values derived for surface site densities were normalized considering the solid to solution ratio used in the acidification experiments.

Depending on goodness of fit with the experimental data, the Hybrid-Isotherm and GC-BET models were iteratively run to achieve the best fits by optimizing the complexation reaction constants for surface species at each site. Hybrid-Isotherm model simulations were initially run using the surface complexation reaction constant values reported for HFO in literature as default values (Table 4). FITEQL (Herbelin and Westall, 1999) was employed to estimate the new adsorption equilibrium constants (log K values) fitting the experimental data in the GC-BET models by using nonlinear least square optimization method. The surface complexation constants in the GC-BET model were fitted first individually and then in combination for the reactions associated with the dominant surface species that would improve the fits. Generic surface sites

(site_z) without electrostatic considerations were defined and used instead of the default HFO database in the PHREEQC input to react with As(V).

The increase observed in concentrations of dissolved Ca from acidification experiments were used to estimate the starting amount of calcite present as the mineral phase in each site. The models were also run and compared to the acid titration experiments in order to revise the concentrations and phases responsible for the observed buffering to be included in the inputs.

The modeling was carried out first to simulate the acidification experiments as explained above and then used with certain alterations to assess several possible remediation approaches. Figure 2 illustrates the schematic conceptual framework for constructing the models.

3. Results

3.1. Historical Data.

Figure 3 shows the summary of historical pH trends and corresponding As(V) concentrations from selected groundwater monitoring wells within the area impacted by the contamination. A general relationship between the trends of elevated As(V) concentrations and occurrence of high pH values exists, suggesting that pH was a major factor controlling the mobility of As(V) in the groundwater.

3.2. Total As and Sequential Extractions

Total As in sediments ranged from 4.1 to 11.3 mg/kg, comparable to the global average of 5-7.5 mg/kg (Alloway 2013). Locations composed of brown sand, sites 2, 7 and 8 had lower total solid phase As concentrations (5.5, 4.1, and 4.7 mg/kg) while gray till sites 4 and 6 had higher values of 11.3 and 10.3 mg/kg, respectively.

In sites 4 and 6, however, the percentages of As associated with either of the labile phases, strongly adsorbed or amorphous Fe, were lower than for the other three sites, indicating a larger

fraction of As was present in recalcitrant forms (see Figure 4 and Table 5 for sequential extraction results).

The results also indicate that the downgradient sites (7 and 8) have lower total As, but a higher percentage of exchangeable As. While sites 2, 7, and 8 are similar with higher fractions in both labile phases, site 2 which is upgradient, has lower As (both in absolute terms and percentage) in the adsorbed phase. This is what would be expected after significant mobilization of As occurring in upgradient locations.

The similarity observed between the solid As fractions for Site 7, which lies within the As(V) plume, and the un-impacted Site 8 could indicate the minimal sorption of As(V) mobilized from upstream sites occurring at Site 7. Presence of significant phosphate concentration at Site 7 groundwater and competition for available sorption sites could be the major factor for explaining the lower than expected total solid bound As.

3.3. Adsorption Isotherms

Adsorption isotherms are useful empirical tools for studying mobility and fate of contaminants in natural environments. Researchers have used the Langmuir isotherm in both pH dependent adsorption and transport models for As (Jeppu et al., 2012; Radu et al., 2008). The maximum sorption capacity derived from the Langmuir model was one of the methods used in this study to estimate the concentration of sorption sites in the CA/GC approach.

The Langmuir isotherm parameters of K (binding strength coefficient, L/mg) and S_t (maximum sorption capacity, mg/kg) were calculated by using the non-linear regression fit spreadsheet developed by Bolster, 2007 (See Table 6). The use of non-linear regression was selected in order to avoid the statistical limitations caused by using the linearized forms of the Langmuir equation.

The adsorption isotherm results generally fall into the category of "L" isotherms without a strict plateau although such interpretations are often difficult (Limousin et al, 2007). The As(V) concentration range used in the isotherm experiments was selected to be environmentally relevant for the adsorptive processes. At higher concentrations of solutes, the retention mechanism generally transitions from monolayer surface coverage (i.e. adsorption) to multi-layer surface precipitation resulting in a continuous increase observed in the sorptive capacity (Farley et al., 1985).

Results showed that the un-impacted Site 8 has the highest S_t value and consequently largest number of sorption sites for As(V) sorption (Table 6 and Figure 5). Dramatic differences were observed in the fraction adsorbed at the lowest initial concentration in the isotherms.

At C_0 of 50µg/L, Sites 4 and 7 which are the most impacted sites with highest As concentrations in groundwater are the least sorptive sediments (0-5%) while un-impacted Site 8 sediment sorbs the As(V) in solution completely to below detection limit (<1 ppb). Site 6 which historically has been exposed to lower As concentrations in the range of 100-200 ppb and adsorbs 85% of the spiked concentration.

3.4. Acidification Experiments

As a preliminary investigation of the potential for groundwater acidification as a remediation scheme, batch acidification experiments were conducted with the purpose of measuring the changes in dissolved As concentrations (Table 7). The most significant change in As(V) concentrations occurs in Site 4 with a 63% decrease at pH 7.3 relative to the control. At this location, the control (no acidification) had 460 µg/L As at pH 8.4 while the treated samples at pH 7.7 and 7.3 had As(V) levels of 269 and 170 µg/L respectively. For Sites 6, a 50% decrease in

As(V) concentration was observed at pH 7. At site 7 however, As(V) levels did not significantly change and remained relatively stable (<10% decrease).

The insignificant changes observed in Site 7 could be related to the significantly higher concentrations of phosphate acting as a competing ion in the groundwater from this site and therefore inhibiting the As(V) sorption. Groundwater from Site 8 was already at relatively much lower initial dissolved As(V) concentrations that underwent further removal by lowering the pH.

The substantial increase in dissolved Ca concentrations in Sites 4 and 6 indicates that the dissolution of calcite minerals, known to be present at these two sites, is occurring. The increase in Ca concentration was used to calculate the initial amount of calcite present in the geochemical model inputs for the two mentioned sites. At Site 7 however, the dissolved Ca increased very moderately in agreement with the lower level of pH buffering observed.

3.5. Acid Titration Results

Different levels of pH-buffering were observed during the acidification experiments. Site 4 had the highest buffering capacity which corresponds to the significant increase in dissolved Ca concentrations during the acidification experiments followed by Sites 6 and 7.

Understanding the pH-buffering capacity of the sediment and groundwater is critical for assessing the potential effectiveness and practicality of in-situ remediation by acidification. The acid titration experiments in Sites 4 and 7 were conducted to investigate buffering in more detail. Site 4 sediment and the sediment-grounwater combination exhibited a significantly larger buffering capacity, which is also supported by presence of significant calcite pool evident in acidification experiments (Figure 6).

For groundwater, while having a similar initial pH as Site 4, groundwater in Site 7 exhibited a somewhat higher level of buffering. This is in agreement with the higher alkalinity measured at

Site 7 groundwater (150 mg/L as $CaCO_3$) compared to Site 4 (100 mg/L as $CaCO_3$). These results suggest that the overall more significant pH-buffering evident in Site 4 is mostly due to the solid phase reactions such as carbonates dissolution, whereas in Site 7 buffering is mainly controlled by the reactions in the aqueous phase.

It is noteworthy that the experiments in the current study were conducted at the sediment/solution ratio of 1:10. Therefore it could be anticipated that the aquifer will exhibit a significantly higher level of pH- buffering.

3.6. Geochemical Modeling Results

3.6.1. Thermodynamic and buffering calculations

Aqueous speciation by PHREEQC indicates that As is mainly present as the arsenate oxyanions $H_2AsO_4^-$ and$HAsO_4^{2-}$which is expected for an oxic groundwater in the pH range studied here.

Calculated saturation indices (SI) by PHREEQC indicated that the solutions for all sites are undersaturated with respect to common As bearing minerals and metal arsenates.

Fe (III) oxides, ferrihydrite, goethite and hematite are found to be all supersaturated in the studied sites with assumption of an oxidizing environment based on the field data (pe = 4). The calculated SI values indicate that the system in Site 7 with noticeable phosphate concentrations (8.9 mg/L) is supersaturated with respect to several apatite minerals such as hydroxylapatite and FCO3apatite. Calcium phosphate mineral phases $CaHPO_4$ and $Ca_3(PO_4)_2$, however, have SI values closer to zero, indicating equilibrium

PHREEQC was also used to model the solid phase pH buffering in Sites 4 and 7 and the models fit the experimental data well (Figure 6). These simulations are based only on the calcite content estimated from acidification experiments and without including any gas phase inputted in the model.

3.6.2.Acidification simulation

Models for the selected sampling locations (Sites 4, 6, 7 and 8) built in PHREEQC used surface site densities derived from adsorption isotherms, two different chemical extractions of amorphous Fe oxides, and BET surface area measurements. The goodness of fit of the model predictions to experimental data was quantified by calculating the normalized root mean square error (NRMSE):

$$NRMSE = \sqrt{\frac{\sum\left(\frac{C_{exp}-C_{mod}}{C_0}\right)^2}{n_{exp}}}$$

where, C_{exp} is the measured aqueous concentration, C_{mod} is the simulated aqueous concentration, C_0 is the initial aqueous concentration, and n_{exp} is the number of experimental data points. Results of the different model simulations for As and phosphate concentrations are illustrated in Figure 7 and Table 8 lists the NRMSE values for model fits.

The CA-Hydroxylamine and CA-Oxalate models underestimate the sorption of As in Site 4 while overestimating the results in Site 6 for the higher pH ranges. Bigger disagreement between these two models and experimental data exist in Site 7 where the CA model predictions show increase in dissolved As(V) concentration instead of the slight decreasing trend of As(V) observed. In Site 8, due to the low initial concentration of As(V) and lack of significant adsorption competition, all models exhibit similar trends and yield reasonably good fits with the data. The CA-Oxalate model yields good fits (NRMSE<5%) to phosphate data in Sites 6 and 7 (Figure 7e) while the CA-Hydroxylamine model overestimates the adsorption at most pH values. The Hybrid-Isotherm and GC-BET models exhibit moderate to good agreements in fitting the experimental As(V) and phosphate data in all sites.

In the Hybrid-Isotherm based method, a single surface site type based on the HFO characteristics and consistent with the DDL model was employed to simulate the data by allowing the modification of the reaction constants. Table 9 lists the adjusted surface reaction constants for -Hybrid-Isotherm model in comparison to the default values for HFO database. It can be noted that only the two reactions for the negatively charges surface species needed to be modified and the reaction constant for the neutral As-surface species was not modified in any of the sites as this reaction is only important at the lower range of pH values.

The Hybrid-Isotherm models were capable of adequately simulating the adsorption of As(V) in all four sites. The different rates of modeled As(V) removal among the studied sites were strongly influenced by the magnitude of phosphate concentrations present and the consequent competition for sorption sites. This was verified by calculating and comparing the distribution of surface species in equilibrium with the groundwater. Figure 8 shows the calculated distribution of surface species by Hybrid-Isotherm model for Sites 4 and 7 at pH 7. In Site 7, about 98% of available sorption sites are occupied by other solutes, mainly competing ions PO_4, Si and CO_3. In Site 4 however, As(V) outcompetes the much lower level of phosphate present, occupying 12% of surface sites which corresponds to the higher level of As(V) adsorption observed experimentally.

Due to the surface reaction constants being sensitive to the total surface site number used and the fact that values derived from the BET method were significantly larger than the value estimated from other methods, FITEQL was utilized for the GC-BET models in order to obtain a quantitative goodness of fit for the fitted K values. The indicator for how well the experimental data are fitted is the weighted sum of squares of residuals divided by degrees of freedom (WSOS/DF) with the value of between 0.1 and 20 considered a good fit achieved in all cases.

It must be noted that all the surface reactions for complexation of other solutes with HFO were excluded from the input in the GC-BET models as these reactions and their log K values are only valid for adsorption on ferrihydrite surface (600 m^2/g) with a diffuse double layer model and assumed density of 0.2 moles sites per mole Fe. Therefore the fitted constants for As adsorption in GC-BET models are considered specific to the sediments studied and the total concentration of competing ions present. In the case of Site 6 and 7, surface reactions and species for complexation of dissolved phosphate were also included in the optimization process using FITEQL.

Derived reaction constants from FITEQL used in the GC-BET models are displayed in Table 10. With the exception of Site 7, in all cases only two surface reactions were needed to model the data. Similar to the Hybrid-Isotherm models, the neutrally charged surface species had no influence on fitting the data as the formation of negatively charged species are more important in the pH range studied. There are currently very scarce reaction constant values reported for natural oxidized sediments for direct comparison with the derived constants in this study.

4. Discussion

4.1. Acidification Experiments

While acidification in Site 4 produced the highest removal rates, the As(V) concentration at pH 7 was still significantly higher than the EPA standard limit of 10 μg/L. The other two sites (6 and 7) with high As(V) concentrations achieved moderate to minor decline in aqueous levels.

The acidification experiment results exhibit lower levels of As(V) retention on sediments with increasing levels of phosphate in solution. There are significantly higher levels of phosphate present in Site 6 and 7 groundwater which results in sorbed phosphate concentrations exceeding the sum of sorbed As(V) species and therefore limiting the overall As(V) removal rates. A

substantial body of research reported in the literature has shown that, phosphate is a major competing anion for adsorption of As(V) on solid phases due to similarities in aqueous chemical form and surface complexation behavior. Consequently a general relation exists between increasing dissolved phosphate and As in groundwaters.

The experimental and modeling results indicate that acidification alone will not be an effective remediation method for controlling the aqueous As(V) levels and needs to be implemented in combination with other approaches.

4.2.Surface Complexation Modeling

The CA-Hydroxylamine and CA-Oxalate models yield very similar results due to their comparable values of derived surface site densities. Using the default database reaction constants, the CA models are able to predict the general trend of experimental data in Site 4 and 8. However the CA models do not yield a good fit to As(V) data in Site 6 and 7 where multi-component adsorption becomes important and experimental results do not show appreciable changes in the As(V) concentrations. The Fe extraction based model, CA-Hydroxylamine overestimates the As(V) adsorption in Site 6 by about 50%, and predict desoprtion of As below pH 7.5 in Site 7. These results show the limited predictive application of CA models in more complex systems with a larger number of variables present.

The DDL database (Dzombak and Morel, 1990) contains three reactions for describing the sorption of As(V) on HFO but it does not include the constant for reaction resulting in formation of doubly negative charged species ($Hfo\_AsO_4^{-2}$) as it was indicated to be not effective in improving the fitting of data. The analogous reaction for formation of ($Site\_zAsO_4^{-2}$) was included in the non-electrostatic GC-BET models in this study to and it was found to improve the model fit significantly in Site 7 where highest level of competitive adsorption was present. However,

including it in the other models did not have any impact on the goodness of fit and therefore it was omitted.

Since the surface complexation constants in the GC-BET models are fitted to the experimental data at pH values >7 and do not include the uncharged complexes, the resulting models will not be capable of predicting As(V) or phosphate adsorption at lower pH values where these surface complexes become important. On the other hand, the Hybrid-Isotherm models which include the unchanged reaction constants from DDL database for these uncharged complexes, can be used for obtaining predictions in the lower pH range but their performances need to be further evaluated.

It should be noted that the equilibrium constants for the analogous surface reactions and species should not be directly compared between the Hybrid-isotherm and GC-BET models as there are wide differences between the values of total surface site concentration used in the two models. The choice of determining the number of surface sites affects the resulting reaction constants significantly. Also, the pH dependence of adsorption is simulated differently between the two models as the Hybrid-Isotherm model incorporates the HFO surface acidity constants and the DDL theory, but the GC-BET model compensates for the absence of these factors by changing the distribution of surface speciation as a function of pH.

4.3. Comparison of Methods for Determining the Adsorption Capacity of Sediments

Quantification of the total number of surface sites is an essential component of any SCM. There is an inherent difficulty in accurately determining the relative abundance of sorbent constituents of a heterogeneous mixture and such data are rarely available for describing the retention of solutes by sediments. In this study, four different methods for calculating the concentration of total sorption sites for use in the models were implemented (see Figure 9). These methods

include using the Langmuir S_t parameter, two extraction methods aimed at dissolving amorphous iron oxides, and the BET surface area measurement.

The method of using the S_t parameter from the empirical Langmuir isotherm model in developing a mechanistic SCM seems promising since it could be used as a normalizing measure for determining the maximum number of sorption sites not exclusive to any specific sorbent solid phases. In this method, the maximum sorption capacity for As(V), (S_t) is converted to moles of sorption sites by assuming a 1:1 molar ratio between As and sorption sites. This values is then normalized to the solid/solution ratio and converted to moles of HFO by using the density of 0.2 sites/mol HFO (Dzombak and Morel, 1990).

Compared to the other estimation methods, using the adsorption isotherm could minimize the risk of overestimation of available surface sites by not including the sites pre-occupied by other adsorbates. Using S_t could also avoid potential underestimation by acting as a pool for the contribution of all reactive sorption sites and not just considering certain phases as is the case with extraction methods. Nonetheless, interpretation of adsorption isotherm results could be difficult to definitively determine what general shape they follow. Another difficulty is determining whether the isotherm has reached maximum monolayer surface coverage or surface precipitation is occurring and being responsible for the observed sorption. As the concentration of dissolved solute increases, the sorption mechanism transitions from surface adsorption reaction to solid solution surface precipitation. Consequently, the choice of maximum concentration of solute in an adsorption isotherm experiment becomes important as it could also be a factor in underestimating or overestimating the sorption site density.

A great number of the published studies have used chemical extraction of poorly crystalline Fe oxides as the method for determining the surface site densities of sorbents used in SCM (Jung et

al., 2012; Robinson et al., 2011;Sharif et al., 2011). The assumption used is that the Fe oxide phases are principally responsible for the sorption of solutes.

In this study, hydroxylamine extraction method yields larger number of sites comparing to oxalate method in all cases. This is in contrast with the fact that oxalate is reported to be a more aggressive extractant than hydroxylamine hydrochloride as it is not strictly selective to amorphous phases and could potentially extract crystalline constituents (Anwar et al., 2008; Rodriguez et al., 2003).

With the exception of the un-impacted Site 8, the extraction and isotherm methods result in relatively similar number of sites and values are in the same order of magnitude. In the upgradient contaminated sites, Langmuir St estimation gives the smallest value relative to other methods, suggesting that the sorption sites are already occupied to some extent by As or other solutes in the plume. Therefore, using Fe concentrations from chemical extractions as often done in the published studies, could lead to potential overestimation of adsorption results if not taking into consideration the sites previously occupied by adsorbates and/or not reactive with regard to the solute of interest.

However, Site 8 exhibits a different behavior and the isotherm derived value is much larger than values from extraction methods and only slightly smaller than the BET derived number. The Langmuir isotherm and BET surface area derived values generally represent the contribution of all of the sorptive surfaces as opposed to the selective extractions targeting specific phases such as amorphous Fe oxides. This suggests that the un-impacted Site 8 has significantly larger number of available surface sites for As adsorption which are not only attributed to amorphous Fe oxides but also to other sorptive phases present in the solid matrix. This indicates that

selective extraction methods could also lead to underestimation of adsorption results in these aquifer sediments by neglecting the other available adsorbent phases.

Characterization of the aquifer sediments with respect to ability for re-adsorbing As is of critical importance if efforts for remediation of As at this site are to be considered. The findings from the batch adsorption experiments show that the highest number of available sites for sorption of As exist at the un-impacted Site 8 outside of the known boundaries of high-pH groundwater affected areas.

Although sequential extractions data show close similarities between the solid phase distribution and total content of As between Sites 7 and 8, Site 8 exhibits more than a 2 fold higher number of total adsorption sites (S_t). A combination of induced geochemical changes due to high pH waste plume and occupation of active surface sites by competing ions could be responsible for the significantly lower adsorption sites in Site 7.

It has been shown in the literature that iron and aluminum oxide content in addition to pH and cation exchange capacity are the most important soil parameters that correlate with adsorption isotherm coefficients (Selim, 2014). Greater content of metal oxides result in more significant retention of anions such as the dominant oxidized arsenic species.

Positive correlation exists between the total solid phase Fe concentrations and the Langmuir St values among the studied impacted sites (Supplementary material). However the un-impacted Site 8 does not follow this trend which could be evidence for presence of major sorbent constituents other than Fe oxides or larger fraction of free binding sites compared to the impacted sediments due to lack of historical contamination at this site.

In the contaminated sites (4, 6 and 7), the determination of surface sites based on BET surface area measurements results in significantly larger values than those derived from the Langmuir

S_t. However, in the un-contaminated Site 8, the BET and Langmuir St derived values are very close. This suggests that the maximum surface site given by the BET measurement has been diminished in the historically contaminated zone and only a fraction of sites are available for adsorption of As(V).

Also, among the contaminated sites, the upgradient Sites 4 and 6 solids, have been in contact with the contaminants for a longer period compared to the downgradient Site 7 and have higher concentrations of pre-adsorbed solutes; therefore the average ratio of free sites (Langmuir derived) to Fe oxide sites (extraction derived) increases from upgradient to downgradient.

4.4. Future Studies

The SCM simulations are strongly influenced by the amount of total surface sites assigned in the models (HFO or generic sites). Although the competing ions concentrations at Site 4 are relatively lower than Sites 6 and 7, the number of surface sites is still not sufficient to decrease As(V) in the liquid phase to the regulatory levels.

Thermodynamic calculations by PHREEQC show that several Fe (III) (hydr)oxides are supersaturated over a wide range of pH. In the acidification models, the dissolved Fe in groundwater instantly precipitates as the mineral phase which is allowed to form in the model input (ferrihydrite, goethite or hematite). Although this finding does not bear any kinetic information, it has implications for potential remediation strategies by promoting the precipitation and formation of additional surface sites.

Only few studies have used SCM tools to study the natural attenuation and effectiveness of using stabilizing amendments for metal contaminated sites (Komarek et al., 2013). In particular, there is also a lack of data available in the literature from applications of geochemical modeling for remediation of As contaminated environments (Moldovan et al., 2005).

The developed Hybrid-Isotherm models for simulating the acidification experiments in PHREEQC were subsequently used to assess several potential schemes of As remediation by acidification and promoted natural attenuation (Figure 10). Site 4 acidification model was modified by using the solid characteristics of un-impacted Site 8. This alteration and increase in the number of sorption sites (S_t) in addition to lowering the pH resulted in significant improvement of As(V) removal. This method achieved desirable As levels below the standard drinking water limits at pH 7.5. However the strategy of equilibrating the groundwater with Site 8 solid phase did not achieve the same results in Sites 6 and 7. At these two sites, in order to decrease As(V) concentration to desirable levels within a practical pH range, dissolved phosphate concentrations also had to be lowered to 1 ppm prior to acidifying the solution.

The knowledge gained from these batch scale experiments was used to develop models that will serve as a building block of future reactive transport models for predicting column scale scenarios. Further experiments will be needed to evaluate the predictive capabilities of the developed models and effectiveness of potential methods for remediation of As(V). Developed models in this study will be applied in future column studies to study the transport of As(V) in both contaminated and un-contaminated zones.

5. Conclusions

Arsenic is mainly present as As(V), arsenate under oxidizing conditions at the study site and was desorbed from the host iron oxide minerals at high pH values. Laboratory experiments on natural sediment and groundwater samples were conducted to characterize the geochemical conditions at the site, and in order to contribute to the development of a model that will allow simulating various remediation strategies. The experimental results show that the dissolved As concentration in this oxidizing system is overall controlled by pH, number of available sorption

sites and presence of competing ions

In the current study, we used modeling tools PHREEQC and FITEQL, site-specific field and laboratory data, default SCM databases for surface site characteristics (HFO) and surface reaction constants for major ions from literature in order to develop preliminary geochemical models. Models were refined step-wise and the complexation reaction constants were adjusted for achieving the best fit to the experimental data for As(V) and other major competing ion. The developed Hybrid-Isotherm models were used to simulate different remediation scenarios by incorporating the obtained site-specific reaction constants. This model is based on a hybrid approach to implementing SCM for heterogeneous sorbents and could be used as a best engineering estimate for practical applications.

The different results among the impacted and un-impacted sites indicate that the historical levels of solutes in contact with the sediments play a significant role in analyzing and interpreting the sorptive behavior and retention capacity of such heterogeneous systems.

If the source of As(V) contamination at this site is the mobilization from natural soils, then the remediation question that needs to be answered is whether and how the conditions can be reversed to immobilize the As(V). The acidification experiments were moderately successful at lowering As(V) concentration in Sites 4 and 6. An indication of the modeling results is that even with the extension of the acidification process the As(V) concentrations in the most affected sites would not meet the EPA standard levels of 10 μg/L. Both experimental and modeling outcomes demonstrate the significant influence of phosphate concentrations on As(V) attenuation. The results indicate that combining methods for removal of dissolved phosphate from sites 6 and 7 could be beneficial to As(V) immobilization process by reducing the competition factor. The modeling results also show that in addition to lower pH, the number of total HFO sorption sites

is the major controlling factor for As(V) removal. Future column studies are needed to evaluate the predictive capabilities of models for reactive transport of contaminants.

Figures

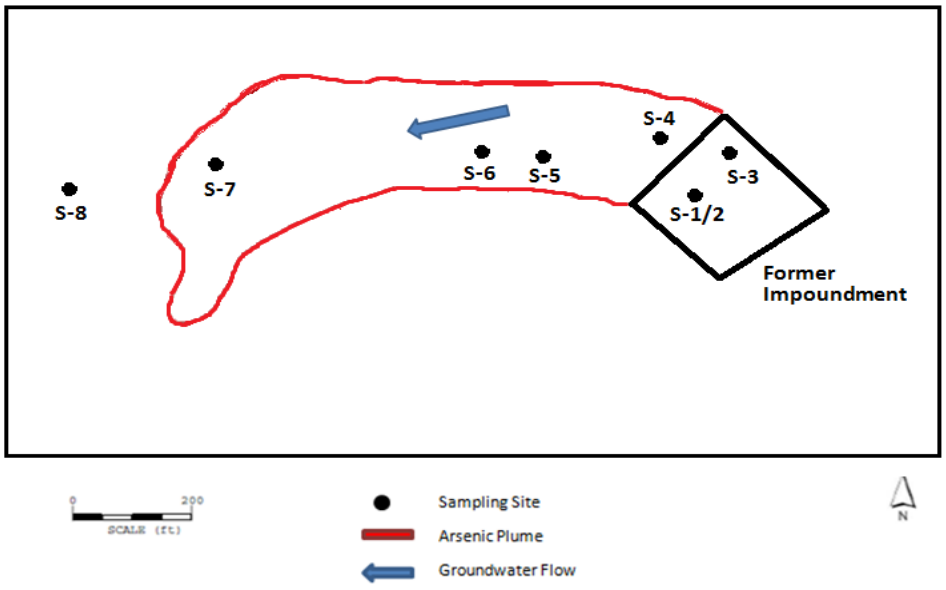

Figure 1. Map of the site showing the former impoundment location and extent of As plume

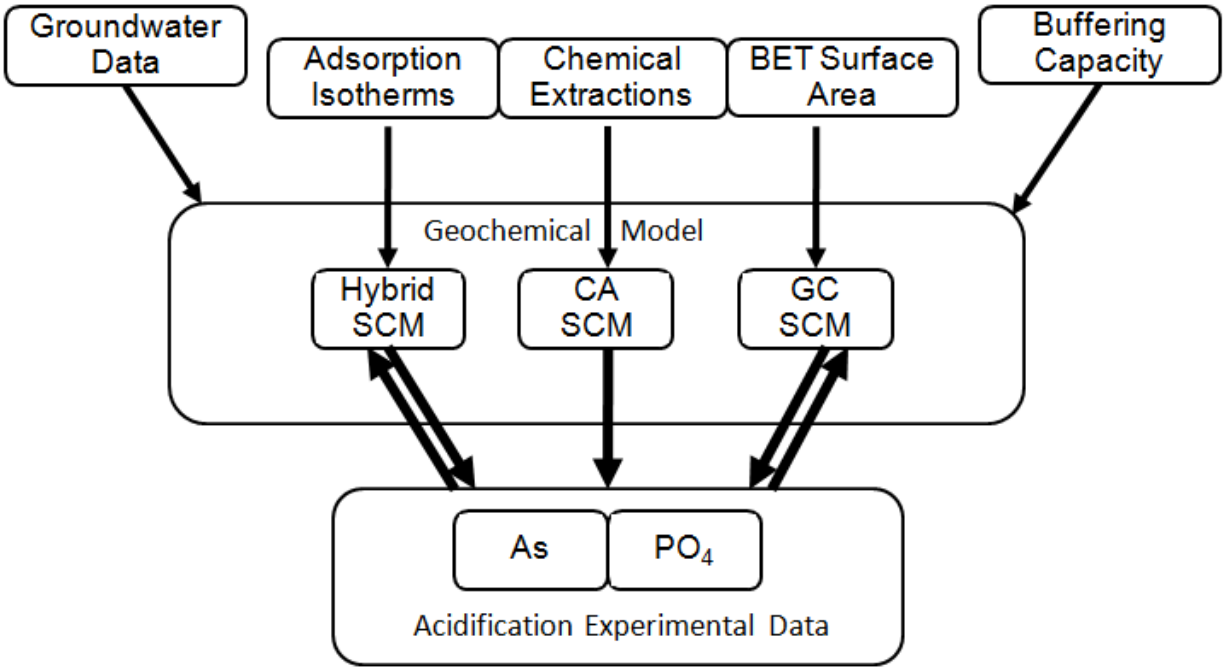

Figure 2. Schematic framework of geochemical modeling procedure implemented in this study

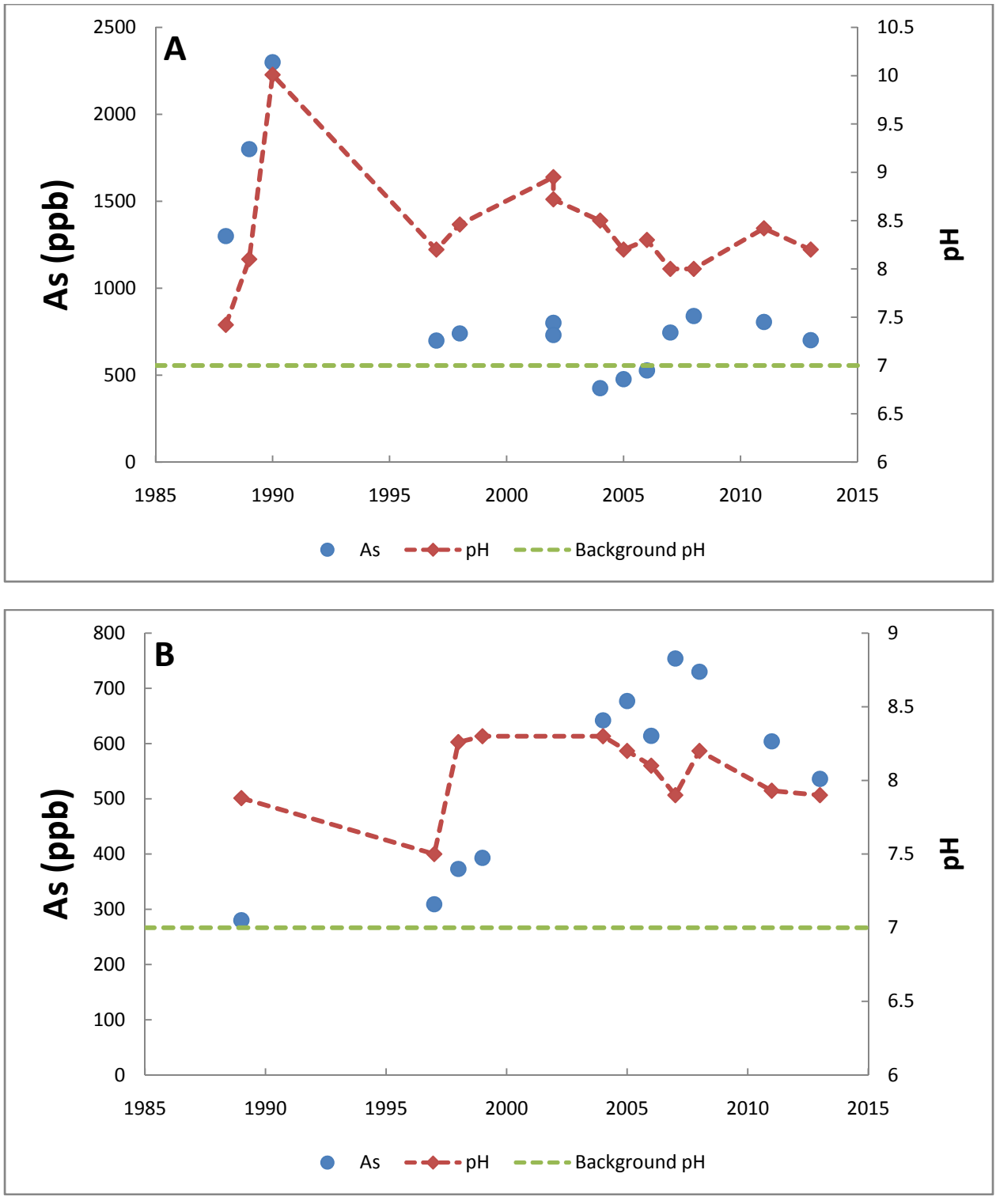

Figure 3. As concentrations and pH values at monitoring wells near (A) Site 4 and (B) Site 7 sampling locations, downgradient of waste impoundments.

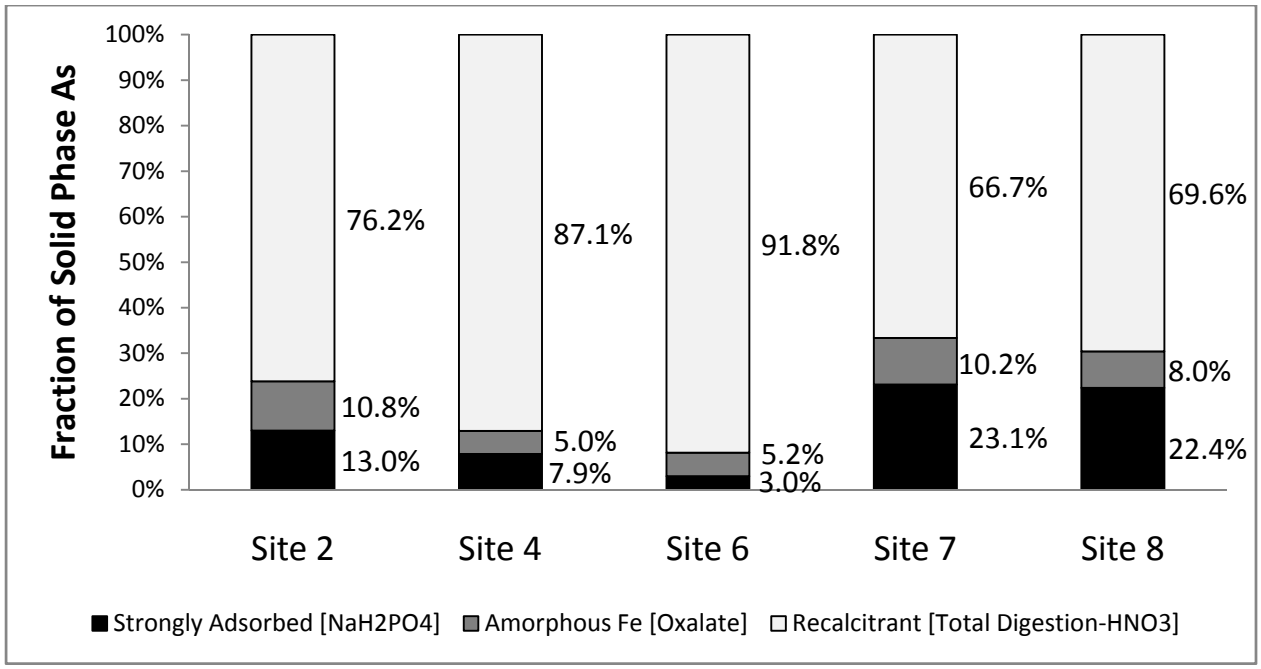

Figure 4. Distribution of solid phase As concentrations derived from sequential extraction of sediment samples.

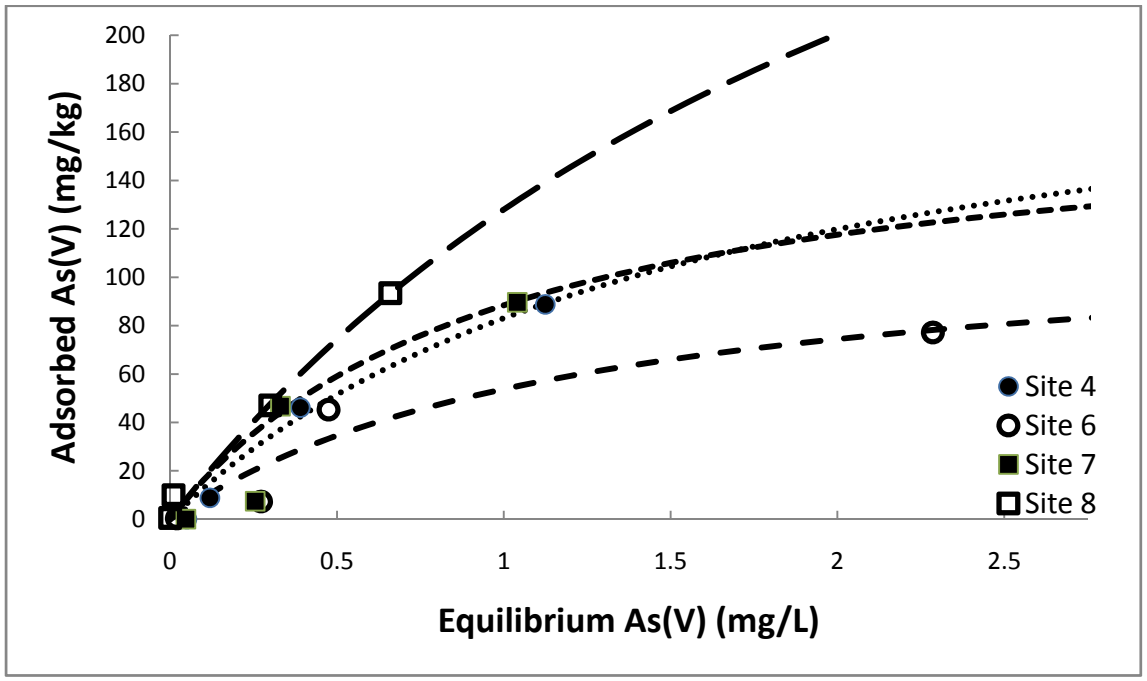

Figure 5. Experimental As(V) adsorption as a function of equilibrium concentration. Dashed lines represent Langmuir model fitted to experimental data using nonlinear least squares regression.

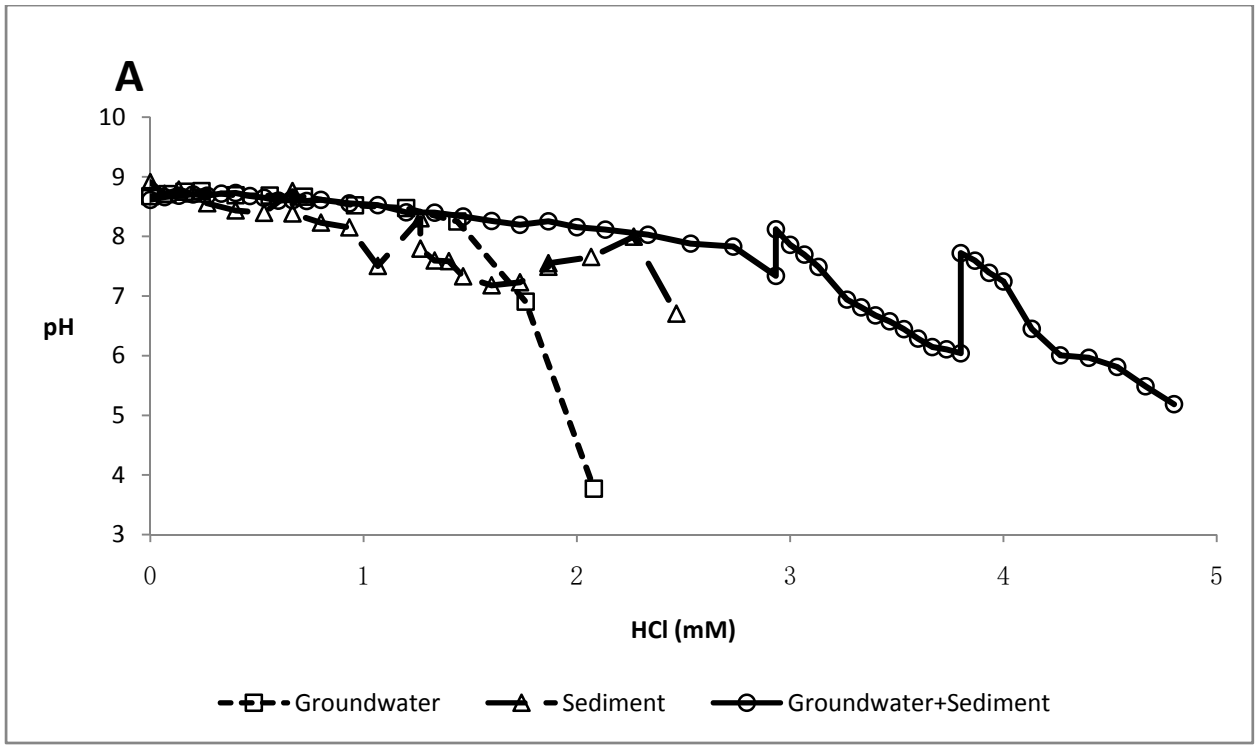
A
10
9
8
7
6
5
4
3
pH
0
1
2
3
4
5
HCl (mM)
Groundwater
Sediment
Groundwater+Sediment

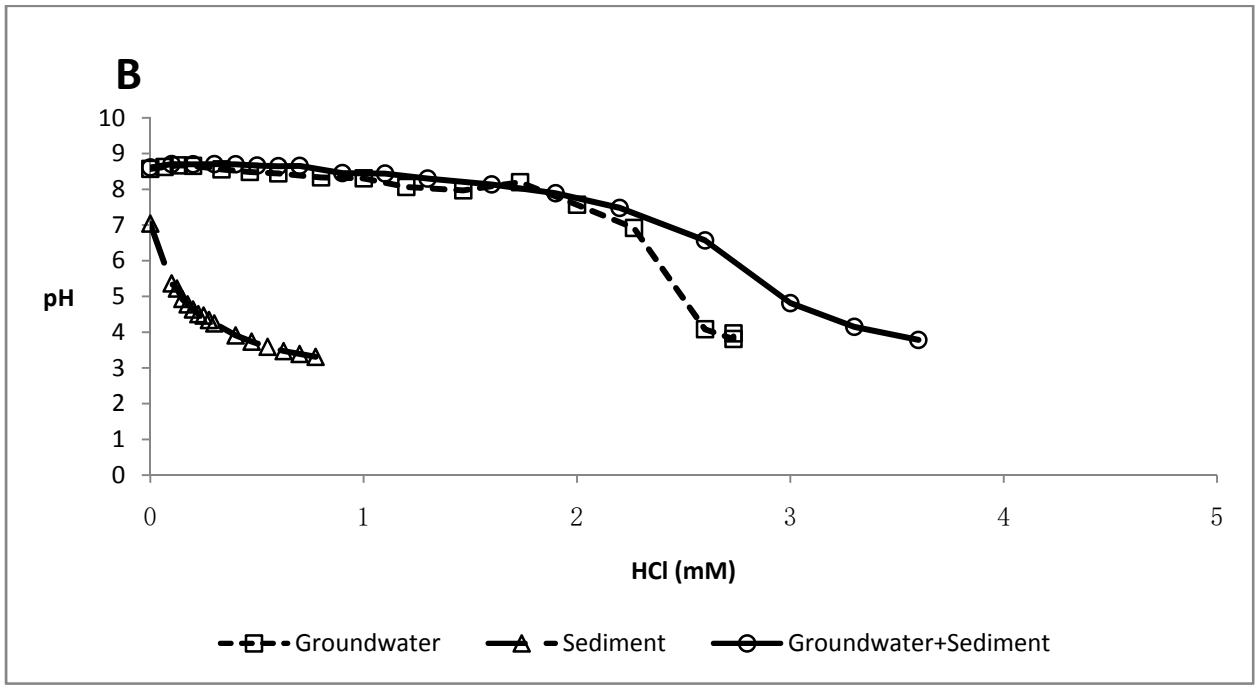
B
10
9
8
7
6
5
4
3
2
1
0
pH
0
1
2
3
4
5
HCl (mM)
Groundwater
Sediment
Groundwater+Sediment

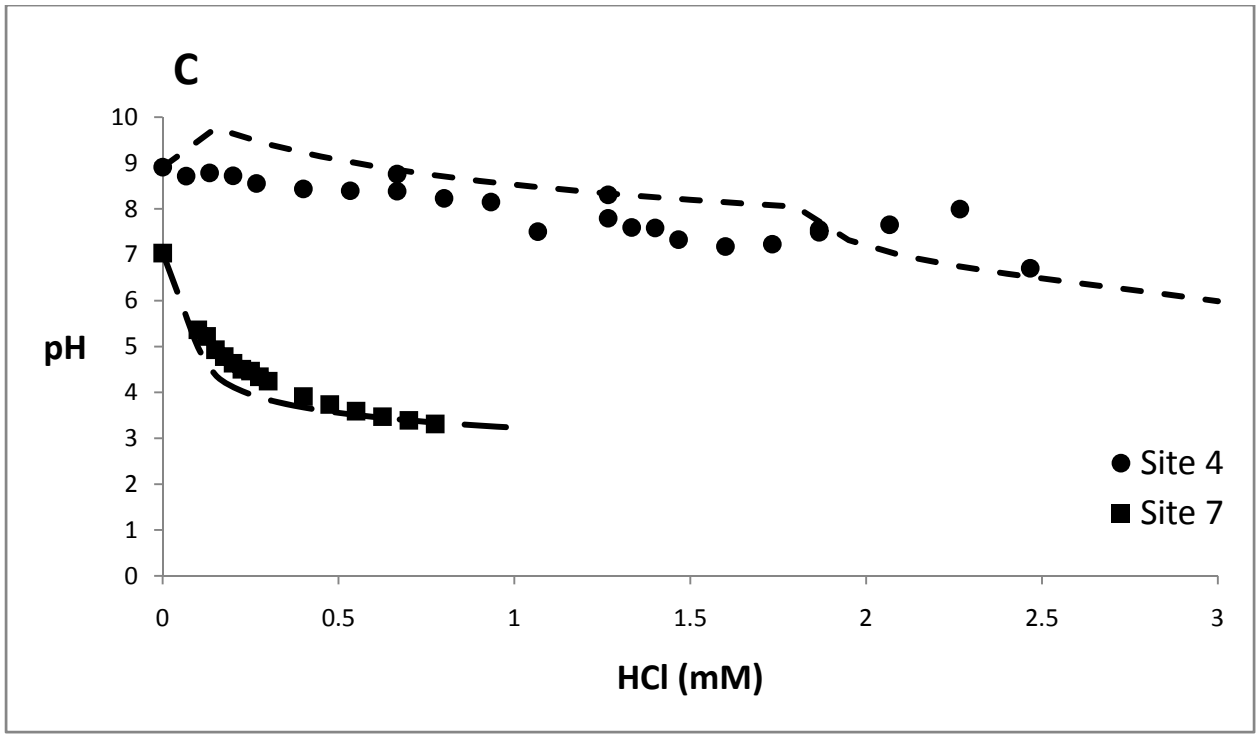

Figure 6. Acid titration experimental results for (A) Site 4, (B) Site 7. Experimental and modeling results (dashed lines) for pH buffering of sediments (C).

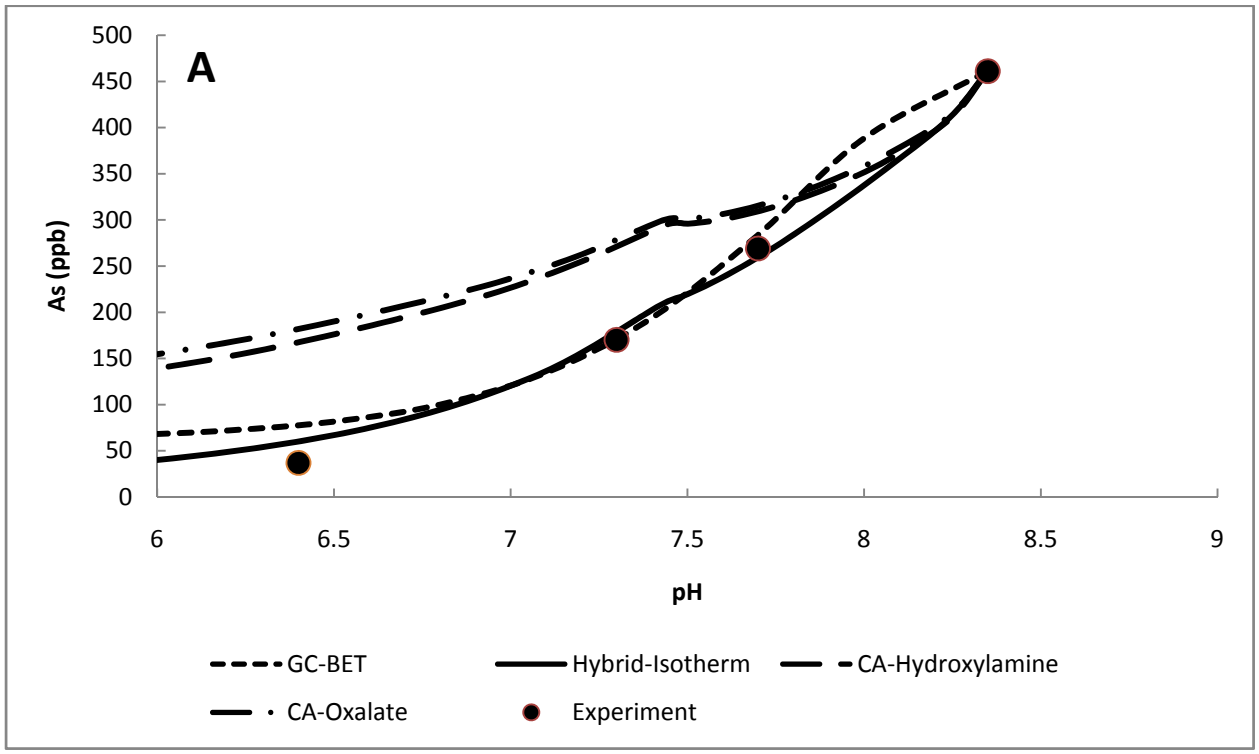

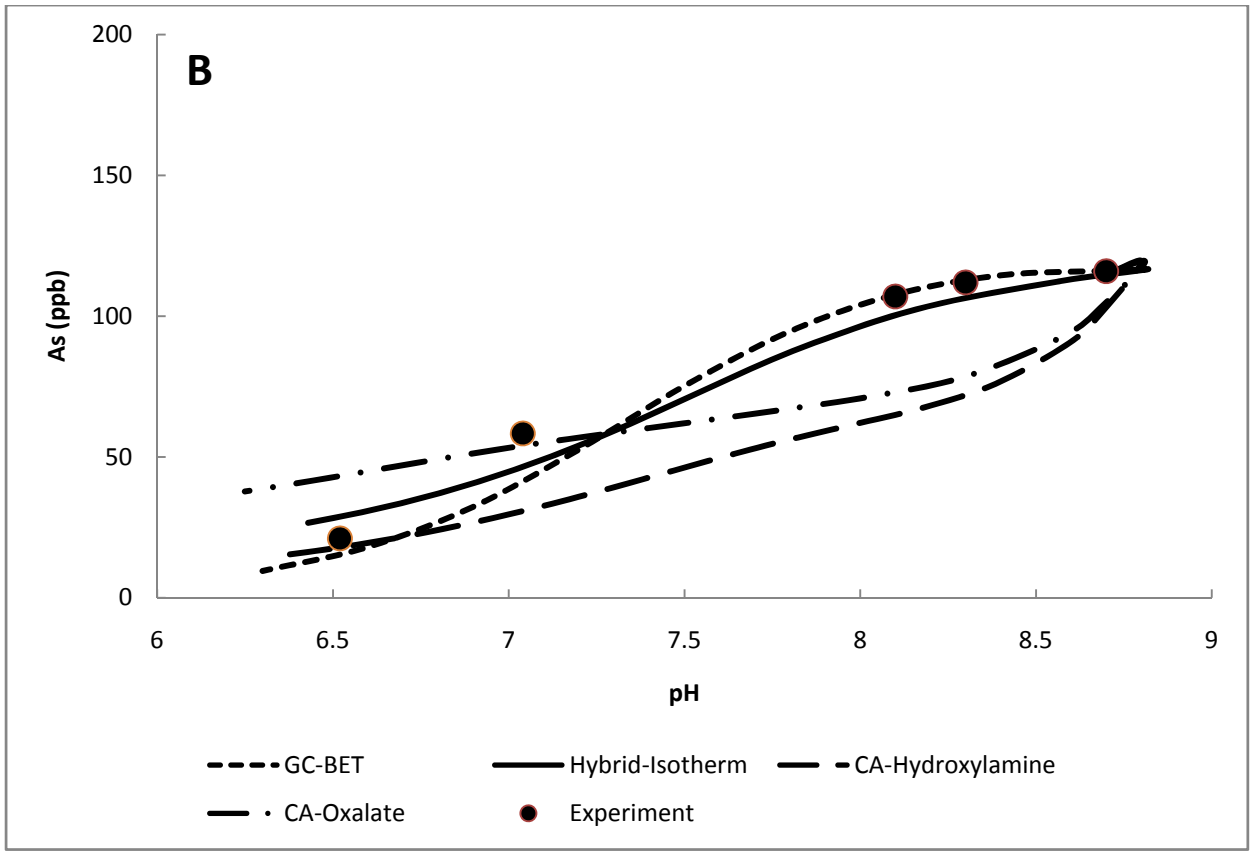
B
200
150
100
50
0
As (ppb)
6
6.5
7
7.5
8
8.5
9
pH
GC-BET
Hybrid-Isotherm
CA-Hydroxylamine
CA-Oxalate
Experiment

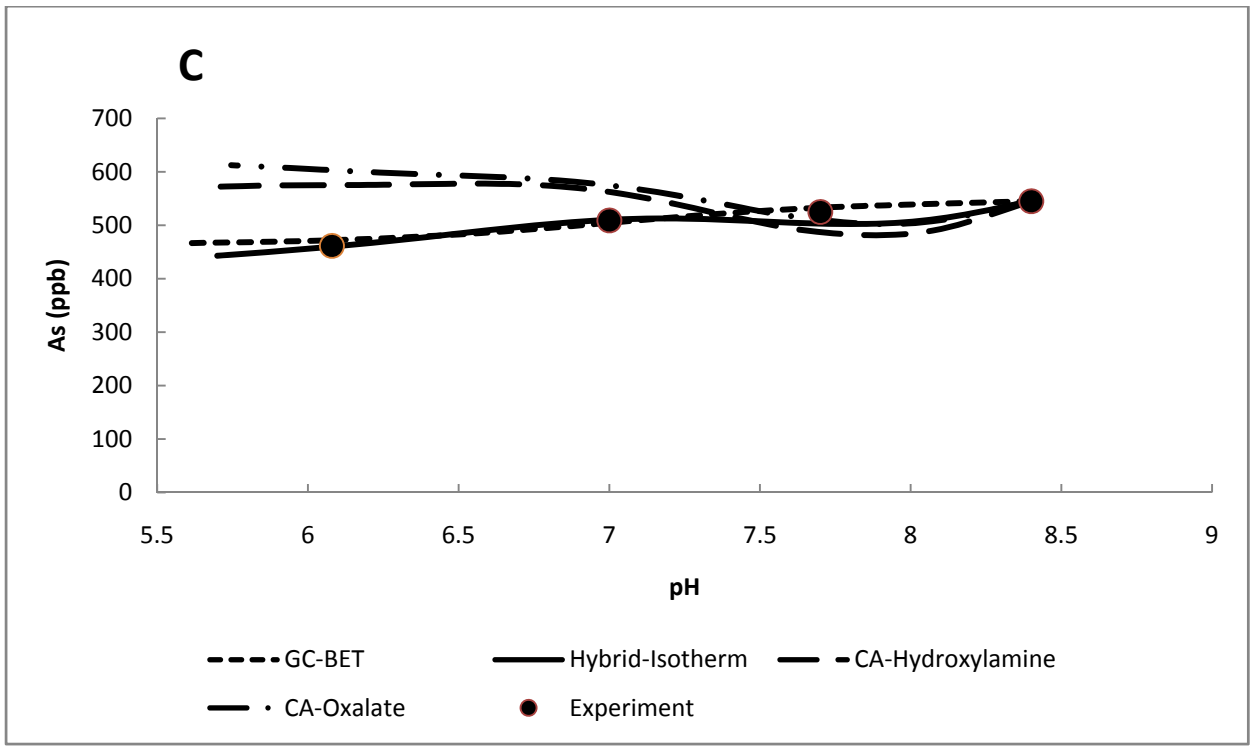
C
700
600
500
400
300
200
100
0
As (ppb)
5.5
6
6.5
7
7.5
8
8.5
9
pH
GC-BET
Hybrid-Isotherm
CA-Hydroxylamine
CA-Oxalate
Experiment

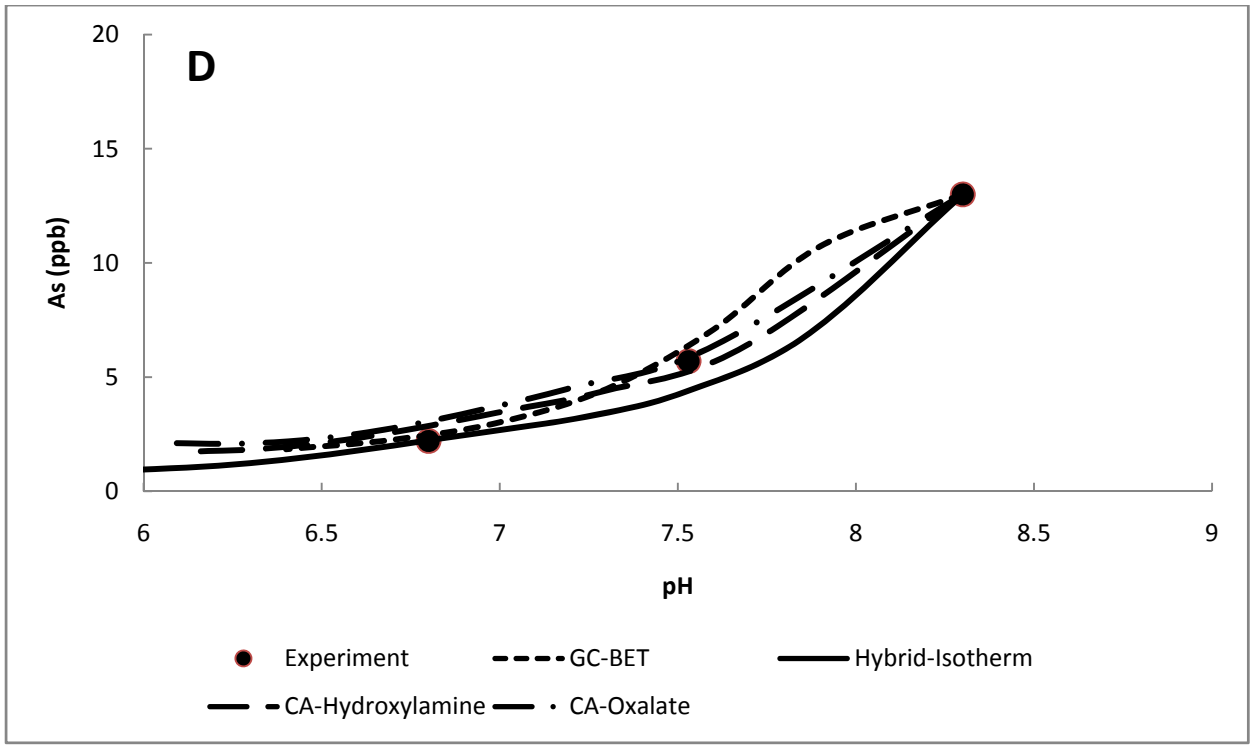
D
20
15
10
5
0
As (ppb)
6
6.5
7
7.5
8
8.5
9
pH
Experiment
GC-BET
Hybrid-Isotherm
CA-Hydroxylamine
CA-Oxalate

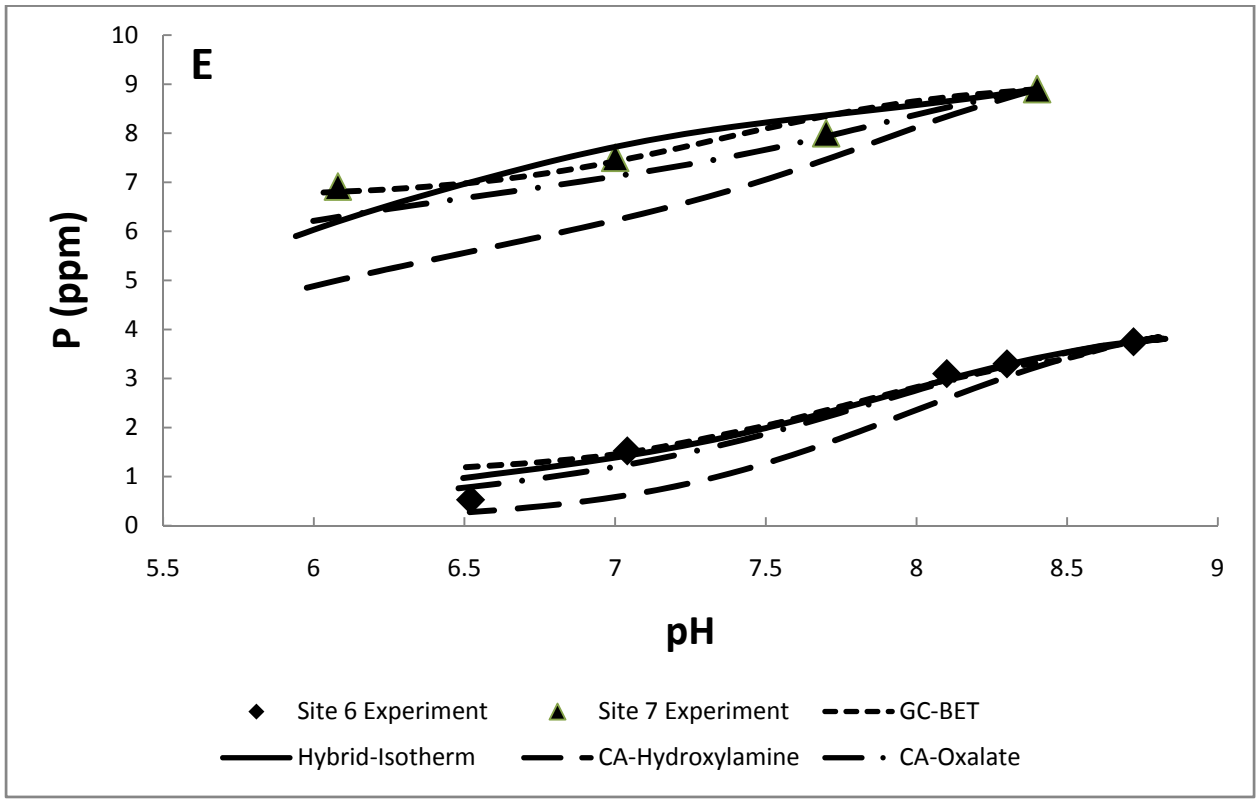
E
10
9
8
7
6
5
4
3
2
1
0
P (ppm)
5.5
6
6.5
7
7.5
8
8.5
9
pH
Site 6 Experiment
Site 7 Experiment
GC-BET
Hybrid-Isotherm
CA-Hydroxylamine
CA-Oxalate

Figure 7. Dissolved As(V) in acidification experiments compared with the modeling simulations for (A) Sites 4, (B) Site 6, (C) Site 7, and (D) Site 8. Dissolved phosphate concentrations in acidification experiments compared with the modeling simulations for Sites 6 and 7 (E)

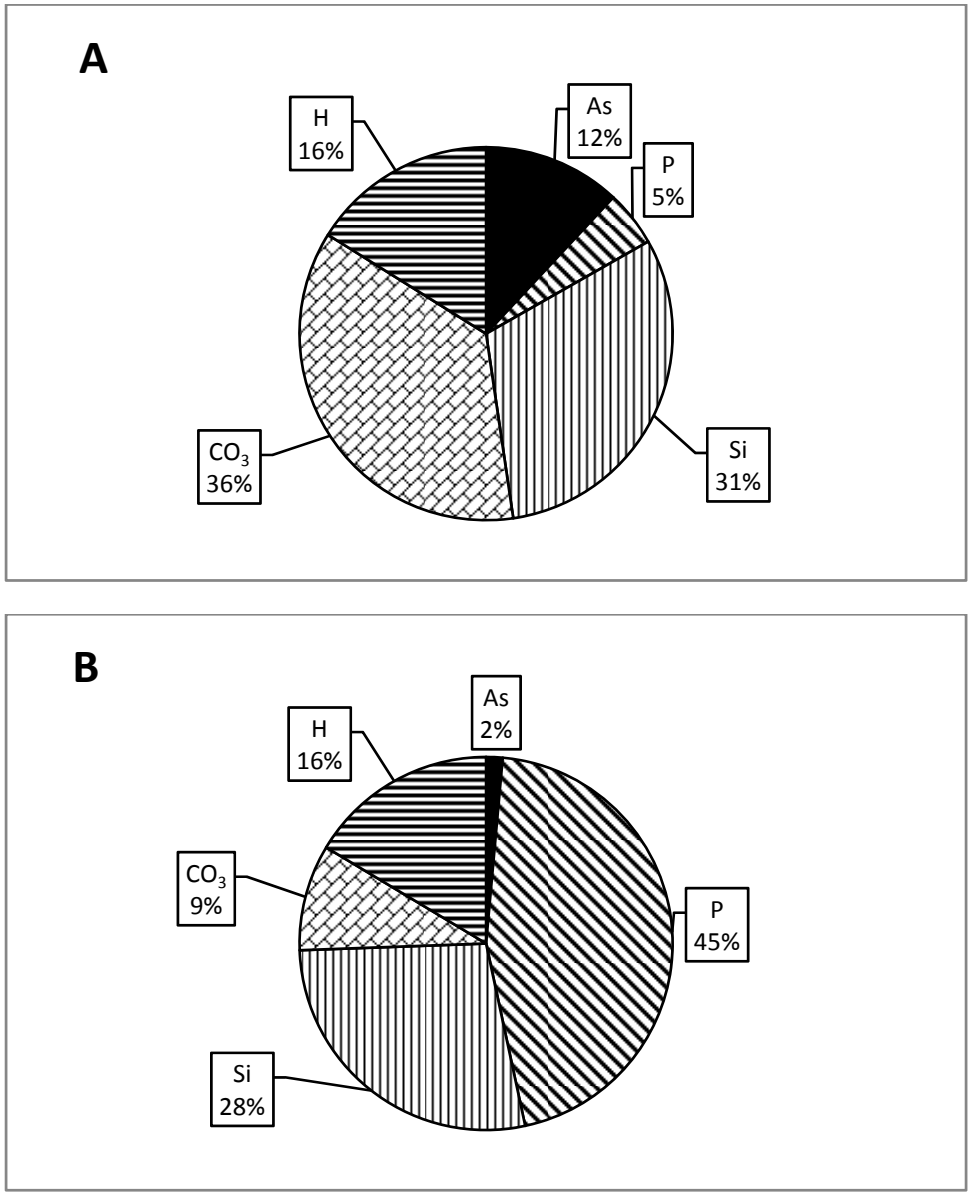

Figure 8. Simulated distribution (%) of surface species at pH 7 for (A) Site 4, (B) Site 7.
The field for each parameter in the pie chart is the sum of all surface species associate with the solute.

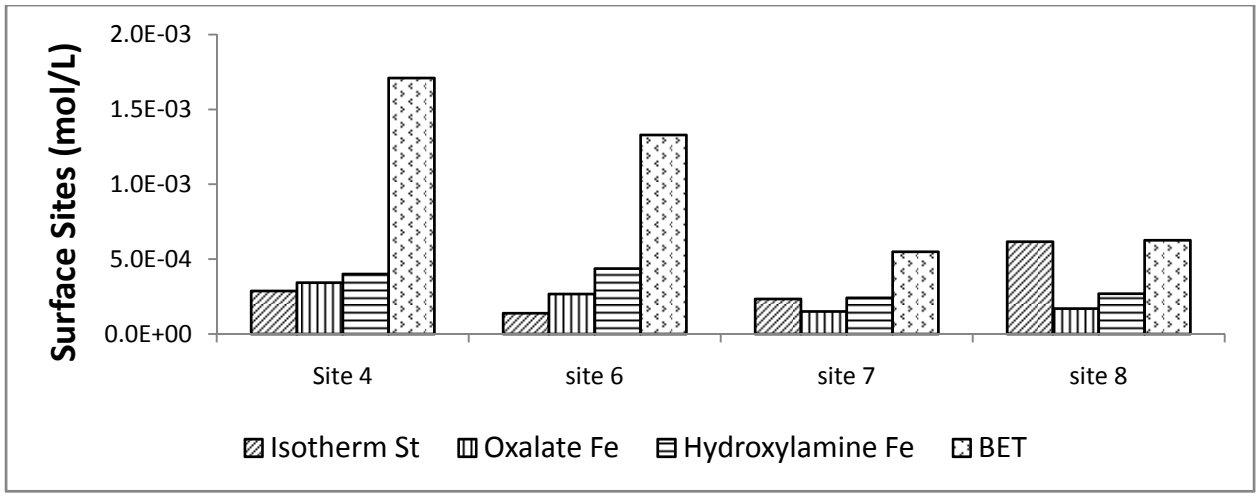

Figure 9. Surface site concentration calculated from four different methods; S_t from the Langmuir adsorption isotherm, Fe concentration extracted by oxalate, Fe concentration extracted by hydroxylamine hydrochloride, and BET surface area measurement.

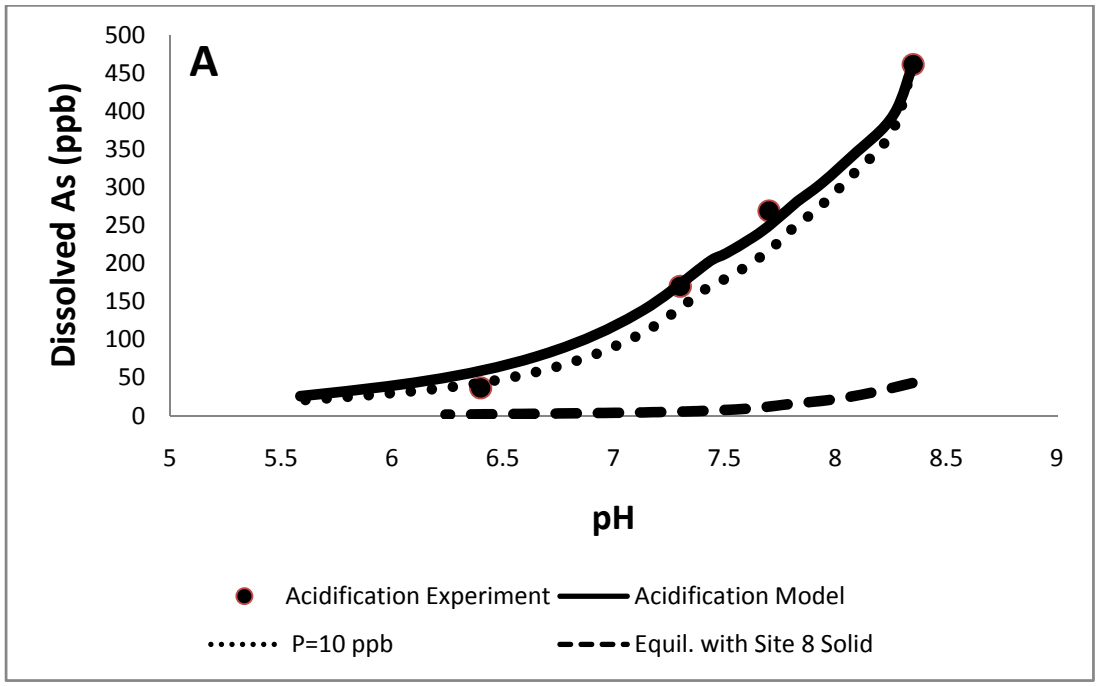

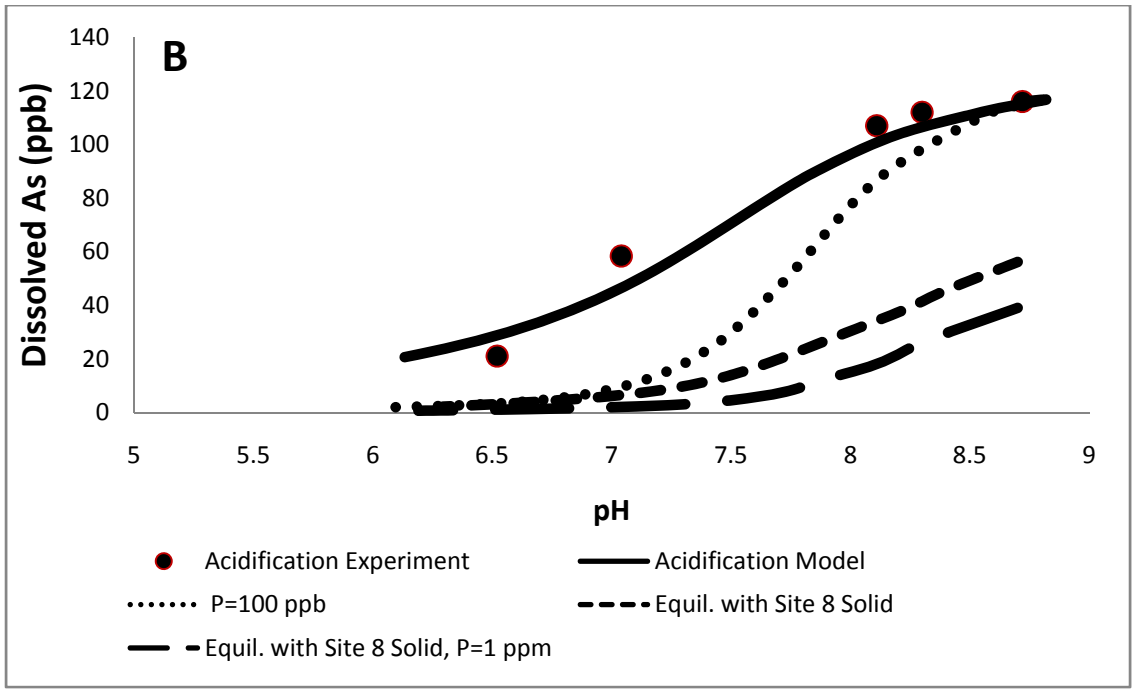

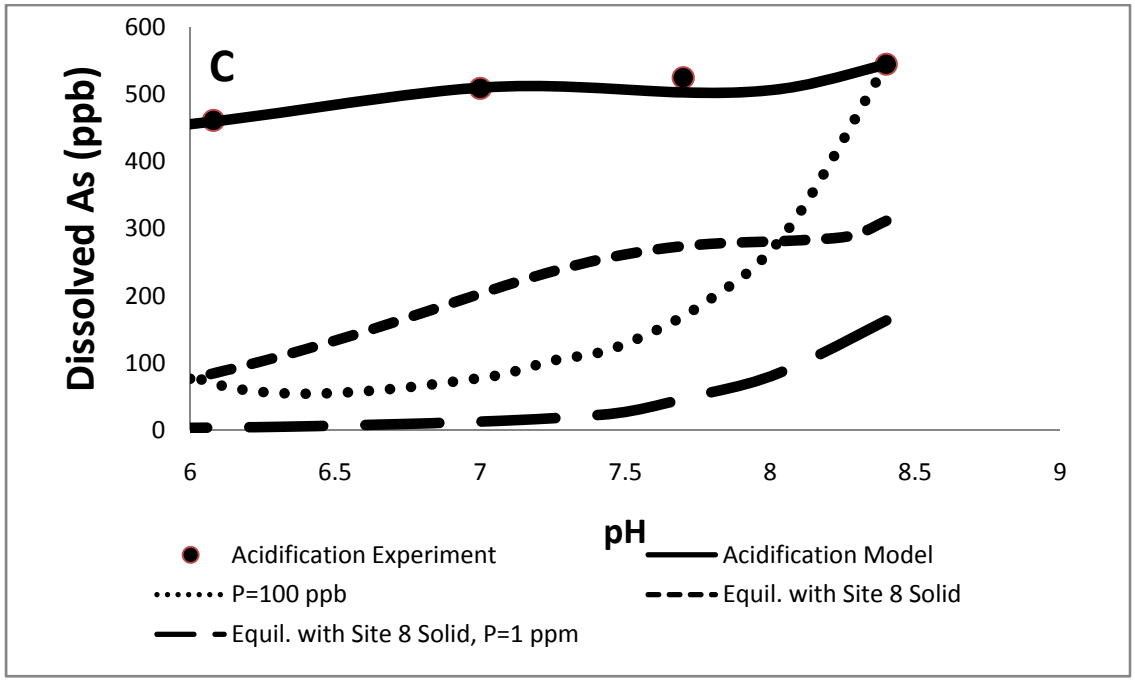

Figure 10. Hybrid-Isotherm Model predictions for different potential remediation schemes at (A) Site 4, (B) Site 6, and (C) Site 7.

Tables

Table 1. Sediment samples properties and descriptions

Boring	Sample ID	Depth Interval (ft)	Soil pH	Organic Matter (%)	CEC (meq/100g)	Description
A	Site 1	22-29	9.6	0.4	2.4	Gray Silty Sand (Till)
A	Site 2	24-26	9.3	0.2	1.1	Brown Fine-Medium Sand
B	Site 3	25-31	7.9	0.2	1.9	Gray-Brown Silty Sand (Till)
C	Site 4	29-35	8.3	0.2	1.2	Gray Silty Sand (Till)
D	Site 5	25-28	9.1	0.2	1.4	Brown Fine Sand
D	Site 6	31-35	8.3	0.2	1.8	Gray Silty Sand (Till)
E	Site 7	47-55	8.2	0.4	0.7	Brown Medium Sand
F	Site 8	51-58	7.2	0.2	0.8	Brown Fine to Coarse Sand

Table 2. Sequential extraction method modified from Keon et al (2001)

Step	*Extractant*	*Target Phase*
PO_4	1M NaH_2PO_4, pH 5, 16 & 24 hr, 25°C 1 repetition each time duration, 1 water wash	Strongly-adsorbed As
Oxalate	0.2M ammonium oxalate/oxalic acid, pH 3, 2hr, 25°C in dark 1 repetition, 1 water wash	As precipitated with amorphous Fe oxyhydroxides
Hot HNO_3	15N HNO_3 + 30% H_2O_2 , EPA method 3050B	As oxides, As coprecipitated with silicates, pyrites, and amorphous As_2S_3, orpiment & other remaining recalcitrant As minerals

Table 3. Surface Complexation Model parameters and assumptions

Model Name	Total Surface Site Estimation	Surface Site Type	Electrostatic Model	Surface Reaction Constants
CA-Hydroxylamine	Chemical Extraction of Amorphous Fe Oxides (Hydroxylamine Hydrochloride)	HFO Weak Site	DDL	HFO Database (Non-fitted)
CA-Oxalate	Chemical Extraction of Amorphous Fe Oxides (Ammonium Oxalate/Oxalic Acid)	HFO Weak Site	DDL	HFO Database (Non-fitted)
GC-BET	BET Surface Area Measurement	Generic Site	Non-Electrostatic	Experimental Data (Fitted)
Hybrid-Isotherm	Adsorption Isotherm (Langmuir)	HFO Weak Site	DDL	Experimental Data (Fitted) and HFO Database (Non-fitted)

Table 4. Surface complexation stoichiometry and reaction constants used in the diffuse double layer model for HFO

Surface Complexation Reaction	Log K	Reference
Surface Acidity		
Hfo_sOH + H+ = Hfo_sOH2+	7.29	Dzombak and Morel (1990)
Hfo_wOH + H+ = Hfo_wOH2+	7.29	
Hfo_sOH = Hfo_sO- + H+	-8.93	
Hfo_wOH = Hfo_wO- + H+	-8.93	
Arsenate		
Hfo_sOH + H3AsO4 = Hfo_sH2AsO4 + H2O	8.61	Dzombak and Morel (1990)
Hfo_wOH + H3AsO4 = Hfo_wH2AsO4 + H2O	8.61	
Hfo_sOH + H3AsO4 = Hfo_sHAsO4- + H2O + H+	2.81	
Hfo_wOH + H3AsO4 = Hfo_wHAsO4- + H2O + H+	2.81	
Hfo_sOH + H3AsO4 = Hfo_sHAsO4-2 + H2O + 2H+	-4.7	
Hfo_wOH + H3AsO4 = Hfo_wHAsO4-2 + H2O + 2H+	-4.7	
Hfo_sOH + H3AsO4 = Hfo_sOHAsO4-3 + 3H+	-10.12	
Hfo_wOH + H3AsO4 = Hfo_wOHAsO4-3 + 3H+	-10.12	
Arsenite		
Hfo_sOH + H3AsO3 = Hfo_sH2AsO3 + H2O	5.41	Dzombak and Morel (1990)
Hfo_wOH + H3AsO3 = Hfo_wH2AsO3 + H2O	5.41	

Phosphate		
Hfo_sOH + PO4-3 + 3H+ = Hfo_sH2PO4 + H2O	31.29	Dzombak and Morel (1990)
Hfo_wOH + PO4-3 + 3H+ = Hfo_wH2PO4 + H2O	31.29	
Hfo_sOH + PO4-3 + 2H+ = Hfo_sHPO4- + H2O	25.39	
Hfo_wOH + PO4-3 + 2H+ = Hfo_wHPO4- + H2O	25.39	
Hfo_sOH + PO4-3 + H+ = Hfo_sPO4-2 + H2O	17.72	
Hfo_wOH + PO4-3 + H+ = Hfo_wPO4-2 + H2O	17.72	
Carbonate		
Hfo_wOH + CO3-2 + H+ = Hfo_wCO3- + H2O	12.56	Appelo et al. (2002)
Hfo_wOH + CO3-2 + 2H+ = Hfo_wHCO3 + H2O	20.62	
Silicic Acid		
Hfo_sOH + H4SiO4 = Hfo_sH3SiO4 + H2O	4.28	Swedlund and Webster (1999)
Hfo_wOH + H4SiO4 = Hfo_wH3SiO4 + H2O	4.28	
Hfo_sOH + H4SiO4 = Hfo_sH2SiO4- + H2O + H+	-3.22	
Hfo_wOH + H4SiO4 = Hfo_wH2SiO4- + H2O + H+	-3.22	
Hfo_sOH + H4SiO4 = Hfo_sHSiO4-2 + H2O + 2H+	-11.69	
Hfo_wOH + H4SiO4 = Hfo_wHSiO4-2 + H2O + 2H+	-11.69	
Calcium		
Hfo_sOH + Ca+2 = Hfo_sOHCa+2	4.97	Dzombak and Morel (1990)
Hfo_wOH + Ca+2 = Hfo_wOCa+ + H+	-5.85	
Ferrous Iron		
Fe+2 + Hfo_wOH = Hfo_wOFe+ + H+	-2.98	Appelo et al. (2002)
Fe+2 + Hfo_wOH + H2O = Hfo_wOFeOH + 2H+	-11.55	
Fe+2 + Hfo_sOH = Hfo_sOFe+ + H+	-0.95	

Table 5. Distribution of solid phase As concentrations from sequential extractions

Sample	As Fractions [Extractants] (mg/kg)			Total As (mg/kg)
	Strongly Adsorbed [NaH_2PO_4]	Amorphous Fe [Oxalate]	Recalcitrant [Total Digestion-HNO_3]	
Site 2	0.71	0.59	4.2	5.5
Site 4	0.89	0.57	9.9	11.3
Site 6	0.31	0.53	9.5	10.3
Site 7	0.94	0.42	2.7	4.1
Site 8	1.1	0.38	3.3	4.7

Table 6. Langmuir Isotherm parameters derived from adsorption experiments

Sample	K(L/mg)	S_t(mg/Kg)	R^2
Site 4	0.63	215	0.981
Site 6	0.92	104	0.901
Site 7	1.01	175	0.982
Site 8	0.38	462	0.987

Table 7. Acidification Experiment Results (All concentrations in mg/L)

		PH	As	Ca	Fe	Mg	Si	P	Al	B	Mn	K	Na
Site 4	**Groundwater**	8.2	0.701	4.09	<0.1	0.74	4.76	0.84					
	Control Sample	8.4	0.461	10.3	0.4	1.62	5.52	0.4	0.42	0.17	0.02	6.2	56.2
	Acidified Samples	7.7	0.269	48.4	<0.1	3.05	6.09	0.33	0.13	0.4	0.12	8.5	58.5
		7.3	0.17	76.1	<0.1	3.57	6.32	0.21	0.16	0.34	0.27	9.8	56.7
		6.4	0.04					<0.1					
Site 6	**Groundwater**	9.4	0.101	0.1	<0.1	<0.1	3.25	4.6					
	Control Sample	8.7	0.116	4.7	2.26	1.1	6.16	2.9	1.88	0.23	0.04	3.8	50.7
	Acidified Samples	8.3	0.112	8.9	0.69	1.04	5.17	3.3	0.65	0.23	0.02	4.8	52
		8.1	0.107	12.6	0.05	1.22	5.4	3.1	0.51	0.25	0.02	5.7	55.3
		7	0.06					1.5					
		6.5	0.02					0.5					
Site 7	**Groundwater**	7.9	0.536	1.6	<0.1	0.32	9.01	7.5					
	Control Sample	8.4	0.545	1.9	1.53	0.5	11.5	8.9	0.86	1.03	0.09	4	120.3
	Acidified Samples	7.7	0.525	2.2	2.06	0.63	13.3	8	1.17	1.03	0.09	6.5	127.8
		7	0.509	2.3	2.45	0.74	14.3	7.5	1.8	1.18	0.11	5.1	124.8
		6.1	0.461					6.9					
Site 8	**Groundwater**	7	<0.008	49.6	<0.1	13.2	8.56	<0.1					
	Control Sample	8.3	0.013	49.6	<0.1	12.2	8.81	<0.2	0.04	0.13	0	4.2	26
	Acidified Samples	7.5	0.006	50.4	<0.1	12.6	9.6	<0.2	0.04	0.14	0.03	6.2	25.9
		6.8	0.002	51.1	<0.1	12.9	9.13	<0.2	0.07	0.11	0.05	5.3	26.1

Table 8. Comparison of the goodness of fit values (NRMSE, %) for different model simulations of acidification experiments

	Site 4	Site 6		Site 7		Site 8
Model	As(V)	As(V)	PO4	As(V)	PO4	As(V)
CA-Hydroxylamine	18.5	24.6	13.1	12.0	13.3	3.0
CA-Oxalate	20.3	20.3	5.0	14.4	4.1	4.1
GC-BET	4.8	6.7	8.2	1.3	2.1	3.7
Hybrid-Isotherm	2.9	6.5	5.8	1.9	4.7	4.9

Table 9. Surface complexation reaction constants modified for Hybrid-Isotherm model

	Default	Site 4	Site 6	Site 7	Site 8
Arsenate					
Hfo_wH_2AsO_4	8.61	8.61	8.61	8.61	8.61
Hfo_s$HAsO_4^-$	2.81	3.8	3.6	2.9	3.7
Hfo_w$OHAsO_4^{-3}$	-10.12	-10.12	-11.5	-10.5	-10.12
Phosphate					
Hfo_w$H2PO_4$	31.29	31.29	32.5	31.29	31.29
Hfo_wHPO_4^-	25.39	24.5	25.7	23.5	25.39
Hfo_wPO_4^{-2}	17.72	17.72	17.72	19.1	17.72

Table 10. Surface complexation reaction constants optimized by FITEQL for GC-BET model

	Site 4	Site 6	Site 7	Site 8
Arsenate				
Site_z$H2AsO_4$	-	-	-	-
Site_z$HAsO_4^-$	6.91	7.66	6.43	8.7
Site_zAsO_4^{-2}	-	-	-0.81	-
Site_z$OHAsO4^{-3}$	-9.93	-9.34	-10.58	-7.72
Phosphate				
Site_zH_2PO_4		-	-	
Site_zHPO_4^-		27.89	26.9	
Site_zPO_4^{-2}		17.14	18.87	

Acknowledgments

We gratefully acknowledge support from Drumlin Environmental, LLC for conducting this work. This material is based upon research performed in a renovated collaboratory by the National Science Foundation under Grant No. 0963183, which is an award funded under the American Recovery and Reinvestment Act of 2009 (ARRA).

References

Alloway, B. J. (2013). *Introduction* (pp. 3-9). In *Heavy metals in soils*. Springer Netherlands.

Anawar, H. M., Garcia-Sanchez, a., & Santa Regina, I. (2008). Evaluation of various chemical extraction methods to estimate plant-available arsenic in mine soils. *Chemosphere*, *70*(8), 1459–1467.

Anawar, H. M., Akai, J., Mostofa, K. M. G., Safiullah, S., & Tareq, S. M. (2002). Arsenic poisoning in groundwater: Health risk and geochemical sources in Bangladesh. *Environment International*, *27*(7), 597–604.

Appelo, C. A. J., & Postma, D. (2005). *Geochemistry, groundwater and pollution*. CRC press.

Appelo, C. A. J., & De Vet, W. W. J. M. (2003). Modeling in situ iron removal from groundwater with trace elements such as As. In *Arsenic in Ground Water* (pp. 381-401). Springer US.

Appelo, C. a J., Van Der Weiden, M. J. J., Tournassat, C., & Charlet, L. (2002). Surface complexation of ferrous iron and carbonate on ferrihydrite and the mobilization of arsenic. *Environmental Science & Technology*, *36*(14), 3096–103.

Ayotte, J. D., Nolan, B. T., Nuckols, J. R., Cantor, K. P., Robinson, G. R., Baris, D., … Lubin, J. H. (2006). Modeling the probability of arsenic in groundwater in New England as a tool for exposure assessment. *Environmental Science & Technology*, *40*(11), 3578–85.

Ayotte, J. D., Montgomery, D. L., Flanagan, S. M., & Robinson, K. W. (2003). Arsenic in groundwater in eastern New England: occurrence, controls, and human health implications. *Environmental science & technology*, *37*(10), 2075-2083.

Bhattacharya, P., Claesson, M., Bundschuh, J., Sracek, O., Fagerberg, J., Jacks, G., … Thir, J. M. (2006). Distribution and mobility of arsenic in the Rio Dulce alluvial aquifers in Santiago del Estero Province, Argentina. *Science of the Total Environment*, *358*(1-3), 97–120.

Berg, M., Tran, H. C., Nguyen, T. C., Pham, H. V, Schertenleib, R., & Giger, W. (2001). Arsenic contamination of groundwater and drinking water in Vietnam: a human health threat. *Environmental Science & Technology*, *35*(13), 2621–6.

Biswas, A., Gustafsson, J. P., Neidhardt, H., Halder, D., Kundu, A. K., Chatterjee, D., … Bhattacharya, P. (2014). Role of competing ions in the mobilization of arsenic in groundwater of Bengal Basin: insight from surface complexation modeling. *Water Research*, *55*, 30–9.

Bolster, C. H., & Hornberger, G. M. (2008). On the Use of Linearized Langmuir Equations. *Soil Science Society of America Journal*, *72*(6), 1848.

Bond, D. L., Davis, J. A., & Zachara, J. M. (2007). Uranium (VI) release from contaminated vadose zone sediments: Estimation of potential contributions from dissolution and desorption. *Developments in Earth and Environmental Sciences*, *7*, 375-416.

Currell, M., Cartwright, I., Raveggi, M., & Han, D. (2011). Controls on elevated fluoride and arsenic concentrations in groundwater from the Yuncheng Basin, China. *Applied Geochemistry*, *26*(4), 540–552.

Davis, J. A., Meece, D. E., Kohler, M., & Curtis, G. P. (2004). Approaches to surface complexation modeling of uranium (VI) adsorption on aquifer sediments. *Geochimica et Cosmochimica Acta*, *68*(18), 3621-3641.

Davis, J. A., Coston, J. A., Kent, D. B., & Fuller, C. C. (1998). Application of the surface complexation concept to complex mineral assemblages. *Environmental Science & Technology*, *32*(19), 2820-2828.

Dixit, S., & Hering, J. G. (2003). Comparison of arsenic(V) and arsenic(III) sorption onto iron oxide minerals: implications for arsenic mobility. *Environmental Science & Technology*, *37*(18), 4182–9.

Dzombak, D. A., & Morel, F. M. (1990). *Surface complexation modeling: hydrous ferric oxide*. John Wiley & Sons.

EPA, U. S. (2002). Arsenic treatment technologies for solid, waste, and water. *USEPA Report EPA-542-R-02-004*.

Farley, K. J., Dzombak, D. A., & Morel, F. M. (1985). A surface precipitation model for the sorption of cations on metal oxides. *Journal of Colloid and Interface Science*, *106*(1), 226-242.

Harvey, C. F., Ashfaque, K. N., Yu, W., Badruzzaman, a. B. M., Ali, M. A., Oates, P. M., … Ahmed, M. F. (2006). Groundwater dynamics and arsenic contamination in Bangladesh. *Chemical Geology*, *228*(1-3), 112–136.

Herbelin, A. L., & Westall, J. C. (1999). FITEQL: A computer program for determination of chemical equilibrium constants from experimental data. *Version*, *4*, 99-01.

Hiemstra, T., Antelo, J., Rahnemaie, R., & Riemsdijk, W. H. Van. (2010). Nanoparticles in natural systems I: The effective reactive surface area of the natural oxide fraction in field samples. *Geochimica et Cosmochimica Acta*, *74*(1), 41–58.

Hongshao, Z., & Stanforth, R. (2001). Competitive adsorption of phosphate and arsenate on goethite. *Environmental Science & Technology*, *35*(24), 4753–7.

Hyun, S. P., Fox, P. M., Davis, J. A., Campbell, K. M., Hayes, K. F., & Long, P. E. (2009). Surface complexation modeling of U (VI) adsorption by aquifer sediments from a former mill tailings site at Rifle, Colorado. *Environmental science & technology*, *43*(24), 9368-9373.

Islam, F. S., Gault, A. G., Boothman, C., Polya, D. a, Charnock, J. M., Chatterjee, D., & Lloyd, J. R. (2004). Role of metal-reducing bacteria in arsenic release from Bengal delta sediments. *Nature*, *430*(6995), 68–71.

Jeppu, G. P., & Clement, T. P. (2012). A modified Langmuir-Freundlich isotherm model for simulating pH-dependent adsorption effects. *Journal of Contaminant Hydrology*, *129-130*, 46–53.

Jessen, S., Postma, D., Larsen, F., Nhan, P. Q., Hoa, L. Q., Trang, P. T. K., … Jakobsen, R. (2012). Surface complexation modeling of groundwater arsenic mobility: Results of a forced gradient experiment in a Red River flood plain aquifer, Vietnam. *Geochimica et Cosmochimica Acta*, *98*, 186–201.

Jung, H. B., Bostick, B. C., & Zheng, Y. (2012). Field, experimental, and modeling study of arsenic partitioning across a redox transition in a bangladesh aquifer. *Environmental Science and Technology*, *46*(3), 1388–1395.

Kanel, S. R., Manning, B., Charlet, L., & Choi, H. (2005). Removal of arsenic(III) from groundwater by nanoscale zero-valent iron. *Environmental Science & Technology*, *39*(5), 1291–8.

Kanematsu, M., Young, T. M., Fukushi, K., Green, P. G., & Darby, J. L. (2012). Individual and combined effects of water quality and empty bed contact time on As(V) removal by a fixed-bed iron oxide adsorber: implication for silicate precoating. *Water Research*, *46*(16), 5061–70.

Larsen, F., Pham, N. Q., Dang, N. D., Postma, D., Jessen, S., Pham, V. H., … Refsgaard, J. C. (2008). Controlling geological and hydrogeological processes in an arsenic contaminated aquifer on the Red River flood plain, Vietnam. *Applied Geochemistry*, *23*(11), 3099–3115.

Lawson, M., Polya, D. a, Boyce, A. J., Bryant, C., Mondal, D., Shantz, A., & Ballentine, C. J. (2013). Pond-derived organic carbon driving changes in arsenic hazard found in Asian groundwaters. *Environmental Science & Technology*, *47*(13), 7085–94.

Limousin, G., Gaudet, J. P., Charlet, L., Szenknect, S., Barthès, V., & Krimissa, M. (2007). Sorption isotherms: A review on physical bases, modeling and measurement. *Applied Geochemistry*, *22*(2), 249–275.

Keon, N. E., Swartz, C. H., Brabander, D. J., Harvey, C., & Hemond, H. F. (2001). Validation of an arsenic sequential extraction method for evaluating mobility in sediments. *Environmental Science & Technology*, *35*(13), 2778–84.

Komárek, M., Vaněk, A., & Ettler, V. (2013). Chemical stabilization of metals and arsenic in contaminated soils using oxides--a review. *Environmental Pollution (Barking, Essex : 1987)*, *172*, 9–22.

Mai, N. T. H., Postma, D., Trang, P. T. K., Jessen, S., Viet, P. H., & Larsen, F. (2014). Adsorption and desorption of arsenic to aquifer sediment on the Red River floodplain at Nam Du, Vietnam. *Geochimica et Cosmochimica Acta*, *142*, 587-600.

Manning, B. A., & Goldberg, S. (1996). Modeling Competitive Adsorption of Arsenate with Phosphate and Molybdate on Oxide Minerals. *Soil Science Society of America Journal*, *60*(1), 121.

Martínez-Villegas, N., Briones-Gallardo, R., Ramos-Leal, J. a, Avalos-Borja, M., Castañón-Sandoval, A. D., Razo-Flores, E., & Villalobos, M. (2013). Arsenic mobility controlled by solid calcium arsenates: a case study in Mexico showcasing a potentially widespread environmental problem. *Environmental Pollution (Barking, Essex : 1987)*, *176*, 114–22.

Masue, Y., Loeppert, R. H., & Kramer, T. a. (2007). Arsenate and arsenite adsorption and desorption behavior on coprecipitated aluminum:iron hydroxides. *Environmental Science & Technology*, *41*(3), 837–42.

McArthur, J. ., Banerjee, D. ., Hudson-Edwards, K. ., Mishra, R., Purohit, R., Ravenscroft, P., … Chadha, D. . (2004). Natural organic matter in sedimentary basins and its relation to arsenic in anoxic ground water: the example of West Bengal and its worldwide implications. *Applied Geochemistry*, *19*(8), 1255–1293.

Moldovan, B. I., & Hendry, M. J. (2005). Characterizing and quantilying controls on arsenic solubility over a pH range of 1-11 in a uranium mill-scale experiment. *Environmental Science & Technology*, *39*(13), 4913–20.

Neumann, R. B., Ashfaque, K. N., Badruzzaman, a. B. M., Ashraf Ali, M., Shoemaker, J. K., & Harvey, C. F. (2009). Anthropogenic influences on groundwater arsenic concentrations in Bangladesh. *Nature Geoscience*, *3*(1), 46–52.

Neupane, G., Donahoe, R. J., & Arai, Y. (2014). Kinetics of competitive adsorption/desorption of arsenate and phosphate at the ferrihydrite–water interface. *Chemical Geology*, *368*, 31–38.

Neidhardt, H., Berner, Z. A., Freikowski, D., Biswas, A., Majumder, S., Winter, J., … Norra, S. (2014). Organic carbon induced mobilization of iron and manganese in a West Bengal aquifer and the muted response of groundwater arsenic concentrations. *Chemical Geology*, *367*, 51–62.

Omoregie, E. O., Couture, R.-M., Van Cappellen, P., Corkhill, C. L., Charnock, J. M., Polya, D. a, … Lloyd, J. R. (2013). Arsenic bioremediation by biogenic iron oxides and sulfides. *Applied and Environmental Microbiology*, *79*(14), 4325–35.

Parkhurst, D. L., & Appelo, C. A. J. (2013). *Description of input and examples for PHREEQC version 3: a computer program for speciation, batch-reaction, one-dimensional transport, and inverse geochemical calculations* (No. 6-A43). US Geological Survey.

Polya, D. a., Gault, a. G., Diebe, N., Feldman, P., Rosenboom, J. W., Gilligan, E., … Cooke, D. a. (2005). Arsenic hazard in shallow Cambodian groundwaters. *Mineralogical Magazine*, *69*(5), 807–823.

Postma, D., Larsen, F., Minh Hue, N. T., Duc, M. T., Viet, P. H., Nhan, P. Q., & Jessen, S. (2007). Arsenic in groundwater of the Red River floodplain, Vietnam: Controlling geochemical processes and reactive transport modeling. *Geochimica et Cosmochimica Acta*, *71*(21), 5054–5071.

Quicksall, A. N., Bostick, B. C., & Sampson, M. L. (2008). Linking organic matter deposition and iron mineral transformations to groundwater arsenic levels in the Mekong delta, Cambodia. *Applied Geochemistry*, *23*(11), 3088–3098.

Radloff, K. a., Zheng, Y., Michael, H. a., Stute, M., Bostick, B. C., Mihajlov, I., … van Geen, a. (2011). Arsenic migration to deep groundwater in Bangladesh influenced by adsorption and water demand. *Nature Geoscience*, *4*(11), 793–798.

Radu, T., Kumar, A., Clement, T. P., Jeppu, G., & Barnett, M. O. (2008). Development of a scalable model for predicting arsenic transport coupled with oxidation and adsorption reactions. *Journal of contaminant hydrology*, *95*(1), 30-41.

Raven, K. P., Jain, A., & Loeppert, R. H. (1998). Arsenite and arsenate adsorption on ferrihydrite: Kinetics, equilibrium, and adsorption envelopes. *Environmental Science and Technology*, *32*(3), 344–349.

Ravenscroft, P., Brammer, H., & Richards, K. (2009). *Arsenic pollution: a global synthesis* (Vol. 28). John Wiley & Sons.

Robertson, F. N. (1989). Arsenic in ground-water under oxidizing conditions, south-west United States. *Environmental Geochemistry and Health*, *11*(3-4), 171–185.

Robinson, C., Brömssen, M. Von, Bhattacharya, P., Häller, S., Bivén, A., Hossain, M., … Thunvik, R. (2011). Dynamics of arsenic adsorption in the targeted arsenic-safe aquifers in Matlab, south-eastern Bangladesh: Insight from experimental studies. *Applied Geochemistry*, *26*(4), 624–635.

Rodriguez, R. R., Basta, N. T., Casteel, S. W., Armstrong, F. P., & Ward, D. C. (2003). Chemical extraction methods to assess bioavailable arsenic in soil and solid media. *Journal of Environmental Quality*, *32*(3), 876-884.

Rowland, H. a L., Pederick, R. L., Polya, D. a., Pancost, R. D., Van Dongen, B. E., Gault, a. G., … Lloyd, J. R. (2007). The control of organic matter on microbially mediated iron reduction and arsenic release in shallow alluvial aquifers, Cambodia. *Geobiology*, *5*(3), 281–292.

Scanlon, B. R., Nicot, J. P., Reedy, R. C., Kurtzman, D., Mukherjee, a., & Nordstrom, D. K. (2009). Elevated naturally occurring arsenic in a semiarid oxidizing system, Southern High Plains aquifer, Texas, USA. *Applied Geochemistry*, *24*(11), 2061–2071.

Selim, H. (2014). *Transport & Fate of Chemicals in Soils*. CRC Press.

Sharif, M. S. U., Davis, R. K., Steele, K. F., Kim, B., Hays, P. D., Kresse, T. M., & Fazio, J. a. (2011). Surface complexation modeling for predicting solid phase arsenic concentrations in the sediments of the Mississippi River Valley alluvial aquifer, Arkansas, USA. *Applied Geochemistry*, *26*(4), 496–504.

Sherman, D. M., & Randall, S. R. (2003). Surface complexation of arsenic (V) to iron (III)(hydr) oxides: structural mechanism from ab initio molecular geometries and EXAFS spectroscopy. *Geochimica et Cosmochimica Acta*, *67*(22), 4223-4230.

Smedley, P. L., Kinniburgh, D. G., Macdonald, D. M. J., Nicolli, H. B., Barros, a. J., Tullio, J. O., … Alonso, M. S. (2005). Arsenic associations in sediments from the loess aquifer of La Pampa, Argentina. *Applied Geochemistry*, *20*, 989–1016.

Smedley, P. L., & Kinniburgh, D. G. (2002). A review of the source, behaviour and distribution of arsenic in natural waters. *Applied Geochemistry*, *17*(5), 517–568.

Smith, a H., Hopenhayn-Rich, C., Bates, M. N., Goeden, H. M., Hertz-Picciotto, I., Duggan, H. M., … Smith, M. T. (1992). Cancer risks from arsenic in drinking water. *Environmental Health Perspectives*, *97*(6), 259–67.

Sracek, O., Bhattacharya, P., Jacks, G., Gustafsson, J.-P., & Brömssen, M. Von. (2004). Behavior of arsenic and geochemical modeling of arsenic enrichment in aqueous environments. *Applied Geochemistry*, *19*(2), 169–180.

Stollenwerk, K. G., Breit, G. N., Welch, A. H., Yount, J. C., Whitney, J. W., Foster, A. L., … Ahmed, N. (2007). Arsenic attenuation by oxidized aquifer sediments in Bangladesh. *The Science of the Total Environment*, *379*(2-3), 133–50.

Stollenwerk, K. G. (2003). Geochemical processes controlling transport of arsenic in groundwater: a review of adsorption. In *Arsenic in ground water* (pp. 67-100). Springer US.

Swedlund, P. J., & Webster, J. G. (1999). Adsorption and polymerisation of silicic acid on ferrihydrite, and its effect on arsenic adsorption. *Water Research*, *33*(16), 3413-3422.

Van Geen, a., Zheng, Y., Cheng, Z., Aziz, Z., Horneman, a., Dhar, R. K., … Ahmed, K. M. (2006). A transect of groundwater and sediment properties in Araihazar, Bangladesh: Further evidence of decoupling between As and Fe mobilization. *Chemical Geology*, *228*(1-3), 85–96.

Wang, S., & Mulligan, C. N. (2006). Natural attenuation processes for remediation of arsenic contaminated soils and groundwater. *Journal of Hazardous Materials*, *138*(3), 459–70.

Welch, A. H., Westjohn, D. B., Helsel, D. R., & Wanty, R. B. (2000). Arsenic in Ground Water of the United States-Occurrence and Geochemistry. *Ground Water*, *38*(4), 589–604.

Wilkie, J. A., & Hering, J. G. (1996). Adsorption of arsenic onto hydrous ferric oxide: effects of adsorbate/adsorbent ratios and co-occurring solutes. *Colloids and Surfaces A: Physicochemical and Engineering Aspects*, *107*, 97-110.

Zheng, Y., Stute, M., Van Geen, a., Gavrieli, I., Dhar, R., Simpson, H. J., … Ahmed, K. M. (2004). Redox control of arsenic mobilization in Bangladesh groundwater. *Applied Geochemistry*, *19*(2), 201–214.

Chapter 4. Remediation of As(V) Contaminated Groundwater Through Enhanced Natural Attenuation: Batch and Column Studies

Abstract

Batch and column laboratory experiments were conducted on natural sediment and groundwater samples from a contaminated site with the aim of lowering the dissolved arsenate [As(V)] concentrations by enhancing natural attenuation. In factorial experiments two levels of treatment for pH adjustment, Ca and Fe additions were studied for impact on As(V) solubility. Results showed statistical significance for the effect of pH, Ca and Fe on increased sorption capacity of sediments. Additionally, adsorption isotherm experiments at three levels of Ca showed consistent increase in adsorption capacity (26-37%) indicating that the beneficial effect of Ca is due to improving the adsorption rates on surfaces likely by increasing the surface positive charges. Column experiments were conducted by flowing contaminated groundwater with elevated pH, As, and PO_4 through both uncontaminated and contaminated sediments. Potential remediation scenarios were simulated by adding a chemical amendment line to the columns input injecting Fe(II) and Ca as well as simultaneous pH adjustment to the groundwater inflow. Results showed temporary and limited decrease in As(V) concentrations by Ca treatment (39-41%) and higher levels of attenuation in Fe(II) treated columns (50-91%) but given the sufficient number of pore volumes(18-20 pore volumes).

1. Introduction

Arsenic is a toxic element with known negative health effects for humans (Duker et al., 2005). Mobilization of naturally occurring Arsenic (As) from the host solid minerals into aqueous phase is a major environmental pollution problem on a global scale. The release of As can take place via dissolution processes such as oxidative weathering of As sulfide minerals and reductive dissolution of iron (Fe) oxides and hydroxides. In oxidizing systems where As is mainly present

as the oxidized form As(V), the main mechanism of mobilization is the alkaline desorption caused by the increased repulsion between the negatively charged As(V) oxyanions and the solid surfaces. Presence of competing ions such as phosphate as well as persistence of high pH values due to high alkalinity of solution and natural pH buffering of solid phases, inhibits the sorption of mobilized As(V) and can lead to enriched As concentrations in soil solutions and groundwaters. Desorption processes can also be caused by the loss of adosrptive capacity of Fe oxide phases due to aging and transformation to more crystalline phases over time (Paktunc et al., 2004).

Conventional methods for remediation of contaminated groundwaters generally involve a form of above-ground pump and treat system. However these systems usually require high cost of installation and maintenance and might not be effective for reducing the contaminants concentrations over long term (Martin and Kempton, 2000). Other methods such as in-situ remediation with focus on promoting the natural processes for retention of contaminant have gained more interest in recent decades.

Sorption to solid phases is the main mechanism applicable to in-situ remediation of As contaminated groundwaters. These solid phases include oxides and hydroxides of Fe, Al, Mn, clay minerals, and organic matter (Wang and Mulligan, 2006). These oxide phases exist as either discrete minerals or more commonly as coatings on other minerals and solid particles (Singer et al., 2013).

Studies have shown the important role of Fe oxides present in soils for immobilizing released As (Savage et al., 2000; Morin et al., 2002; Yang et al., 2002; Cances et al., 2005). The abundance and characteristics of Fe oxides present in soils and sediments can influence the mobility and transport of As both vertically and horizontally. It has been shown that adsorption of As on Fe

oxides such as green rust, goethite and lepidocrocite is orders of magnitude greater than adsorption by clays and feldspars (Lin and Puls, 2003).

In addition to the interactions between the solid phase and As oxyanions, the composition of the solution phase and presence of other solutes also have important effect on fate and transport of mobilized As. Competition of phosphate anion with As species for available sorption sites on a variety of surfaces has been well documented (Manning and Goldber, 1996; Jain and Loeppert, 2000; Gao and Mucci, 2001; Hongshao and Stanforth, 2001; Liu et al., 2001; Goldberg, 2002; Violante and Pigna, 2002; Zeng et al., 2007; Zhang and Selim, 2008). Cations such as Ca^{2+} have been reported by some to increase As adsorption on surfaces through increasing the positive charge on oxide surfaces (Meng et al., 2000; Wilkie and hering, 2003; Masue et al., 2007; Currell et al., 2011).

In this study, sediment and groundwater samples collected from a contaminated site in New England, USA, are used in batch and column experiments to test the effectiveness of chemical amendments for enhancing natural attenuation of As(V). Our hypothesis is that addition of Fe and Ca to the aqueous phase alongside pH adjustment is capable of increasing the natural attenuation of As(V) by providing more sorption sites and improving the adsorption rates. Column experiments are conducted using sediments from locations within and outside known bounds of the contaminant plume. Flowing contaminated groundwater from sampling sites within the plume through columns packed with un-impacted sediments will simulate the worst case scenario of the contaminated groundwater reaching the downgradient sites. Results will be used to assess the natural capacity of sediments in hindering the transport of As.

2. Materials and methods

2.1. Analytical Methods

Sediment samples were stored in sealed zip lock- bags and shipped in coolers on ice. All sediment and groundwater samples were stored refrigerated (4°C) in dark until use. All lab-ware were soaked in 1.2N HCl for at least twelve hours and rinsed with Milli-Q water five times prior to use. All solutions were prepared using Milli-Q water (18MΩ) purified by NANOpure deionization system. The sediments were separated from solutions in batch suspensions by centrifuging at 7800 RPM for 15 minutes and supernatants were syringe filtered through 0.45 μm disposable MCE filters (EMD Millipore). All samples for As analysis were preserved upon collection (2%v/v HNO_3) and refrigerated if not immediately measured.

All chemicals used were of laboratory reagent grade. Arsenic added to factorial experiments was prepared from $Na_2HAsO_4.7H_2O$ (Sigma Aldrich). The pH values were adjusted in all experiments using 0.1N HCl and NaOH. HEPES buffer was used to maintain a constant pH throughout the course of the experiments. HEPES has been shown to have negligible influence on As adsorption processes (Kanematsu et al., 2010). For batch studies, the experimental tubes were shaken using rotisserie rotators for the specified duration at 8 rpm.

Total As concentration in filtered solutions was measured by Graphite Furnace Atomic Absorption Spectrometry (GFAAS) (Perkin Elmer AAnalyst 700) with an electrodeless discharge lamp (EDL). 20 μL of sample plus 5 μL of matrix modifier ($Pd(NO_3)_2$ + $Mg(NO_3)_2$) was used for each measurement. The instrument was calibrated on a daily basis with minimum of five standard solutions (5-100 μg/L) prepared from stock solution obtained from Perkin Elmer. The analyses were conducted in triplicates and the relative standard deviations of measurements were below 5%.

Fe(II) measurements were done spectrophotometrically using the Ferrozine method (Stookey, 1970; Lovley and Phillips1986) at 562 nm.

2.2. Sediment pH Buffering Experiments

Sediments were mixed with deionized water (100g/L ratio) and titrated with a Metrohm Titrando titrator using incremental addition of 0.1 N HCl.

2.3. Remediation Factorial Experiments

Effect of three parameters (pH, Ca, Fe) on retention of As on sediments were studied in batch factorial settings. Constant concentration of As (2.5 mg/L) was added to sediment suspensions (0.3 kg/L ratio). Concentration of phosphate used in the experiments was selected to be representative of levels observed at each site's corresponding groundwater. Each parameter was varied at two specified levels. pH values of 7 and 9 were used to represent the background and elevated pH conditions in the study site. Fe concentrations varied between 1 and 20 mg/L and Ca concentrations of 1 and 50 mg/L were used for the low and high conditions.

2.4. Batch Adsorption Experiments

Batch adsorption experiments were conducted by mixing sediments and background electrolyte solution (0.1M NaCl, 5mM HEPES) with a 100g/L ratio. Final Ca concentrations of 1, 50, and 100 mg/L were achieved in suspensions by adding $CaCl_2$ salt. Suspensions were mixed overnight and then pH adjusted to 7 prior to spiking with As(V).

Suspensions were shaken for 7 days and then centrifuged and filtered to measure the dissolved As(V) remaining in solution. Mass balance was applied and concentrations adsorbed were calculated.

2.5. Batch Acidification Experiments

10 g of air-dried and sieved (<2 mm) sediment was mixed with 100 mL of groundwater in glass flasks sealed with stoppers. The suspensions were placed on an orbital shaker in room temperature for 7 days until separation and preservations for analysis. pH was monitored and

recorded daily before and after adjustment by addition of HCl. Samples were withdrawn periodically to measure the changes in As concentration over time.

2.6. Sediment Column Experiments

Column studies were conducted using glass columns (Spectra/Chrom) with 0.9 cm diameter and 15 cm length. Sediment samples were air-dried and passed through 2mm sieve prior to packing the columns. Sediment was added in approximately 1 cm increments and compacted by dropping a custom made pestle (weighing 16 g) ten times.

Assuming 2.65 g/cm3 particle density for sand, mass of sediments used to fill the columns was used to calculate the porosity achieved by this packing method. Tracer studies using a dye (Brilliant Blue FCF) were conducted on control columns using the corresponding sediment type to verify the porosity calculations. All determined porosities were below 5% margin of error. Table 1 lists the achieved porosity values for all columns used in this study.

The Peristaltic pumps were run for a week to first calibrate the flow rate through the tubings and then to validate the flow rate through an empty column as well as a control column packed with sediment. The minimum achievable flow rate of 0.01 mL/min was used for running the columns with groundwater in order to ensure the adequate residence time needed for sorption kinetics. For consistency reasons, equal length of tubing was used for all columns and the columns were positioned at identical heights. Columns were fed with groundwater continuously and upward at a constant 0.6 mL/h rate at the ambient temperature (~25 ^{o}C). Input solutions were kept refrigerated in dark and were added to 50-mL reservoirs on a daily basis. Solutions were pumped through the columns using high accuracy digital Masterflex pumps and compatible L/S 13 and 14 tubings.

Columns and influent reservoirs were covered with aluminum foil to prevent light exposure and minimize the possibility of any photochemically induced reactions. The effluent of columns were collected at 6-hour intervals (approximately 1-1.2 pore volumes) on a daily basis for the duration of experiments. Collected samples were filtered (0.45m) and a constant aliquot was added to pre-acidified (2% HNO_3) micro-centrifuge tubes for subsequent analysis with GFAAS. Alkalinity, conductivity, dissolved oxygen (DO), pH and temperature of the effluents were monitored for duration of the experiments.

In the first round of experiments, sorption and transport of As within columns packed with un-contaminated sediments from Site 11 and 12 were studied. The experiments were run in three phases. The columns were first equilibrated with the corresponding un-contaminated groundwater for 20 pore volumes to achieve an initial equilibrium condition. Next the input solutions were switched to the As contaminated groundwater collected from Site 7 (Table 2). Finally, about 50 pore volumes after the occurrence of As breakthrough, a second input line containing either Fe(II) (added as $FeCl_2$ salt to columns 11A and 12A) or Ca (added as CaCl2 salt to columns 11B and 12B) was added to each column in order to evaluate the effect of such chemical amendments for remediation. The final concentrations of Fe(II) and Ca in the mixture entering the columns were 10 and 50 mg/L respectively. The amendment chemicals were added with 10% flow rate of groundwater and the level of dilution applied to the groundwater composition was taken into account for analysis of data.

In the second round, contaminated groundwater from Sites 5 and 7 were run through columns packed with corresponding sediments. For these columns, remediation by addition of a second influent stream containing only Fe(II) (20 mg/L) was studied. In both rounds of experiments, pH of Fe(II) solution in the feed reservoir was adjusted to ~2.75 in order to avoid premature

oxidation before entering the columns. After the conclusion of the experiments, sediments were extruded from columns in 2 cm increments and analyzed for total solid phase As and Fe.

3. Results

3. 1.Buffering capacity of sediments

As can be seen in Figure 1, sediments S-6 and S-10 have the highest pH buffering capacity. These two sediments have relatively higher natural pH (9.2 and 8.7) and also are the two grey colored sediments in the study site. They also have relatively higher percent clay according to the particle size distribution analyses conducted previously. The HCl fizzing tests indicated that calcite is present in these sediments and therefore explaining the observed higher level of buffering.

3.2. Factorial Experiments

In all of the studied sediments, the highest level of As(V) removal was observed for the combination of low pH, high Fe and high Ca concentrations (Figure 2). The treatment scheme (additional Fe, Ca, and lowering of pH) significantly affected the removal rate relative to the untreated control samples ($p < 0.001$).

Factorial ANOVA analysis indicates that the results are statistically significant for the effect of Ca ($p < 0.001$), Fe ($p < 0.001$), pH ($p < 0.05$), and PO_4 ($p < 0.05$). The difference in removal rate improvements among the different sediment types are not statistically significant at 95% confidence level ($p = 0.07$), however there is a positive correlation between the Langmuir derived sorption capacity and the average sorption increase by chemical amendments ($R^2 = 0.87$).

Among the independent factors, Fe amendment at 20 ppm shows the highest level of impact by increasing an average of 43% additional sorption ($p < 0.001$). pH adjustments results in the smallest level of increase in additional sorption (18%) by an independent factor. The Ca

treatment at 50 ppm increases the mean of amended sorption amount (relative to control) by 32% among all sediments ($p < 0.001$).

The ANOVA results indicates that the level of phosphate present in the system does not significantly affect the increased removal rate due to Ca amendment ($p = 0.13$). Therefore the main likely effect of Ca in increasing the observed retention rates is improving the adsorption by modifying the surface charge of sediments.

3.3. Effect of Ca on Adsorption

The impact of Ca on As adsorption is illustrated in Figure 3 for two sediment types. Increase in level of Ca treatment increases the adsorption rates across all initial As concentrations. The overall adsorption capacity is increased between 26 and 37% for the highest level of Ca treatment, although the results for the initial As concentrations up to 5000 µg/L at the low and medium levels of Ca do not differ greatly from original isotherm results without addition of Ca. These results provide further proof for the Ca induced increase in adsorption capacity observed in the factorial experiments.

3.4.Acidification Experiments

Results of acidification experiments are show in Figure 4 and listed in Table 4. Results show similar trends as observed in the previous studies with the groundwater from S-7. Dissolved As(V) and PO_4 concentrations decrease gradually with lowering of pH in the suspensions. The acidification experiment can be used for developing a site-specific calibrated geochemical model based on GC or Hybrid approach.

3.4. Column Experiments

Columns 11A and 11B effluents showed breakthrough after 5 pore volumes (Figure 5). The concentration of As(V) in the effluent exceeded the level of As(V) present in the influent groundwater by over 280 µg/L which is an increase of 56% compared to 500 µg/L measured in

the groundwater. This suggests that the incoming groundwater induced desorption of As from the sediments. The As(V) concentrations dropped to an average of 540 µg/L after 12 pore volumes and stayed relatively unchanged until the start of chemical amendment at 60 pore volumes. Column 12A and 12B reached breakthrough after only 1 pore volume and achieved the maximum effluent As concentration of 600 µg/L. The difference observed between the attenuation capacity of sediments S-11 and S-12 is in agreement with the adsorption isotherm results obtained in previous studies indicating that S-11 has higher adsorption capacity than S-12. No desorption of PO_4 from sediments was observed and the effluent levels did not exceed the influent concentrations. In fact the PO4 breakthrough for columns 11A and 11B occurred after 60 pore volumes and in columns 12A and 12B the effluents were slightly below the influent concentrations prior to start of chemical amendment.

The initial desorption of As from sediments is also observed for S-5 and S-7 columns with As concentrations in the effluents reaching 250 and 670 µg/L respectively. For these two sites no natural attenuation of contaminant by sediments was observed and the breakthrough of As(V) occurred immediately after only 1 pore volume.

Addition of Ca in columns 11A and 12A resulted in similar trends observed for the effluent As concentrations. Initially in both columns the Ca amendment caused a drop in the effluent concentrations, suggesting an improvement to the adsorption on the surfaces. This initial improvement can also be seen for the phosphate concentrations. However after certain number of pore volumes (19 in 11A and 8 in 12A) As concentrations returned to the levels before the amendment. Effluents from column 12A experienced another drop in As concentrations lasting for 9 pore volumes until it eventually returned to the levels similar to groundwater influent indicating lack of adsorption in the columns. However the effluent phosphate concentrations

remained lower than the baseline until the last pore volume sampled indicating that the Ca amendment was still effective in lowering concentrations.

Treatment of columns with Fe(II) showed an initial stage (20 pore volumes in 11B and 18 pore volumes in 12B) of fluctuations in As effluent concentrations followed by a slow subsequent removal phase until the last pore volume.

Treatment of column 5A with 20 mg/L of Fe(II) resulted in successfully lowering the As concentration in the effluent to below the target level of 10 μg/L after 6 pore volumes. Column 5B experienced loss of effluent volume after 5 pore volumes probably due to clogging. Columns 7A and 7B achieved an average removal rate of 61% after 5 to 9 pore volumes.

The pH in effluents of S-11 and S-12 columns remained relatively unchanged during the course of the experiments at a range of 8.2-8.4. In S-5 and S-7 columns, effluent pH before the amendments were at 8.3-8.4 range and was lowered to 7.5-7.8 range following the start of amendments. These results imply the presence of major pH buffering capacity within the sediments. Other factors such as CO_2 outgassing from the groundwater samples due to the difference between the partial pressures in an aquifer and the laboratory atmosphere could also be partly responsible for increase in pH levels of groundwater.

Effluents were measured continuously for presence of Fe(II) however the concentrations were never above detection limit (<1 mg/L) indicating that the added Fe(II) is mostly oxidized after mixing with the groundwater at the injection port and through the columns. Figure 7 shows the changes in solid phase concentrations of Fe and As along the distance from bottom to top of the columns.

4. Discussion

Different levels of contaminants sorption within the columns were observed. Maximum removal rates of As(V) and PO_4 achieved in the column experiments are shown in Figure 6. Column results show an initial fast rate desorption of As from sediments followed by a steady desorption rate until the start of remediation. This finding is important for understanding the historical contamination of the site and can imply that the original source of As in the plume was in fact the naturally occurring As in the sediments released due to alkaline and competitive desorption processes.

Results also clearly show that phosphate outcompetes As(V). While the As breakthrough takes place after only a few pore volumes, phosphate maintains a small but steady level of adsorption up to 60 pore volumes.

Ca amendments seem to initially improve the adsorption rates however this impact is temporary for As(V) and the increased adsorption capacity apparently becomes exhausted perhaps due to the incoming flux of high pH and PO_4 solution neutralizing the Ca effect and outcompeting As. Three main mechanisms can be hypothesized to explain the results of Ca addition to suspensions. First is through adsorption of Ca^{2+} cations onto solid surfaces and neutralizing the negative surface charges, hence increasing the affinity of surface to adsorption of negatively charged arsenate species. The second possibility is by super-saturation and consequent precipitation of Ca-phosphate phases which reduces the competition factor and therefore could increase As adsorption. Third possible mechanism is formation of Ca-arsenate precipitates. PHREEQC was used with updating the miteq.v4 database with metal arsenate solubility product constants (Martínez-Villegas et a., 2013) to calculate the saturation indices for Ca-arsenate and Ca-phosphate precipitates. The chemical equilibrium calculations by PHREEQC indicate that none

of such phases are supersaturated and therefore ruling out the possibility of Ca influencing the results through precipitation reactions.

Analyzing the isotherm results show that at the low concentrations, Ca addition does not improve the As adsorption rate compared to the isotherm experiment without Ca addition. At significantly higher Ca concentrations of 50 and 100 mg/L however, As sorption capacity is improved. This beneficial impact can be explained by the surface charge neutralizing effect of Ca^{2+} cation. The additional soprtion capacity observed increases with increasing As concentrations. These results indicate that there is a threshold amount of Ca needed for modifying the solid surface charges to a level that compensate the competing effect of Ca by greatly higher affinity for As(V) oxyanions.

Application of Fe oxides or their precursors as amendments for chemical stabilization of As in soils has been reported in the literature (Komarek et al., 2013; Kumpiene et al., 2008). Salts such as Fe (II)/(III) sulfates, or elemental Fe(0) have been used to control As mobility in soils by formation of insoluble secondary Fe-As minerals (e.g., scorodite, $FeAsO_4.H_2O$) and more importantly sorption onto precipitated Fe oxide minerals such as goethite and ferrihydrite. Application of Fe salts will also cause acidification of treated soils (Welch et al., 2003).

There have been a few attempts made to remediate As through use of in-situ methods and applying Fe to increase sorption capacity of aquifers (Welch et al., 2003; Paul et al., 2010). Paul et al. (2010) conducted laboratory column experiments as part of a remediation study to test the results of aeration, Fe addition and pH adjustment on effluent level of As. Welch et al., (2003) utilized addition of ferric chloride ($FeCl_3$) in order to cause precipitation of HFO and facilitate As(v) adsorption. The study found very effective removal rates of As in laboratory experiments

by combination of lowering the pH and increasing the iron oxide content however this practice resulted only in moderate As removal in the field.

Fe(II) application in this study resulted in maximum removal rates between 50 and 91% however the beneficial results for As removal were only yielded alter a significant number of pore volumes. This could be due to the lack of sufficient reaction time for adsorption of As(V) on the freshly formed Fe phases. The absence of Fe(II) in the column effluents indicates complete oxidation taking place within the columns, however the formation of Fe oxide phases and adsorption of As(V) might require longer reaction times than the average residence time of solution in the columns.

5. Conclusion

Any efforts to facilitate the immobilization of As in such contaminated systems need to take into account the different parameters controlling the attenuation processes such as pH, redox potential, competing ions, soil chemical and physical characteristics. A single parameter immobilization strategy is rarely successful for stabilizing trace contaminants (Kumpiene et al., 2008).

Factorial remediation results show that the combination of low pH, high Fe and high Ca results in highest level of As(V) removal from solution phase compared to control samples. This effect however, decreases with increase in phosphate levels due to competition.

Iron oxides are known to have significant affinity for adsorbing As from solution phase via forming inner-sphere surface complexes and are commonly present and widely distributed in sediments and have been used extensively for treating contaminated waters. Addition of Fe containing compounds leading to precipitation of oxides and hydroxide phases in the aquifer

could enhance the natural attenuation by creating more sorption sites and capacity for immobilization of contaminants such as As. However, the kinetics of Fe(II) oxidation and precipitation of Fe(III) phases, as well as kinetics of As(V) adsorption onto the freshly formed solids could be a major factor limiting the removal rates.

In this study, beneficial effect of Ca amendments were observed both in batch factorial and isotherm experiments, as well as limited effect on the sorption rates in column studies. Calculated SI values from PHREEQC indicate that none of the Ca-arsenate or Ca-phosphate species are supersaturated, therefore ruling out the possibility of precipitation of these phases as secondary minerals. Future studies are needed to investigate the interactions between Ca and As on the surfaces of minerals in more detail.

Figures

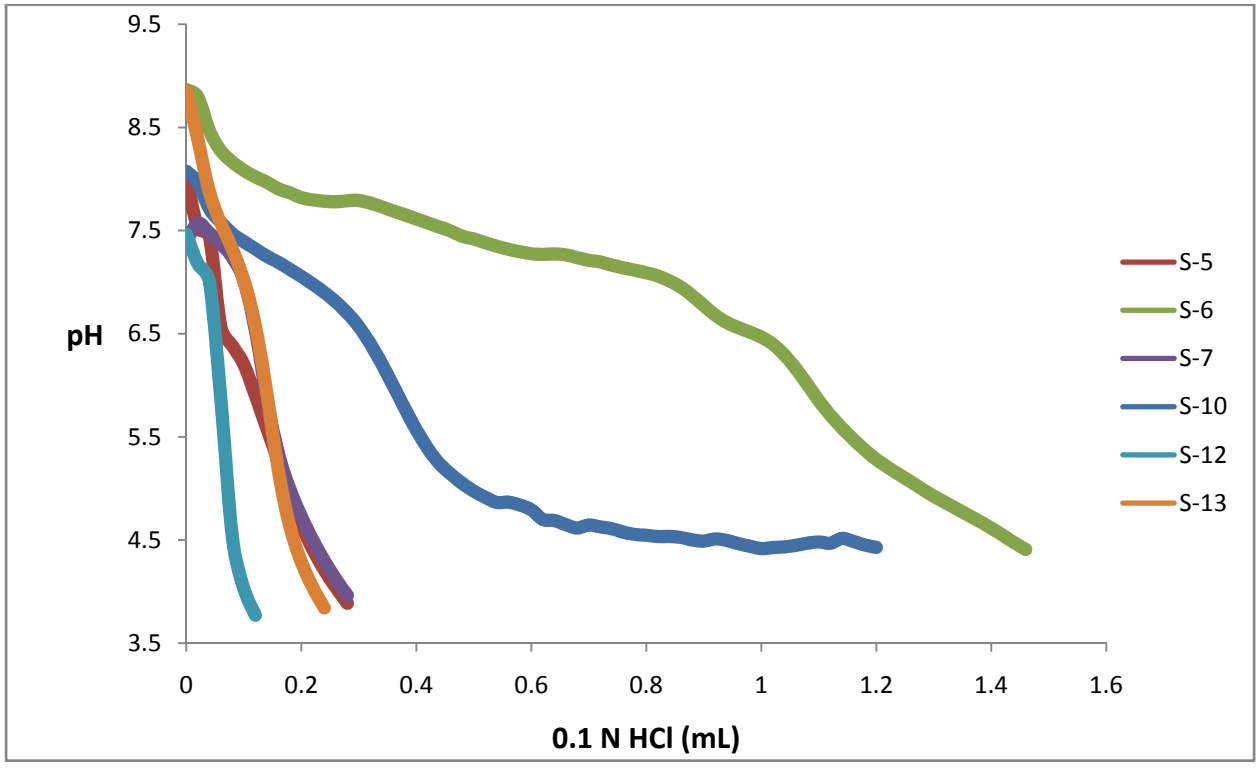

Figure 1. Acid titration of sediment suspensions

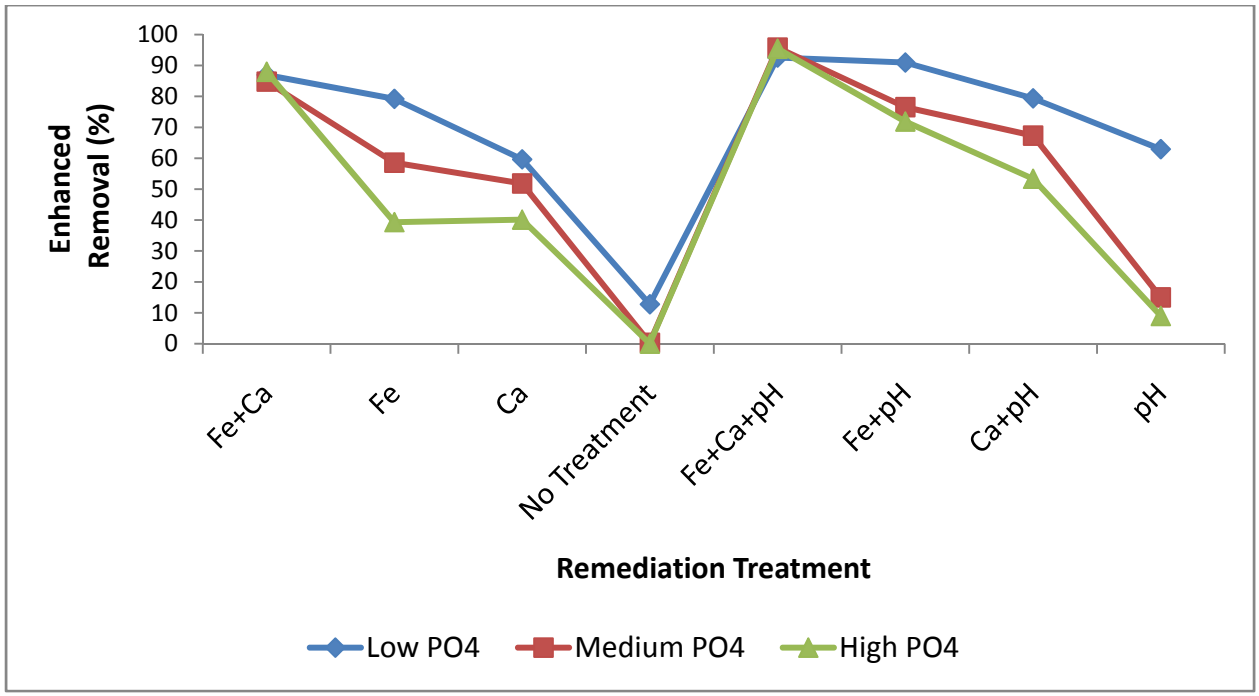

Figure 2. Average effect of remediation treatments on increased As(V) removal relative to control samples from batch factorial tests under three levels of phosphate (0.03 , 0.7, 2 mg/L).

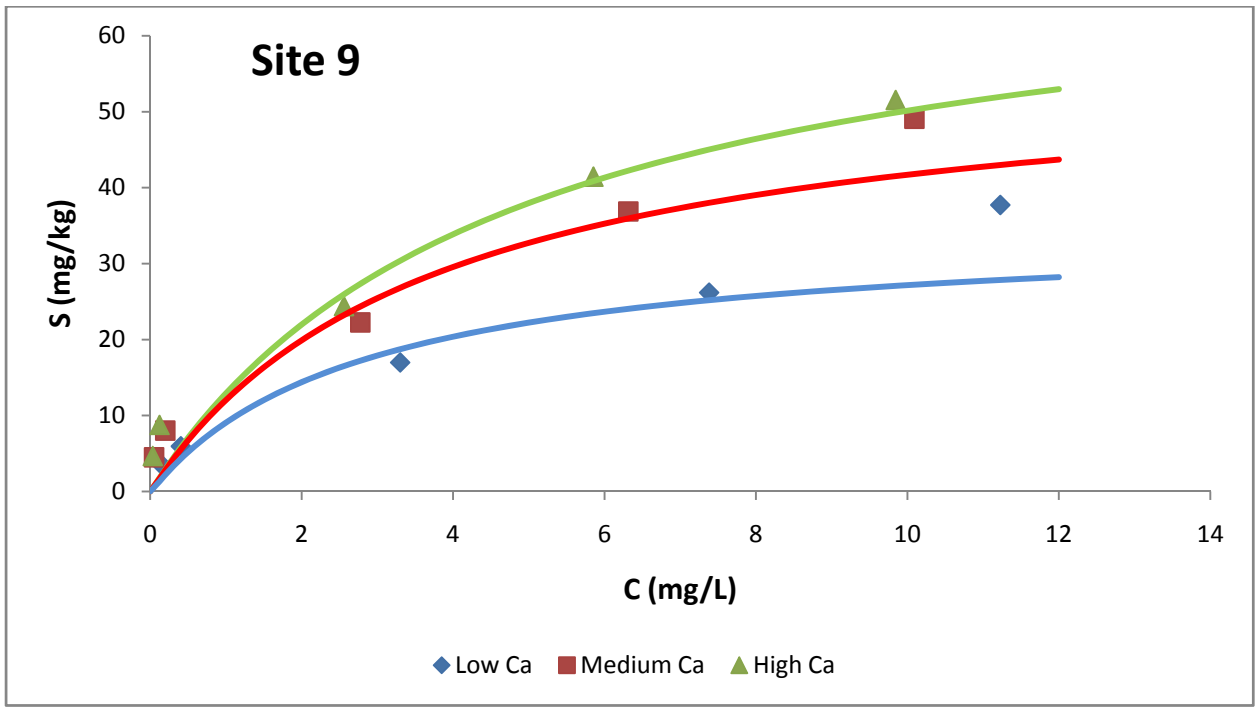

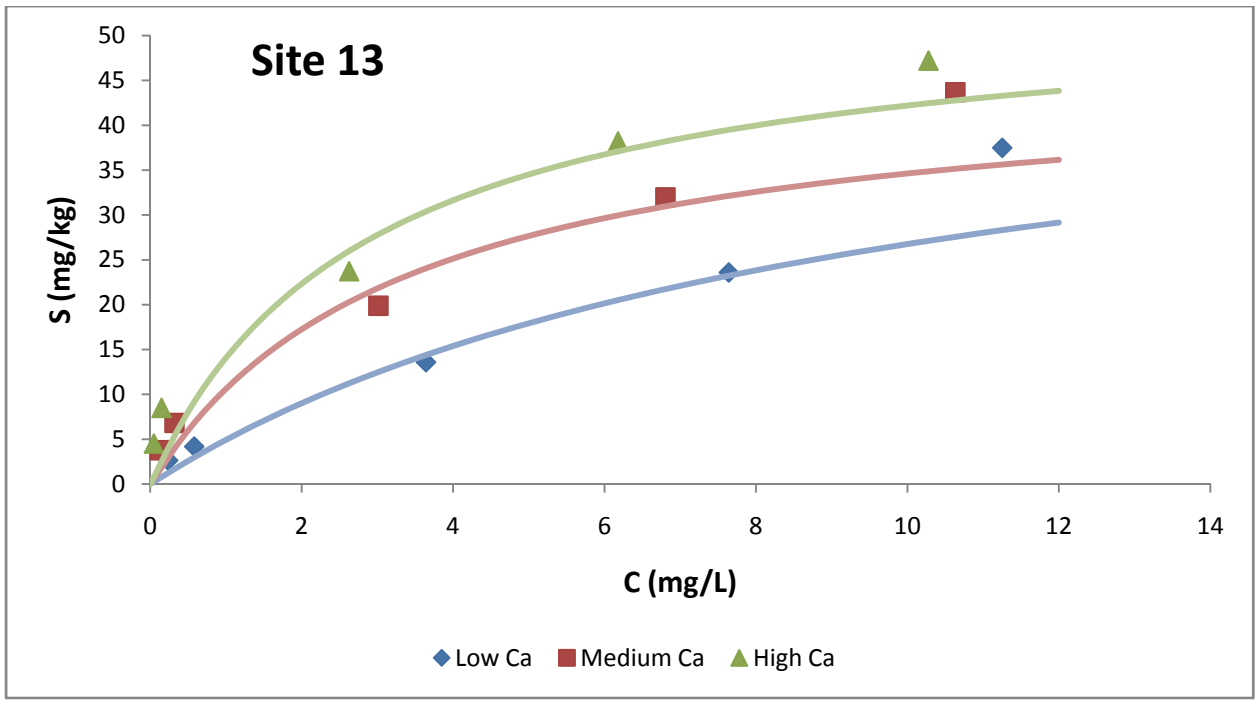

Figure 3. Adsorption isotherm results for three levels of Ca (Low=1 mg/L, Medium=50 mg/L, High=100 mg/L)

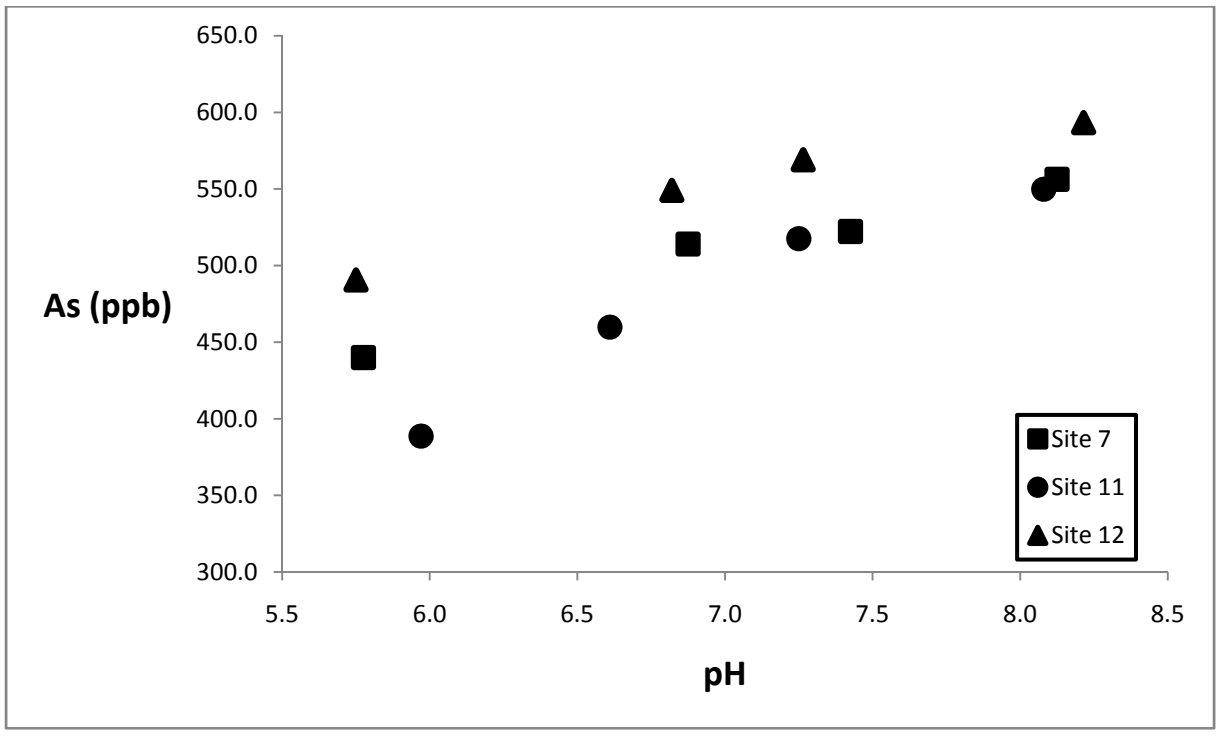

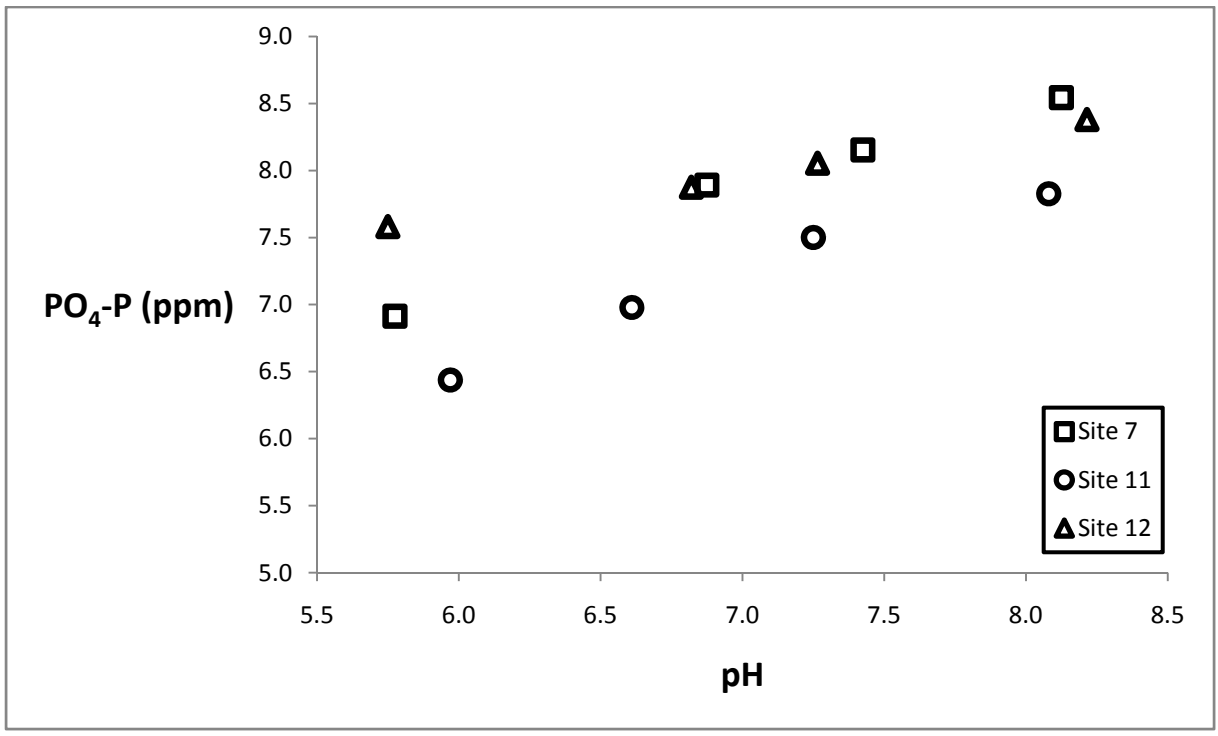

Figure 4. Concentrations of As and PO_4 from sediment suspensions with contaminated groundwater from S-7 as a function of pH (acidification experiments)

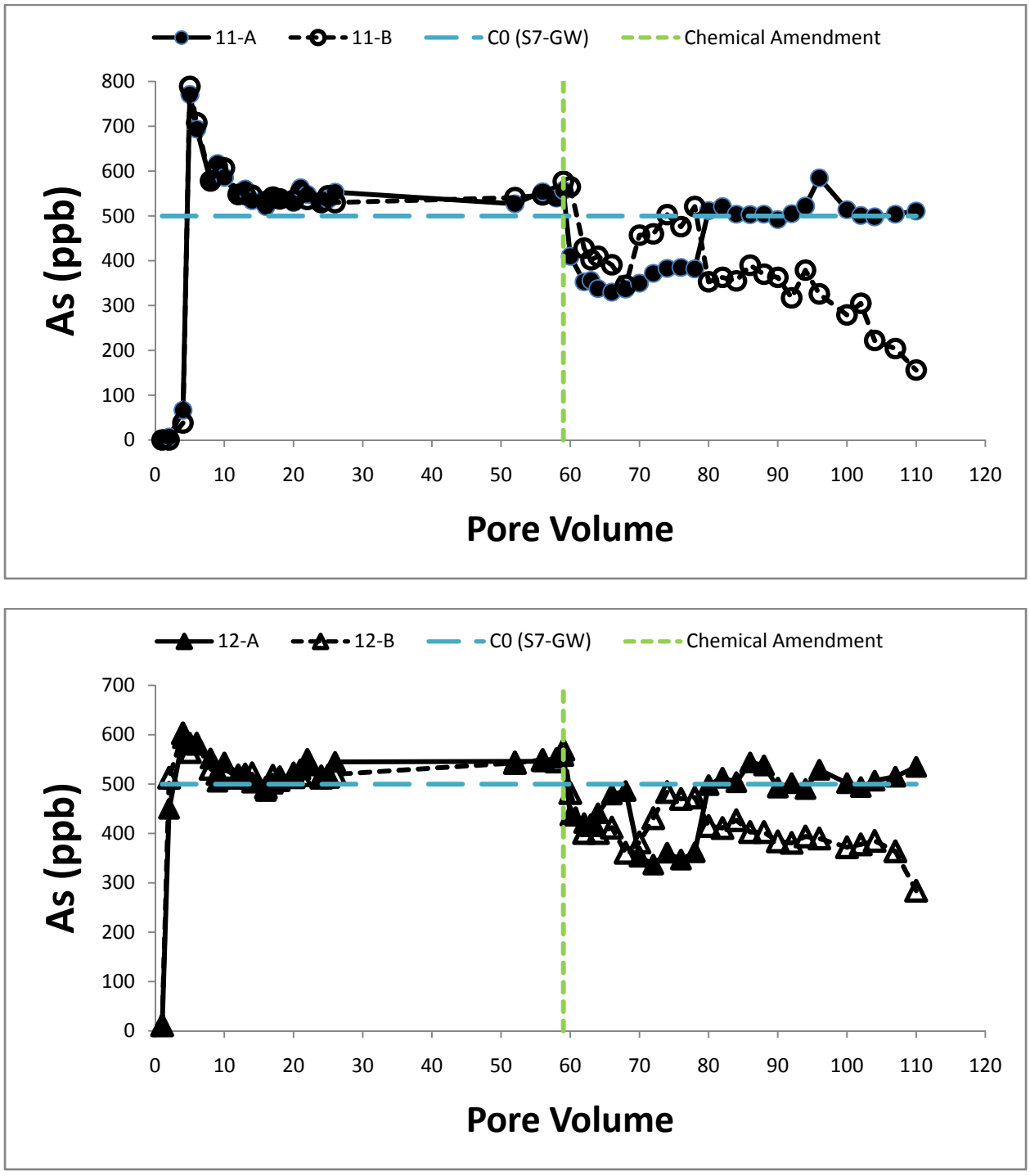

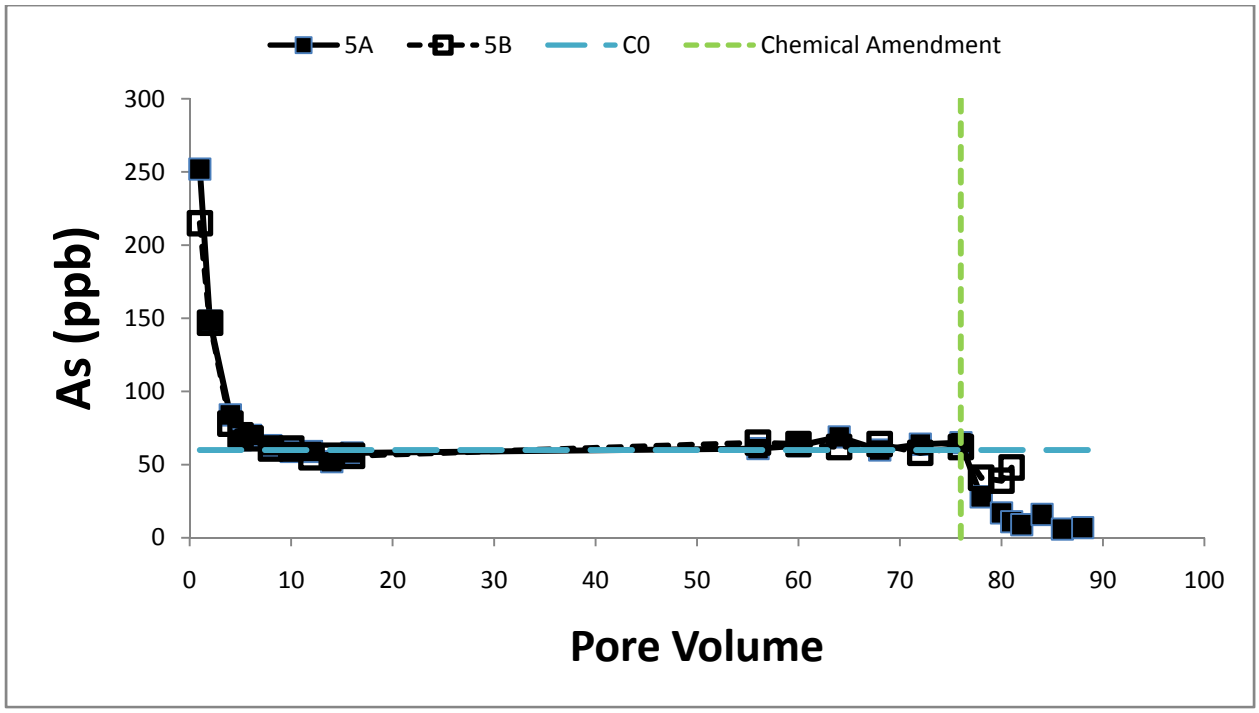
5A
5B
C0
Chemical Amendment
As (ppb)
300
250
200
150
100
50
0
0
10
20
30
40
50
60
70
80
90
100
Pore Volume

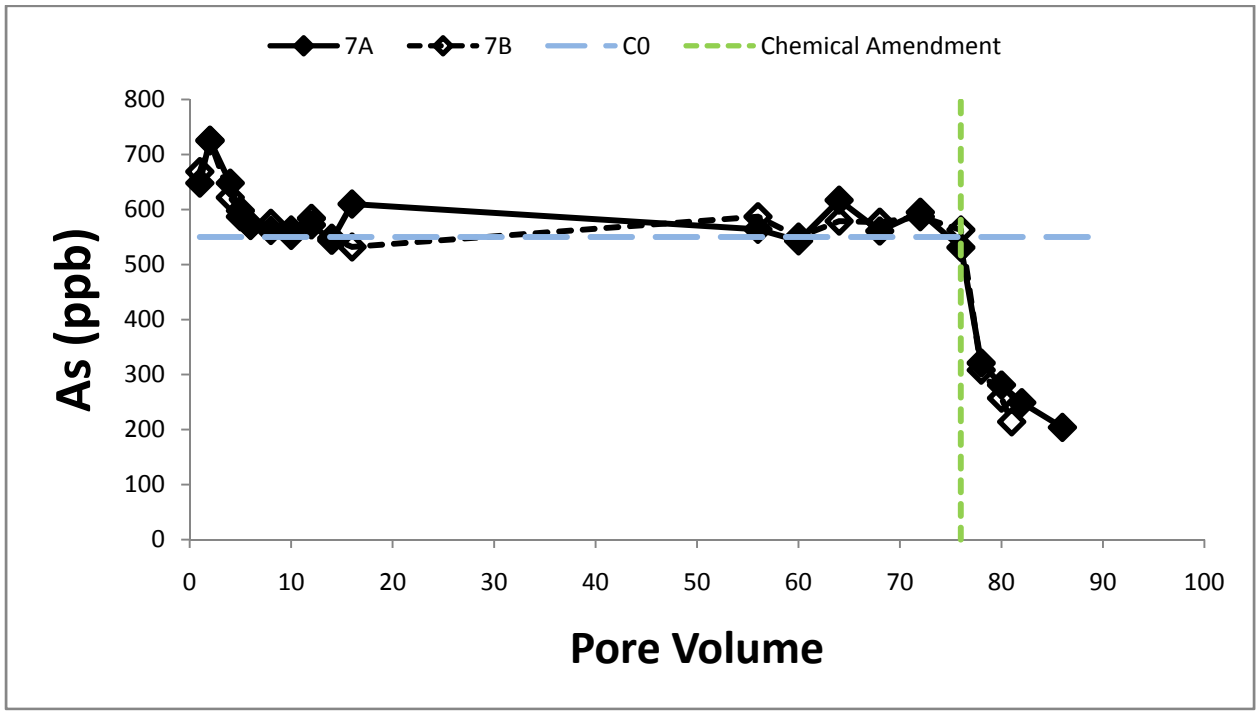
7A
7B
C0
Chemical Amendment
As (ppb)
800
700
600
500
400
300
200
100
0
0
10
20
30
40
50
60
70
80
90
100
Pore Volume

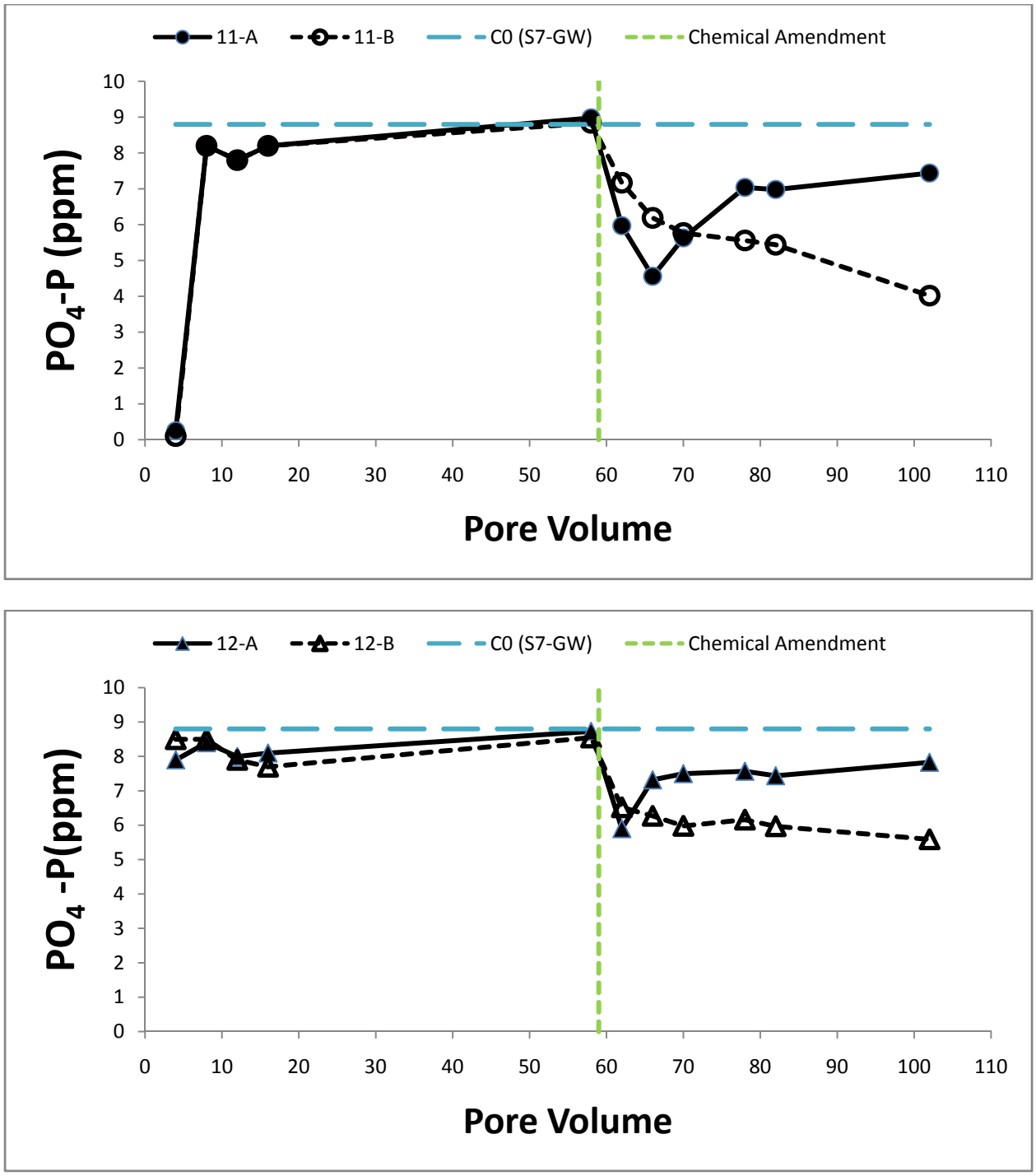

Figure 5. Concentrations of As and PO_4-P in the effluents of columns

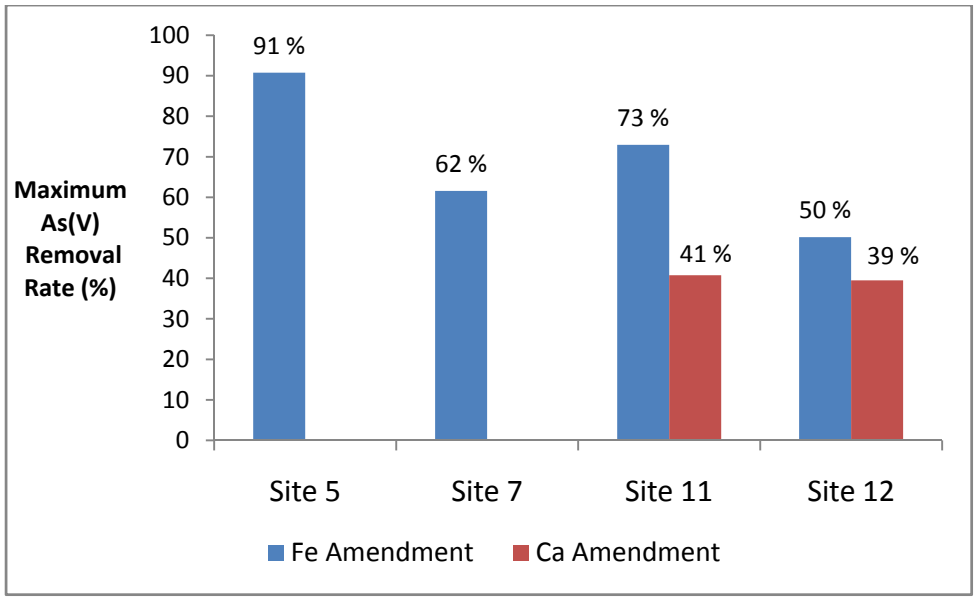

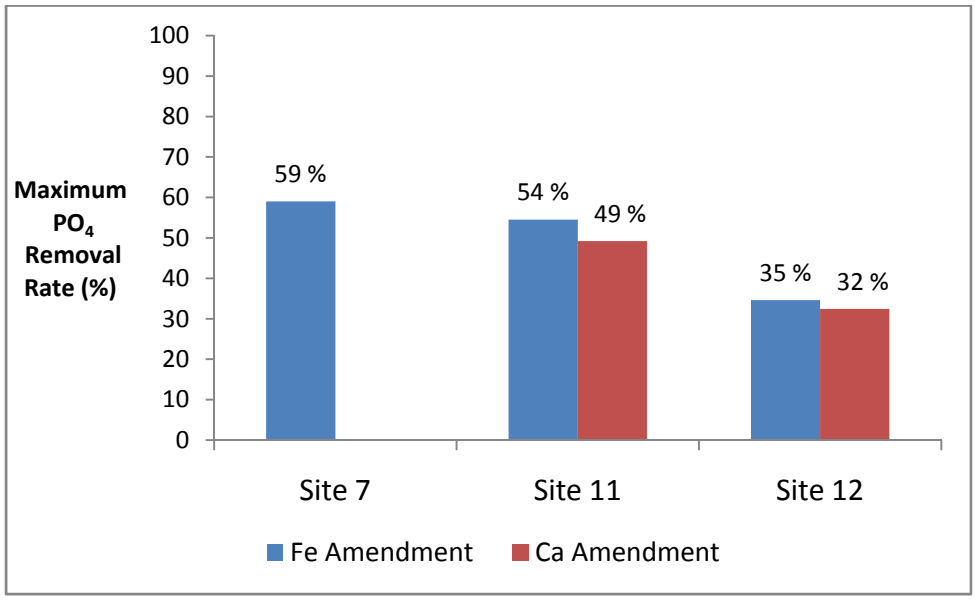

Figure 6. Summary of maximum removal rates (%) for As and PO_4 achieved in columns with chemical amendments

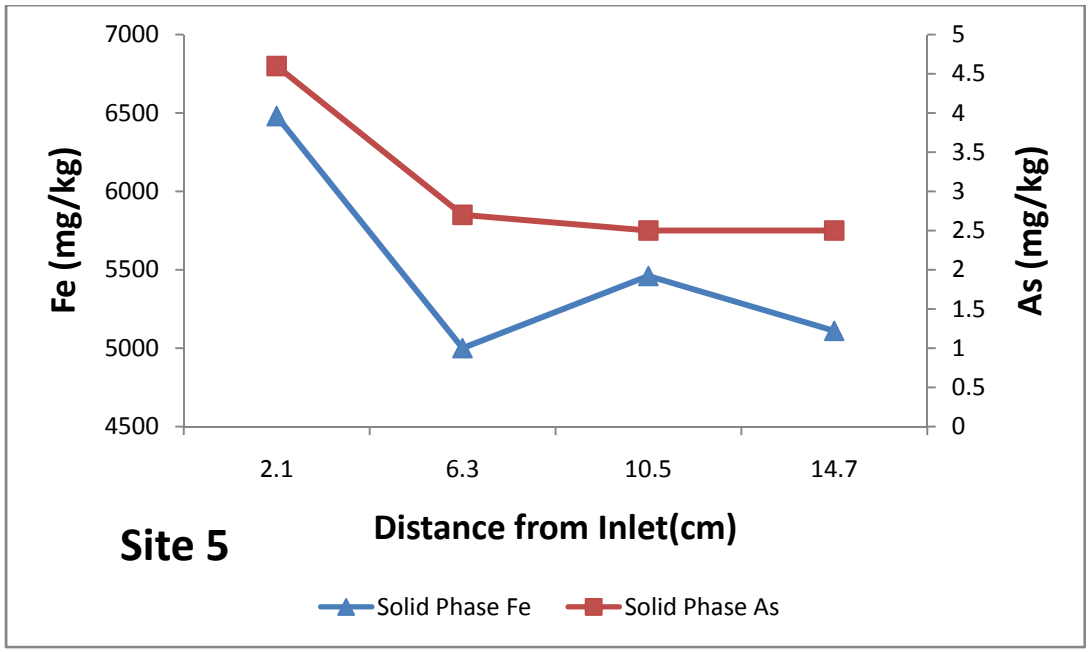
7000
6500
6000
5500
5000
4500
Fe (mg/kg)
5
4.5
4
3.5
3
2.5
2
1.5
1
0.5
0
As (mg/kg)
2.1
6.3
10.5
14.7
Site 5
Distance from Inlet(cm)
Solid Phase Fe
Solid Phase As

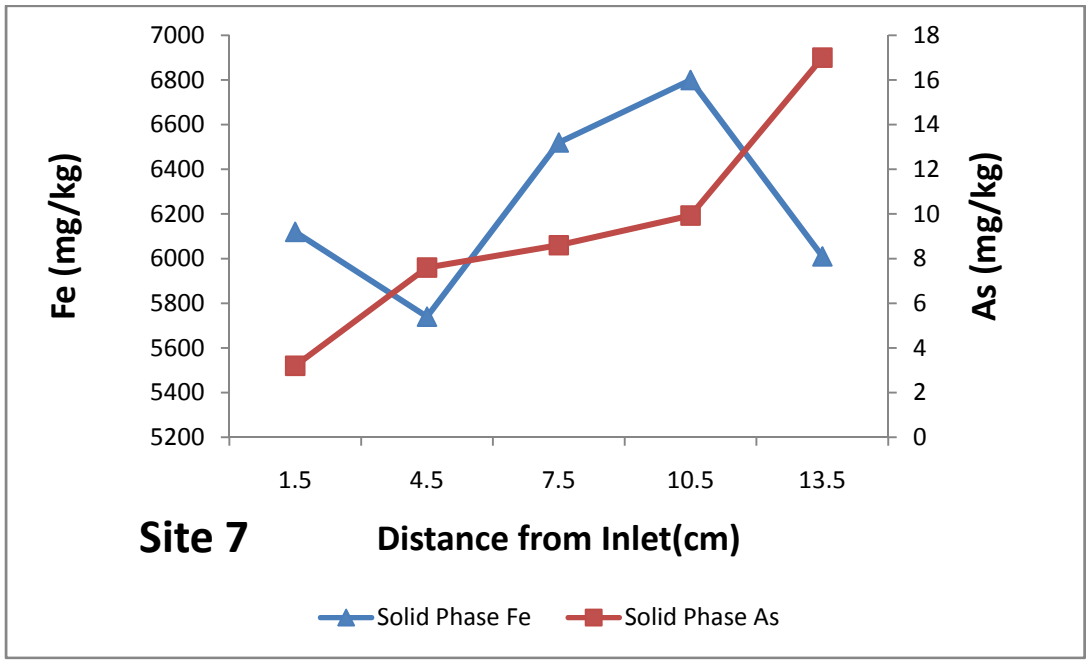
7000
6800
6600
6400
6200
6000
5800
5600
5400
5200
Fe (mg/kg)
18
16
14
12
10
8
6
4
2
0
As (mg/kg)
1.5
4.5
7.5
10.5
13.5
Site 7
Distance from Inlet(cm)
Solid Phase Fe
Solid Phase As

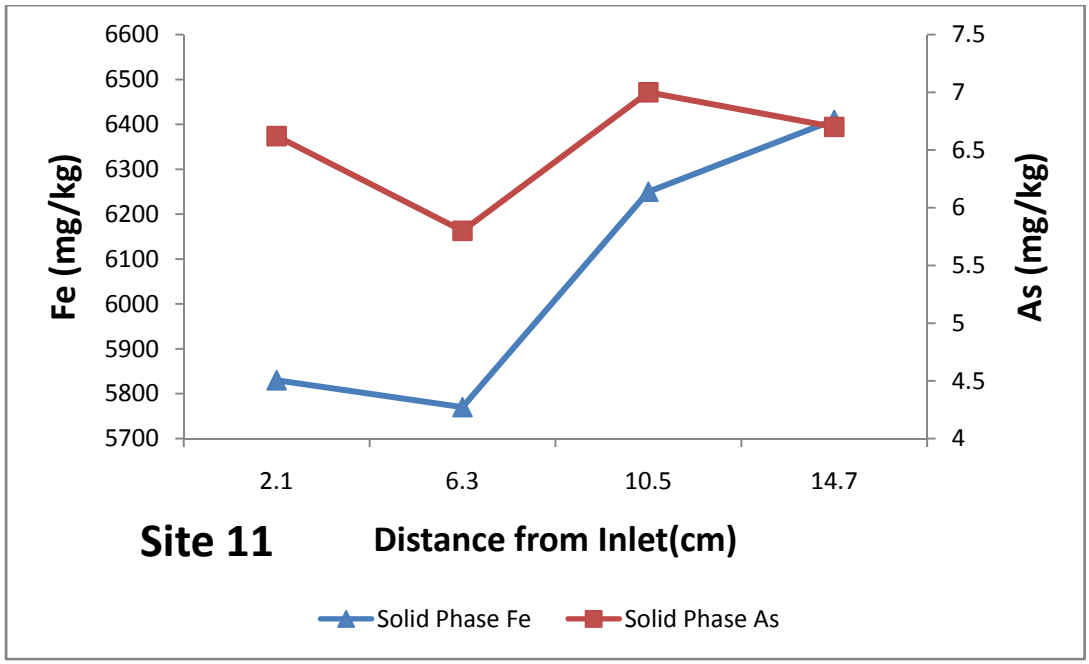

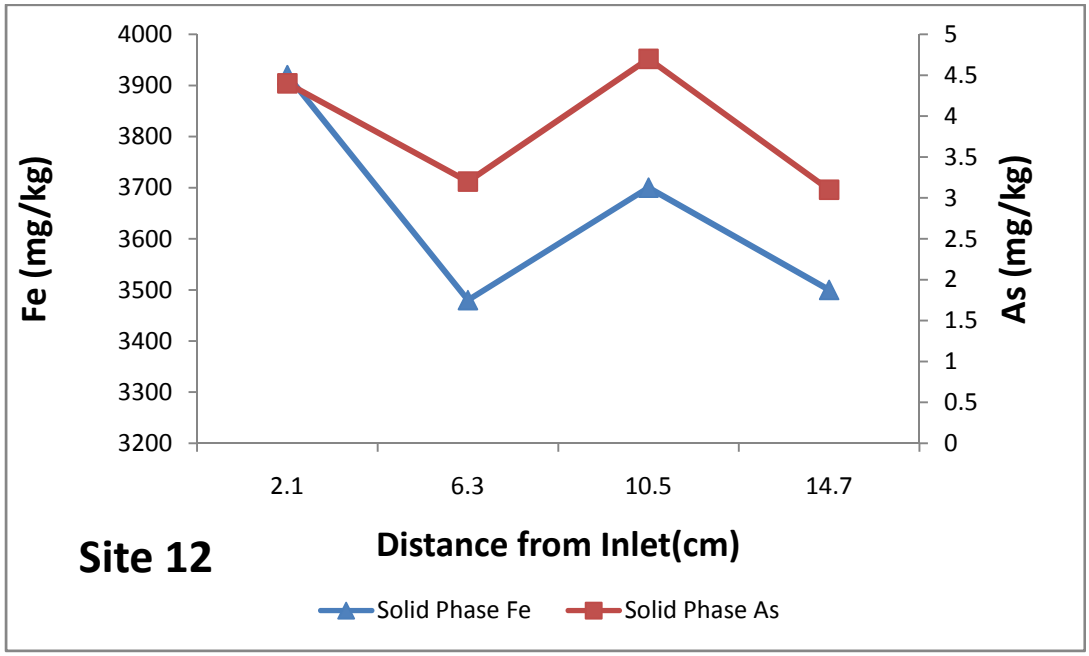

Figure 7. Solid phase concentrations of Fe and As (mg/kg) along the column profile

Tables

Table 1. Column physical properties

Column	Sediment Mass(g)	Porosity(%)	Solid/Solution (kg/L)	Residence Time (h)	Dry bulk density (g/cm^3)	Flow(mL/hr)
S-11A	16.87	38.2	4.29	6.56	1.64	0.60
S-11B	17.39	36.3	4.65	6.23	1.69	0.60
S-12A	17.59	35.6	4.80	6.10	1.71	0.60
S-12B	17.89	34.5	5.04	5.92	1.74	0.60
S-7A	20.04	26.6	7.32	4.56	1.95	0.60
S-7B	20.14	26.2	7.46	4.50	1.96	0.60
S-5A	16.65	39.0	4.14	6.69	1.62	0.60
S-5B	16.44	39.8	4.01	6.83	1.60	0.60

Table 2. Groundwater quality data

Site	pH	As (ppb)	Fe (ppb)	PO_4-P(ppm)
S-5	9.6	60	130	1.4
S-7	8	510	190	8.8
S-11	7.1	<5	10	<0.1
S-12	7.5	<5	300	<0.1

Table 3. Results of factorial remediation experiments. Subscripts 0 and 7 indicate the concentration initial and at equilibrium after 7 days. Enhanced removal percentages are calculated relative to control samples. (*ND=not detected)

Sediment Site	Sample ID	pH	Fe (ppm)	Ca (ppm)	P_0 (ppm)	As_0 (ppb)	As_7 (ppb)	As Removal (%)	P_7 (mg/L)	Enhanced Reoval (%)
	1	9	20	50	0.7	2500	75.2	97.0	0.1	69.6
	2	9	20	1	0.7	2500	191.7	92.3	1.1	22.4
	3	9	0.5	50	0.7	2500	201.8	91.9	0.9	18.3
	4	9	0.5	1	0.7	2500	259.4	89.6	1.0	-5.0
5	5	7	20	50	0.7	2500	20.8	99.2	0.0	91.6
	6	7	20	1	0.7	2500	115.9	95.4	0.4	53.1
	7	7	0.5	50	0.7	2500	143.1	94.3	0.6	42.1
	8	7	0.5	1	0.7	2500	245.1	90.2	1.2	0.8
	Control	9.2	-	-	0.7	2500	247.1	90.1	1.3	0.0
	1	9	20	50	0.03	2500	137.9	94.5		79.4
	2	9	20	1	0.03	2500	195.1	92.2		70.8
	3	9	0.5	50	0.03	2500	409.8	83.6		38.7
	4	9	0.5	1	0.03	2500	618.9	75.2		7.4
6	5	7	20	50	0.03	2500	81.9	96.7	ND	87.7
	6	7	20	1	0.03	2500	101.0	96.0		84.9
	7	7	0.5	50	0.03	2500	238.5	90.5		64.3
	8	7	0.5	1	0.03	2500	333.3	86.7		50.1
	Control	8.8	-	-	0.03	2500	668.3	73.3		0.0
	1	9	20	50	2	2500	155.5	93.8	0.0	85.5
	2	9	20	1	2	2500	665.3	73.4	0.1	37.9
	3	9	0.5	50	2	2500	462.3	81.5	0.0	56.8
	4	9	0.5	1	2	2500	1036.8	58.5	0.6	3.2
7	5	7	20	50	2	2500	43.3	98.3	0.0	96.0
	6	7	20	1	2	2500	88.3	96.5	0.0	91.8
	7	7	0.5	50	2	2500	319.0	87.2	0.0	70.2
	8	7	0.5	1	2	2500	979.9	60.8	0.3	8.5
	Control	8.5	-	-	2	2500	1070.9	57.2	0.5	0.0
	1	9	20	50	0.7	2500	0.0	100.0	0.0	100.0
	2	9	20	1	0.7	2500	17.0	99.3	0.0	94.7
	3	9	0.5	50	0.7	2500	47.2	98.1	0.0	85.4
9	4	9	0.5	1	0.7	2500	304.7	87.8	0.4	5.5
	5	7	20	50	0.7	2500	0.0	100.0	0.0	100.0
	6	7	20	1	0.7	2500	0.0	100.0	0.0	100.0
	7	7	0.5	50	0.7	2500	24.1	99.0	0.0	92.5

	8	7	0.5	1	0.7	2500	228.5	90.9	0.2	29.2
	Control	8.4	-	-	0.7	2500	322.6	87.1	0.0	0.0
	1	9	20	50	0.03	2500	23.5	99.1		94.5
	2	9	20	1	0.03	2500	53.2	97.9		87.6
	3	9	0.5	50	0.03	2500	83.1	96.7		80.6
	4	9	0.5	1	0.03	2500	350.0	86.0		18.1
11	5	7	20	50	0.03	2500	11.2	99.6	ND	97.4
	6	7	20	1	0.03	2500	12.9	99.5		97.0
	7	7	0.5	50	0.03	2500	23.7	99.1		94.4
	8	7	0.5	1	0.03	2500	103.7	95.9		75.7
	Control	7.5	-	-	0.03	2500	427.5	82.9		0.0
	1	9	20	50	1.5	2500	24.0	99.0	0.0	90.5
	2	9	20	1	1.5	2500	149.7	94.0	0.5	40.8
	3	9	0.5	50	1.5	2500	193.6	92.3	0.5	23.4
	4	9	0.5	1	1.5	2500	272.5	89.1	1.1	-7.8
13	5	7	20	50	1.5	2500	12.8	99.5	0.0	94.9
	6	7	20	1	1.5	2500	121.3	95.1	0.0	52.0
	7	7	0.5	50	1.5	2500	160.5	93.6	0.3	36.5
	8	7	0.5	1	1.5	2500	229.0	90.8	0.9	9.4
	Control	9.2	-	-	1.5	2500	252.8	89.9	0.9	0.0

Table 4. Acidification experiment data

Sample Site	pH	As(ppb)	P(ppm)
S-7	8.1	556	8.5
	7.4	522	8.2
	6.9	514	7.9
	5.8	440	6.9
S-11	8.1	550	7.8
	7.3	518	7.5
	6.6	460	7.0
	6.0	389	6.4
S-12	8.2	593	8.4
	7.3	569	8.1
	6.8	549	7.9
	5.8	491	7.6

Chapter 5. Summary

This work aims at providing a better understanding of controls on As(V) dissolved concentrations through experimental studies on natural samples collected from both contaminated and uncontaminated saturated zones of a sandy aquifer and geochemical modeling of the results.

In chapter 2, batch adsorption experiments are conducted on natural sediment samples to study the adsorption as a function of time and aqueous concentration. The kinetic experimental data are fitted using both pseudo-first and pseudo-second order models. The piecewise linear regression of data results in determining two distinct slopes and a cutoff time point highlighting the two kinetic stages of adsorption; a fast adsorption reaction occurring in the first 14-19 hours followed by a gradual step until equilibrium reached after 7 days. Pseudo-second order models provide excellent fits to the data and second order rate constants are derived for adsorption of As(V) on the sediments.

Adsorption isotherm experiments conducted on nine different samples are fitted with both Freundlich and Langmuir models and evaluated. The results the sensitivity of Langmuir model to the highest concentration used in the range of data to be fitted. This is of high importance for interpretation and implementation of isotherm results in SCM and RTM approaches. The derived Langmuir isotherm parameters show significant reduction in adsorption capacity of sediments in contact with contaminated groundwater. The adsorption capacity of sediments show relationship with the amorphous Fe and Al content of sediments, and BET surface area in the uncontaminated areas. Difference in rates of desorption from original samples and samples after loading with As indicate the presence of reversible and irreversible adsorption sites on the sediments. Sequential extraction data and higher ratio of As/Fe provide

evidence that the amorphous phases are crucial to adsoprtion of As and other competing ions such as phosphate.

In chapter 3, four different SCMs are developed and quantitatively compared for predicting and fitting of experimental data obtained from batch acidification experiments conducted on sediment and groundwater samples collected from the study site. The results show that the GC-BET and Hybrid-Isotherm models are promising approaches in terms of calibrating SCMs to conditions of a specific site for the purposes of using the model for assessing different remediation options. The results underscore the inherent complexity of heterogeneous surfaces and the high level of sensitivity of models to the methods for describing and quantifying the sorption sites.

In chapter 4, both batch and column experiments are conducted to test the effectiveness of chemical amendments for lowering dissolved As(V) concentrations in contaminated groundwaters. Factorial remediation experiments show that lower pH and higher concentrations of Fe and Ca improve the adsorption rates of As(V) significantly. Addition of Al provide comparable increase in adsorption capacities of sediments. Addition of Ca in isotherm experiments show consistent increase in adsorption capacity of sediments which is likely due to increased positive charge on the surface of sediments. The methodology used in this work for packing columns was verified by tracer studies and results in consistent and reproducible porosities. The column studies demonstrate varying levels of success in achieving removal of As(V) from aqueous phase. The solid phase analyses indicate that Fe and As concentrations in the sediments vary accordingly.

The work conducted in this dissertation covers portions of a three step framework needed to build a comprehensive geochemical model capable of predicting As concentrations in a

groundwater system. First step is to characterize and quantify the adsorptive properties of aquifer solids with respect to the solute of concern both kinetically and thermodynamically. Next, a model needs to be developed that is capable of predicting adsorption data as a function of solutes concentrations, pH, and presence of major competing ions. This goal is achieved by a hybrid approach for incorporating empirical and mechanistic adsorption models as well as inputting general water quality data, solid phase physical and chemical characteristics. Finally, the developed adsorption model will be used in a transport code to predict the data from column experiments that can mimic the natural conditions.

Future work will be needed to implement the kinetic adsorption rate constants derived in Chapter 2 and the developed GC-BET and Hybrid-Isotherm SCMs from Chapter 3 in a reactive transport model (RTM) to simulate the experimental data obtained from the column studies conducted in Chapter 4.

References

Bothe, J. V., & Brown, P. W. (1999). Arsenic immobilization by calcium arsenate formation. *Environmental Science & Technology*, *33*(21), 3806-3811.

Cances, B., Juillot, F., Morin, G., Laperche, V., Alvarez, L., Proux, O., ... & Calas, G. (2005). XAS evidence of As (V) association with iron oxyhydroxides in a contaminated soil at a former arsenical pesticide processing plant. *environmental science & technology*, *39*(24), 9398-9405.

Currell, M., Cartwright, I., Raveggi, M., & Han, D. (2011). Controls on elevated fluoride and arsenic concentrations in groundwater from the Yuncheng Basin, China. *Applied Geochemistry*, *26*(4), 540–552.

Duker, A. A., Carranza, E. J. M., & Hale, M. (2005). Arsenic geochemistry and health. *Environment international*, *31*(5), 631-641.

Gao, Y., & Mucci, A. (2001). Acid base reactions, phosphate and arsenate complexation, and their competitive adsorption at the surface of goethite in 0.7 M NaCl solution. *Geochimica et Cosmochimica Acta*, *65*(14), 2361-2378.

Goldberg, S. (2002). Competitive adsorption of arsenate and arsenite on oxides and clay minerals. *Soil Science Society of America Journal*, *66*(2), 413-421.

Hongshao, Z., & Stanforth, R. (2001). Competitive adsorption of phosphate and arsenate on goethite. *Environmental Science & Technology*, *35*(24), 4753-4757.

Jain, A., & Loeppert, R. H. (2000). Effect of competing anions on the adsorption of arsenate and arsenite by ferrihydrite. *Journal of environmental quality*, *29*(5), 1422-1430.

Kanel, S. R., Nepal, D., Manning, B., & Choi, H. (2007). Transport of surface-modified iron nanoparticle in porous media and application to arsenic (III) remediation. *Journal of Nanoparticle Research*, *9*(5), 725-735.

Kanematsu, M., Young, T. M., Fukushi, K., Sverjensky, D. A., Green, P. G., & Darby, J. L. (2010). Quantification of the effects of organic and carbonate buffers on arsenate and phosphate adsorption on a goethite-based granular porous adsorbent. *Environmental science & technology*, *45*(2), 561-568.

Lin, Z., & Puls, R. W. (2003). Potential indicators for the assessment of arsenic natural attenuation in the subsurface. *Advances in Environmental Research*, *7*(4), 825-834.

Liu, F., De Cristofaro, A., & Violante, A. (2001). Effect of pH, phosphate and oxalate on the adsorption/desorption of arsenate on/from goethite. *Soil Science*, *166*(3), 197-208.

Lovley, D. R., & Phillips, E. J. (1986). Organic matter mineralization with reduction of ferric iron in anaerobic sediments. *Applied and Environmental Microbiology*, *51*(4), 683-689.

Manning, B. A., & Goldberg, S. (1996). Modeling competitive adsorption of arsenate with phosphate and molybdate on oxide minerals. *Soil Science Society of America Journal*, *60*(1), 121-131.

Martin, T. A., & Kempton, J. H. (2000). In situ stabilization of metal-contaminated groundwater by hydrous ferric oxide: An experimental and modeling investigation. *Environmental science & technology*, *34*(15), 3229-3234.

Martínez-Villegas, N., Briones-Gallardo, R., Ramos-Leal, J. A., Avalos-Borja, M., Castañón-Sandoval, A. D., Razo-Flores, E., & Villalobos, M. (2013). Arsenic mobility controlled by solid calcium arsenates: A case study in Mexico showcasing a potentially widespread environmental problem. *Environmental Pollution*, *176*, 114-122.

Masue, Y., Loeppert, R. H., & Kramer, T. a. (2007). Arsenate and arsenite adsorption and desorption behavior on coprecipitated aluminum:iron hydroxides. *Environmental Science & Technology*, *41*(3), 837–42.

Meng, X., Bang, S., & Korfiatis, G. P. (2000). Effects of silicate, sulfate, and carbonate on arsenic removal by ferric chloride. *Water Research*, *34*(4), 1255-1261.

Morin, G., Lecocq, D., Juillot, F., Calas, G., Ildefonse, P., Belin, S., ... & Borensztajn, S. (2002). EXAFS evidence of sorbed arsenic (V) and pharmacosiderite in a soil overlying the Echassières geochemical anomaly, Allier, France. *Bulletin de la Société Géologique de France*, *173*(3), 281-291.

Paktunc, D., Foster, A., Heald, S., & Laflamme, G. (2004). Speciation and characterization of arsenic in gold ores and cyanidation tailings using X-ray absorption spectroscopy. *Geochimica et Cosmochimica Acta*, *68*(613), 969–983.

Paul, A. P., Maurer, D. K., Stollenwerk, K. G., Welch, A. H., Kahle, S. C., Taylor, W. A., ... & Olsen, T. D. (2010). *In-situ arsenic remediation in Carson Valley, Douglas County, west-central Nevada* (No. 2010-5161). US Geological Survey.

Savage, K. S., Tingle, T. N., O'Day, P. A., Waychunas, G. A., & Bird, D. K. (2000). Arsenic speciation in pyrite and secondary weathering phases, Mother Lode gold district, Tuolumne County, California. *Applied Geochemistry*, *15*(8), 1219-1244.

Singer, D. M., Fox, P. M., Guo, H., Marcus, M. a, & Davis, J. a. (2013). Sorption and redox reactions of As(III) and As(V) within secondary mineral coatings on aquifer sediment grains. *Environmental Science & Technology*, *47*(20), 11569–76. doi:10.1021/es402754f

Stookey, L. L. (1970). Ferrozine---a new spectrophotometric reagent for iron. *Analytical chemistry*, *42*(7), 779-781.

Su, C., & Puls, R. W. (2003). In situ remediation of arsenic in simulated groundwater using zerovalent iron: laboratory column tests on combined effects of phosphate and silicate. *Environmental science & technology*, *37*(11), 2582-2587.

Su, C., & Puls, R. W. (2001). Arsenate and arsenite removal by zerovalent iron: kinetics, redox transformation, and implications for in situ groundwater remediation. *Environmental science & technology*, *35*(7), 1487-1492.

Violante, A., & Pigna, M. (2002). Competitive sorption of arsenate and phosphate on different clay minerals and soils. *Soil Science Society of America Journal*, *66*(6), 1788-1796.

Vitre, R. D., Belzile, N., & Tessier, A. (1991). Speciation and adsorption of arsenic on diagenetic iron oxyhydroxides. *Limnology and Oceanography*, *36*(7), 1480-1485.

Wang, S., & Mulligan, C. N. (2006). Natural attenuation processes for remediation of arsenic contaminated soils and groundwater. *Journal of Hazardous Materials*, *138*(3), 459–70.

Welch, A. H., & Stollenwerk, K. G. (2003). *Arsenic in ground water: geochemistry and occurrence*. Springer Science & Business Media.

Welch, A. H., Stollenwerk, K. G., Maurer, D. K., & Feinson, L. S. (2003). In situ arsenic remediation in a fractured, alkaline aquifer. In *Arsenic in Ground Water* (pp. 403-419). Springer US.

Yang, J. K., Barnett, M. O., Jardine, P. M., Basta, N. T., & Casteel, S. W. (2002). Adsorption, sequestration, and bioaccessibility of As (V) in soils. *Environmental science & technology*, *36*(21), 4562-4569.

Zeng, H., Fisher, B., & Giammar, D. E. (2007). Individual and competitive adsorption of arsenate and phosphate to a high-surface-area iron oxide-based sorbent. *Environmental science & technology*, *42*(1), 147-152.

Zhang, H., & Selim, H. M. (2008). Competitive sorption-desorption kinetics of arsenate and phosphate in soils. *Soil Science*, *173*(1), 3-12.